THE INTERACTIONS OF CHLORINATED POLYMERS

A Thesis submitted for the Degree of

Doctor of Philosophy of the University of London

and the Diploma of Membership

of the Imperial College of Science and Technology

by

Christopher Philip Doubé B.Sc. (Hons.) A.R.A.C.I.

Department of Chemical Engineering and Chemical Technology

Imperial College of Science and Technology, LONDON SW 7

August 1979

ABSTRACT

The polymers P.V.C. and S.C.P.E. have been shown to be compatible from T_g measurements, and to exhibit an L.C.S.T. The Heat and Volume of Mixing have been estimated and have been shown to be small and negative.

Interaction parameters have been measured for a series of solvents and these polymers using I.G.C. This technique has also been used to calculate the polymer-polymer interaction parameters, and their phase diagram . The behaviour of these substances has been explained in terms of the Equation of State theory.

A new technique has been developed for the solvent free preparation of blends of P.V.C. These blends have been investigated by S.A.X.S. and S.A.N.S. Values of the radius of gyration of d P.V.C. in bulk and in blends with S.C.P.E. have been obtained, and these decrease from 134 Å in bulk to 109 Å in 50% blends. The structure of the blends has been explained in terms of a random density fluctuation associated with overlapping polymer molecules. This structure has been observed in T.E.M. studies. It has been proposed that the 'in-situ' polymerisation of P.V.C. in these blends results in amorphous solids which are free of 'primary particles'.

The influence of an active Kaolin surface on the polymers has been studied by I.G.C. Monolayer formation of S.C.P.E. on the Kaolin has been postulated for a layer $\sim$ 40 Å thick. At this level, S.C.P.E. has been shown to improve the mechanical properties of composites of P.V.C. and Kaolin.

"Applied science, which has a definite object in view, is more in the nature of an art and, like the art of painting a portrait, it is the recognition and isolation of the essential that really counts, though, of course, this art must be backed by sound scientific knowledge and understanding. Fundamental research is the ultimate source of all applied science."

Sir Henry Tizard

Theories are nets : only he who casts will catch.

Novalis

ACKNOWLEDGEMENTS

This thesis has come to fruition because of the wisdom of a number of people. As a small measure of gratitude I should like to acknowledge some of them :

Dr. D. Walsh for his unstinting encouragement and guidance in the resolution of this project.

Dr. A. Challis, Chairman of the Polymer Engineering Directorate of the Science Research Council, for his confidence and assistance in securing the project.

Professor Sir Geoffrey Allen, F.R.S., for his direction and support of the project.

Messrs. G. Burke, J. Cann, L. Barclay and A. Measey of B.P. Chemicals (Int.) Ltd. for their positive contributions and co-operation in industrial related matters.

Dr. G. Parry for his assistance with the diverse aspects of electron microscopy and numerous helpful discussions.

Dr. J. Higgins and Dr. A. Macconachie for their assistance with the organisation of neutron scattering experiments and their subsequent interpretation.

My colleagues, Drs. P. Crosby, V. Chapela, R. Hall and Mr. J. McKeown for their salutary comments and discussions.

Miss D. Eastwood for her very able compilation of this thesis.

Finally, I would like to thank my parents for their encouragement and support, and my wife, Janet, for savoir vivre.

TABLE OF CONTENTS

continued .....

LIST OF TABLES

LIST OF FIGURES

CHAPTER 1

INTRODUCTION

The interactions between atoms or molecules of a substance are responsible for the properties of that substance, for example its state as a solid, liquid or gas. These interactions are the sum of the molecular forces of attraction and repulsion and the thermal effects of disorder between the various components of the substance. In a system of two or more chemically dissimilar substances, one of the most important ways of characterising the interactions in the system is the determination of the thermodynamic phase diagram. These have been developed for crystalline solids such as metal alloys, using sensitive X-ray analysis. In the case of amorphous solids such as glasses and blends of high polymers, it is only recently that techniques[1] have been developed to establish phase diagrams. Similarly, it is difficult to measure exactly the interactions of high polymers with low molecular weight compounds such as solvents in liquid and vapour phase, and of high polymers at an interface with crystalline solids. Many of these difficulties originate in the time dependent viscoelastic properties of polymers, but it is these same properties which make polymers so important in industrial applications[2].

Compositions or formulations used in industry often contain two or more polymers mixed in a common solvent, such as paints, printing inks, adhesives and lubricating oils. Alternatively, these may be prepared in the presence of another solid, such as clay or glass fibre, to form plastic compounds and composites.

Mechanical properties such as adhesion, modulus and impact strength can be controlled by variation of the ratios of the components. Other properties which are of considerable technological importance include flammability, toxicity and ageing. Cost may also be improved in this way.

The main objective of this work was to establish some fundamental data on the system chosen, in order to show that the formulation of these compositions might be better understood.

Of the five main glassy polymers used in large quantity, only poly(vinylchloride) (P.V.C.) contains chlorine, which has some advantages, for instance in reducing flammability.

Much of the exploratory work in this field has been carried out using polystyrene as the main glassy polymer, due to its chemical simplicity and its ability to be prepared in a monodisperse form.

During the last few years, considerable effort has been expended by the polymer industry to identify compatible polymer pairs. The reason for the effort is that compatibility is the exception rather than the rule, so that if such systems can be discovered the possibility exists that novel 'alloy' like transitions and properties may be found. Theories developed to date have not been successful in predicting when compatibility will occur, so the search is empirical.

In this work the question of compatibility was considered by testing chemically similar, but physically dissimilar, polymers. The most common substances compatible with P.V.C. are the dialkyl esters of dicarboxylic acids which form hydrogen bonds,[3] and polymethacrylates, which have the same specific interaction. However, some low molecular weight chlorinated hydrocarbons show limited compatibility, so their higher analogues should show similar behaviour. Chemically similar polymers should have small heats of mixing and therefore could be compatible under some circumstances. Of all the chlorinated polymers available, solution chlorinated polyethylene (S.C.P.E.) has the most regular degree of substitution on a saturated main chain[4].

S.C.P.E. also can be prepared at various degrees of chlorination. Those with approximately 40% chlorine have elastomeric properties and have greater

resistance to degradation reactions than most linear elastomers[5], as typified by their good outdoor weathering characteristics.

It is possible that compatible elastomers could modify the impact properties of P.V.C. whilst not detracting from the tensile properties. Some of these S.C.P.E. polymers incorporate sulfonyl chloride groups in low concentrations to act as cross-link sites, and so are capable of interchain reactions, such as grafting or crosslinking after mixing, which further modify the properties of the composition.

Commercial formulations often include inorganic minerals, such as chalk, clay, diatomaceous earth or talc, and if these behave merely as diluents they are called 'fillers'.[6] In other cases glass spheres or carbon black give dramatic improvements in the properties, and these are called 'reinforcing fillers'.[6] Reinforcement has been intensively studied in glass or carbon fibre reinforced epoxy resins, where silane coupling agents are used to improve adhesion and to reduce the capacity to fail on impact due to delamination at the fibre-resin interface. Fracture mechanics studies of composites indicate this is the main reason for low impact strength[7], and therefore it is important to control the interface between polymers and filler.

Kaolin clays and other silicates have been shown to have surface groups which can, under certain conditions, bond to polymer molecules[8], causing the Kaolin to reinforce the polymer. However, the effect of any surface on polymers must extend beyond the first layer of atoms, and the size of the boundary layer could be equally important[6]. These questions are examined later in more detail.

The techniques for characterising such a system should be capable of resolving these points, and should be quite general for multiphase composites.

Results presented in this thesis are concerned with the measurement of interactions between P.V.C. and S.C.P.E., between each polymer and a number of solvents, and the interactions between each polymer and Kaolin clay particles.

These results are compared with those predicted by various theories, and the implications discussed.

CHAPTER 2

SUBJECT REVIEW

2.1 Polymer Compatibility

2.1.1 History

Studies of the colligative properties of polymer solutions gave results which were different from that expected for mixtures of small molecules[9]. This led to the development of the Flory-Huggins Lattice Theory[10,11]. These were further developed by Tompa[12] and Scott[13] to explain the thermodynamics of mixing two polymers in a common solvent and the general basis of polymer compatibility.

The discovery of numerous deviations from the Flory-Huggins theory[14] led to attempts by Patterson[15] to transpose the theories of Prigogine and others[16], from small molecules to polymers. This "Corresponding States Theory" applied the cell model for liquids to polymers by using reduced thermodynamic variables.

During the 1960's Flory[17] introduced a theory of solutions which stresses the importance of the equation-of-state parameters of the pure components for determining the thermodynamic properties of their solutions.

At present it is apparent that none of the theories is capable of predicting compatible polymer pairs, and empirical searches may be more fruitful. The original Flory-Huggins theory still has much appeal because of the simplicity of the model.

2.1.2 Flory-Huggins Theory

Raoult's Law for simple molecules only applies to ideal solutions, and deviations from this occur even for small molecules. When the solute is a high molecular weight polymer the deviations are very great, and the law applies only at extreme dilutions (where it is approached asymptotically). In the case of simple molecules, the total number of ways of arranging molecules of two types (Ω) [10,11] is :

$$\Omega = \frac{n_0!}{n_1!\ n_2!} \qquad (2.1)$$

where $n_o = n_1 + n_2$, and n_1, n_2 are the numbers of molecules 1 and 2 respectively.

From Boltzmann's Law, the entropy of mixing ΔS_m is given by :

$$\Delta S_m = k \ln \Omega \qquad (2.2)$$

where k is Boltzmann's constant.

Using Stirling's approximation ($\ln n! = n \ln n - n$) this may be rewritten as :

$$\Delta S_m = k \left[(n_1 + n_2) \ln (n_1 + n_2) - n_1 \ln n_1 - n_2 \ln n_2\right]$$

Applying the same argument to a polymer molecule consisting of x segments and arranging these on a lattice of $n_o = n_1 + n_2$ cells gives :

$$\Omega = \left[\frac{n_0!}{(n_0 - xn_2)!\ n_2!}\right] \left[\frac{(z-1)}{n_0}\right]^{n_2(x-1)} \qquad (2.3)$$

where z is the lattice coordination number.

Whence

$$\Delta S_c = -k \left[n_1 \ell n \left(\frac{n_1}{n_1 + xn_2}\right) + n_2 \ell n \left(\frac{n_2}{n_1 + xn_2}\right) - n_2(x_2 - 1) \ell n \frac{(z-1)}{e}\right] \qquad (2.4)$$

This is the configurational entropy of mixing for a perfectly ordered pure polymer and the pure solvent. However, the entropy of disorientation of the pure polymer is given by :

$$\Delta S_{disorientation} = kn_2 \left[\ell n\ x + (x-1) \ell n\ \frac{z-1}{e}\right] \qquad (2.5)$$

The entropy of mixing disoriented polymer may be obtained by subtraction to give

$$\Delta S_m^* = -k\left[n_1 \ell n\ v_1 + n_2 \ell n\ v_2\right] \qquad (2.5)$$

where $v_1 = \frac{n_1}{(n_1 + xn_2)}$ and $v_2 = \frac{xn_2}{(n_1 + xn_2)}$

For a polydisperse polymer of various chain lengths, each called i :

$$\Delta S_m^* = -k\left[n_1 \ln v_1 + \sum_i n_i \ln v_i\right] \qquad (2.6)$$

Computation of the Heat of Mixing was originally given by the empirical Scatchard-Hildebrand expression[18]

$$\Delta H_m = V_m (\delta_A - \delta_B)^2 \phi_A \phi_B \qquad (2.7)$$

where ϕ is the volume fraction and V_m the volume of the mixture, the 'Solubility Parameter' δ_A is $\left(\frac{\Delta E_A \text{ VAP}}{V_A}\right)^{\frac{1}{2}}$ where ΔE_A^V and V_A are the molar energy of vaporisation and molar volume respectively.

Consideration of the argument for the enthalpy of mixing in terms of molecular pair contacts or 'bonds' leads to a new expression[10] :

$$\Delta H_m = Z\Delta\omega_{12} x_1 n_1 v_2 \qquad (2.8)$$

where $\Delta\omega_{12}$ is the energy change for a 1,2 contact compared to themeanof 1,1 and 2,2 contacts,

zx is the number of contacts per molecule of x segments,

v_2 is the volume fraction (probability of contact) of polymer,

and n_1 is the number of solvent molecules.

This was then recast as :

$$\Delta H_m = kT\chi_1 n_1 v_2 \qquad (2.9)$$

where $\chi_1 = z\Delta\omega_{12}\frac{x_1}{kT}$, the 'Interaction Parameter', characterises the interaction energy per solvent molecule divided by kT.

If the configurational entropy change ΔS_m^* is assumed to represent the total entropy change on mixing ΔS_m , the free energy of mixing can be written as :

$$\Delta G_m = \Delta H_m - T\Delta S_m = \Delta H_m - T\Delta S_m^*$$

$$= kT\left[n_1 \ln v_1 + n_2 \ln v_2 + \chi_1 n_1 v_2\right] \qquad (2.10)$$

The assumption that $\Delta S_m^* = \Delta S_m$ is not correct because the entropy may change

due to an ordering conferred on the molecules by the contact energy of interaction associated with ΔH_m. In this case the term $\Delta\omega_{12}$ and hence χ_1 must be considered as $\Delta\omega_h - T\Delta\omega_s = \Delta\omega_{12}$ i.e. an entropy and enthalpy component to the interaction.

This causes some conceptual problems but the experimentally accessible change in chemical potential may be derived from the expression as :

$$\mu_1 - \mu_1^0 = RT \ln \left[(1-v_2) + (1-\frac{1}{x})v_2 + \chi_1 v_2^2\right] \qquad (2.11)$$

where μ_1 is the chemical potential of component 1 in the mixture, and μ_1^0 that in the pure state, or for polydisperse systems = $RT \ln \left[(1-v_2) + (1-\frac{1}{\bar{x}_n})v_2 + \chi_1 v_2^2\right]$ (2.12)

From this the partial molar Heat and Entropy of dilution may be written as respectively

$$\Delta\bar{H}_1 = RT\,\chi_1 v_2^2 \qquad (2.13)$$

$$\Delta\bar{S}_1^* = -RT\left[\ln(1-v_2) + (1-\frac{1}{x})v_2\right] \qquad (2.14)$$

Whilst these mathematical expressions are conveniently simple, the assumption that a non-structured system may be described in terms of a lattice is open to criticism.

Phase equilibria in polymer solutions may also be analysed by this theory. Polymer solutions may be caused to separate by a change in temperature or the addition of a non-solvent. The temperature at which phase separation, or precipitation, occurs on cooling in a solvent is called the cloud point.

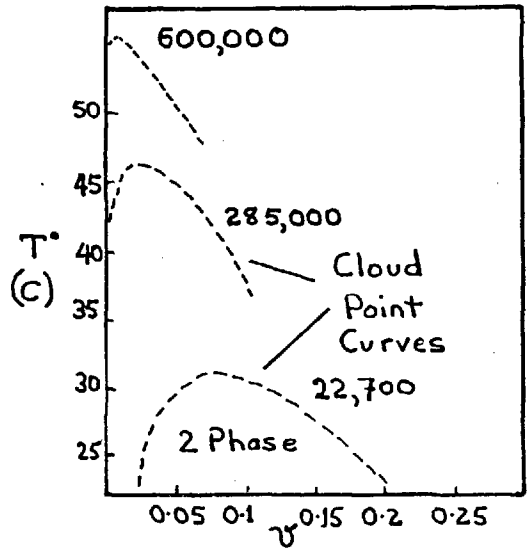

Fig. 2.1 The effect of increasing molecular weight on Polymer-Solvent (cloud points predicted for polyisobutylene and diisobutylketone from the Flory-Huggins theory).

Precipitation occurs on cooling polymer solutions at different temperatures depending on composition and polymer chain length. These cloud point curves also vary for different solvents and different polymers. Two phases are formed at this temperature, one polymer rich and the other polymer poor, and the chemical potential of each component in each of these is equal.

$$\text{Solvent } \mu_1 \text{ (polymer poor)} = \mu_1' \text{(polymer rich)}$$

$$\text{Polymer } \mu_2 \text{ (polymer poor)} = \mu_2' \text{(polymer rich)}$$

The maximum temperature at which this occurs is called the critical temperature T_c and it must fulfil the conditions $\left(\frac{\partial \mu_1}{\partial v_2}\right)_{T,P} = 0$, and $\left(\frac{\partial^2 \mu_1}{\partial v_2^2}\right)_{T,P} = 0$.

Application of these conditions to the expression from dilute solution theory[10] gives :

$$\frac{1}{(1-v_2)} - \left(1 - \frac{1}{x}\right) - 2\chi_1 v_2 = 0 \qquad (2.15)$$

and

$$\frac{1}{(1-v_2)^2} - 2\chi_1 = 0 \qquad (2.16)$$

If x is large

$$v_{2\,crit.} = \frac{1}{x^{\frac{1}{2}}} \qquad (2.17)$$

and

$$\chi_{1\,crit.} = \tfrac{1}{2} + \frac{1}{x^{\frac{1}{2}}} \qquad (2.18)$$

Thus a temperature theta may be defined as the critical solution temperature for a polymer of infinite molecular weight. As the molecular weight decreases the critical temperature also decreases, and the critical concentration increases.

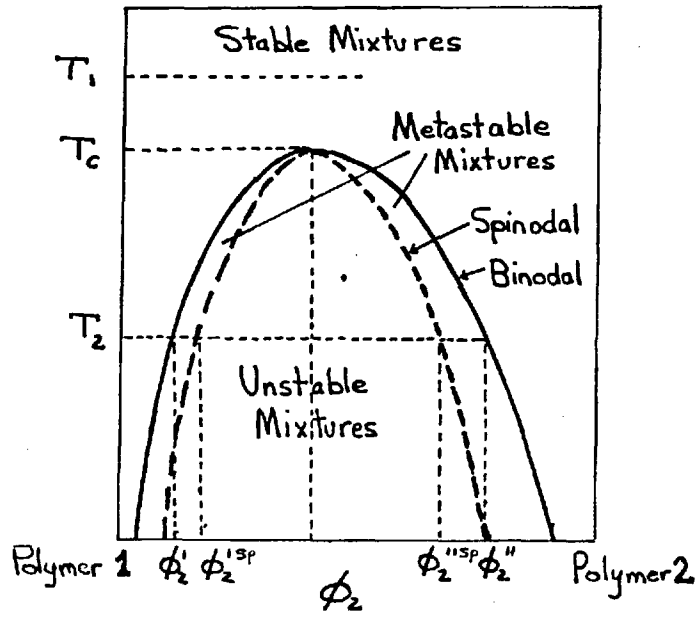

Fig. 2.2 Phase Diagram of a miscible binary polymer system which shows an Upper Critical Solution Temperature (U.C.S.T.)

The situation which occurs on mixing two polymers may be described similarly (Fig. 2.2). The free energy of mixing ΔG_m is

$$\Delta G_m = \Delta H_m - T\Delta S_m \qquad (2.19)$$

and this must be negative for compatibility. The Scatchard-Hildebrand expression, $\Delta H_m = V_m (\delta_A - \delta_B)^2 \phi_A \phi_B$, cannot predict a negative heat of mixing due to the square of the difference in solubility parameters. Also, the Van Laar expression, $\Delta H_m = z\Delta\omega_{12} n_1 v_2$, will not be negative unless there is a specific interaction to make ω_{12} less than the mean of ω_{11} and ω_{22}.

The mechanism of phase separation of polymers is more complicated than that of small molecules. This is because of the slow rates of diffusion of polymers, which means that metastable composition can be observed. In this case the conditions for phase equilibria are :

$$\left(\frac{\partial \Delta G}{\partial \phi}\right)_{T,P} = 0 \quad \text{which defines the binodal} \qquad (2.20)$$

and $\left(\frac{\partial^2 \Delta G}{\partial \phi^2}\right)_{T,P} = 0$ which defines the spinodal (2.21)

and $\left(\frac{\partial^3 \Delta G}{\partial \phi^3}\right)_{T,P} = 0$ at the critical temperature (2.22)

These can be better understood by consideration of the following plots of free energy vs. composition in Fig. 2.3.

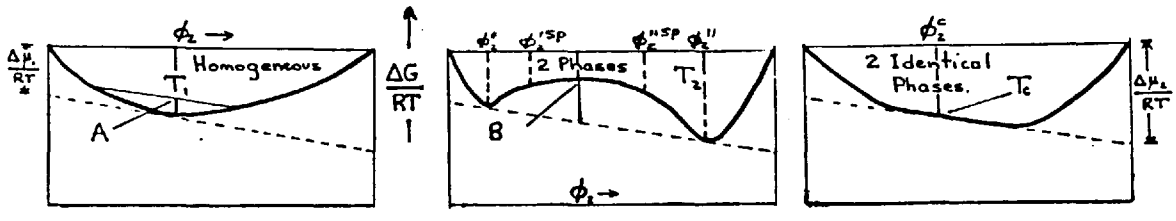

Fig. 2.3 The relation between the Gibbs free energy of mixing and the phase diagram for partially miscible polymers

At temperature T_1 the mixture at point A will not phase separate as the mean of the free energies of the separate phases is greater than that of the single phase.

At temperature T_2 the mixture at point B can go to a lower energy state by phase separation provided the compositions ϕ_2' and ϕ_2'' on the binodal can be formed. Such a composition difference requires a nucleation and growth mechanism, which introduces the interfacial free energy as an activation energy. This means that compositions from B to the points of inflexion on the spinodal should spontaneously phase separate. This spontaneous trend away from a homogeneous mixture must mean diffusion against the concentration gradient, and a negative diffusion coefficient.

Finally at the critical temperature T_c the only possibility is the spontaneous phase separation into two identical phases described above. At T_c there is no possibility of nucleation and growth, so the structure of the 'spinodal decomposition' should be observed.

This suggests that mixtures can be unstable at negative values of ΔG_m, and that variation of ΔG with ϕ is most important. Phase separation is brought about by very small driving forces as only small interfacial energies have to be overcome.

In polymer mixtures there is a problem with the interaction parameter χ_{23} regarding the unit of volume used for normalisation. The normal Flory interaction parameter is determined by the size of V_2, the polymer molar volume, which will be large. Alternatively, the Tompa parameter is determined by the size of a polymer segment for V_2, but the selection of this is arbitrary.

For example, if $\chi_{23} = 1$, for $V_2 = 10^4$

$$\left[\frac{\chi_{23}}{V_2}\right] = 0.0001$$

This is possible only for monodisperse polymers, so most workers use $\left[\frac{\chi_{23}}{V_2}\right]$ as the quantity for analysis.

When two chemically different polymers are mixed, if they have equal molecular weights, their chemical potentials

$$\mu_2 - \mu_2^0 = RT \left[\ell n\ v_2 + \chi_{23}\ v_3^2\right] \qquad (2.23)$$

$$\mu_3 - \mu_3^0 = RT \left[\ell n\ v_3 + \chi_{23}\ v_2^2\right] \qquad (2.24)$$

The critical conditions are satisfied when $\chi_{23}^{crit} = 2$ (or $\frac{\chi_{23}^{c}}{V_2} << 0.2$) as these are the chemical potentials for regular binary solutions. In this case the entropy of mixing is so small that a small positive heat of mixing will ensure compatibility.

If the two polymers are mixed in the presence of a solvent which is completely miscible with each polymer, the conditions are that χ_{12} and χ_{13} must be less than 0.5. From the normal arguments regarding chemical potentials, it can be shown that the critical points are given by

$$\chi_{23} = 2/(1-v_{1c}) \qquad (2.25)$$

where v_{1c} is the critical volume fraction of solvent.

This shows that the values of χ_{12} and χ_{13} are not involved and that the compatibility is independent of solvent, except for the value of v_{1c}. The value of χ_{23} is increased over that with no solvent if v_{1c} is greater than zero, i.e. if phase separation occurs before all solvent is removed.

2.1.3 Limitations of the Flory-Huggins Theory

The Scatchard-Hildebrand expression for heats of mixing is limited because it can predict positive values only. However, the 'solubility parameters' ($\delta_{polymer}$) of the theory have been quite useful as guides to compatibility. These can be experimentally determined by the judicious selection of solvents to swell crosslinked polymers[19]. The improvement of the Flory-Huggins interaction parameter is that it can be used for

positive and negative heats of mixing, although the theory was originally derived for non-polar phantom chains, where negative heats of mixing would not be expected. From the theory it can be seen that the value of χ should be inversely proportional to temperature and independent of concentration.

Initial studies on natural rubber-benzene solutions by Gee and Treloar[9] indicated good agreement with the theory, but later studies[21,22] on other polymers showed a marked concentration dependence of χ. Also Flory and Schultz[23] showed the dependence of χ upon temperature was not as simple as the theory predicted. Although χ decreases with increasing temperature there are deviations from χ being proportional to the reciprocal of the absolute temperature.

Results by Konningsveldt[20] and Gordon[24] have shown the variation of the Upper Critical Solution Temperature (U.C.S.T.) cloud point curves for non-polar components from those predicted by the lattice theory. In general, the theories rely on the 'postulate of the geometric mean'[25] which is a close approximation to London dispersion forces for permanent dipole interactions. Allen, Gee and Nicholson[26] investigated mixtures of oligomers and found an unusually strong entropic contribution to the free energy of mixing, and quite recently Patterson[27] has shown that the compatibility of polymers is dependent on the solvent used for film casting, which contradicts the theoretical assumption that compatibility of polymers should be independent of solvent. These studies of polymer compatibility have shown an asymmetry which could not be related to the ratios of the degrees of polymerisation of the two molecules, or their polydispersity.

These problems were major factors in the reappraisal of the simple lattice theory, and its extension to the Prigogine-Flory equation of state. This theory does predict the concentration dependence of χ^* and the variation of χ^* as a function of temperature. It also predicts higher values for χ^* than χ for polymer-solvent

and polymer-polymer interactions.

It has been shown by McMaster[28] that the Equation of State approach is superior to the lattice treatment as it is capable of explaining the formation of Lower Critical Solution Temperatures (L.C.S.T.) which have been observed in polymer mixtures[20]. This phenomenon is shown in Fig.2.4 and the problem for the lattice theory is evident because in order to explain the L.C.S.T. it is necessary to have a negative ΔH_m and hence a negative ΔS_m.

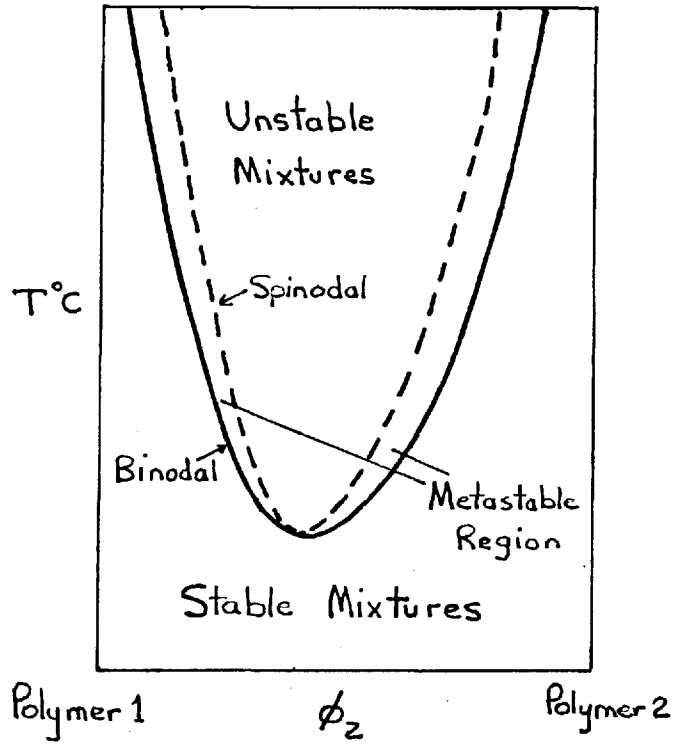

Fig. 2.4 A phase diagram for a binary system with an L.C.S.T.

These can best be explained by the existence of a specific interaction such as a hydrogen bond between the two molecules, so that ΔH_m will be negative, and ΔS_m will also be negative due to the ordering effect conferred by mixing. A second possibility is for two chemically similar polymers where the free volume of mixing ΔV_m is negative, so ΔS_m will again be negative, and ΔH_m will also be negative. It is difficult to resolve these problems as the improvements in the theory obtained by

dealing with the problem of free volume are offset by the loss in simplicity of the model.

Although this theory is capable of explaining L.C.S.T. and the effect of pressure on compatibility, it does not improve the ability of an experimentalist to predict compatible polymer pairs.

2.1.4 Equation of State

The most important omission from the lattice theory described is the effect of the common phenomenon of volume change on mixing. The equation of state theory can take this into account. Three characteristic parameters v^*, T^* and p^*, which scale a reduced partition function, may be evaluated from equation of state data for the pure components such as density, thermal expansion coefficient, and thermal pressure coefficient. The relative surface areas of the molecules are also considered in addition to contact pair exchange interaction parameters. The derivation is comprehensively discussed in reference 17 and only the relevant aspects are given here.

Tonks[29] has shown that the partition function Ω for a one dimensional system of N hard, non-attractive particles arranged on a line of length L is given by

$$\Omega = [(\ell-\ell^*)e]^N \qquad (2.26)$$

where ℓ^* is the hard core length and $\ell = L/N$. This may be extended to three dimensions by defining $\ell = (\gamma_g v)^{\frac{1}{3}}$ and $\ell^* = (\gamma_g v^*)^{\frac{1}{3}}$, where $v = V/N$, γ_g is a numerical factor and v^* is the hard core volume.

In order to maintain generality, the molecule is considered to consist of r segments, and then v^* is the hard core volume of a segment, $v = V/r$, where V is the volume per molecule.

An approximate partition function has been estimated using Monte Carlo calculations[30] considering the limitation on external degrees of freedom for complicated

molecules

$$\Omega = |\gamma_g \, e^3 v^* (\tilde{v}^{1/3} - 1)^3|^{Nrc} \qquad (2.27)$$

where $\tilde{v} = v/v^*$ and c is $\frac{1}{3}$ no. of degrees of freedom per segment.

Now for attractive molecules, the mean intermolecular energy E_o may be written as

$$Z = \Omega \exp(-E_o/kT) \qquad (2.28)$$

In view of the short range of molecular attractions, the energy may be considered to be additive over the area of contact

$$E_o = -N r s \eta / 2 v \qquad (2.29)$$

where s is the number of contact sites per segment (proportional to the surface area per segment) and $-\eta/v$ is the intermolecular energy per contact.

Introduction of the reduced temperature $\tilde{T} = T/T^* = 2v^* ckT/s\eta$ means the partition function may be written as :

$$Z = \text{const} (\tilde{v}^{\frac{1}{3}} - 1)^{3 Nrc} \exp(Nrc/\tilde{v}\tilde{T}) \qquad (2.30)$$

The Equation of State may now be written as :

$$\tilde{p} \, \tilde{v}/\tilde{T} = \tilde{v}^{1/3}/(\tilde{v}^{1/3} - 1) - 1/\tilde{v}\tilde{T} \qquad (2.31)$$

where $\tilde{p} = p/p^* = 2pv^{*2}/s\eta$ and $p^*v^* = ckT^*$.

At $p = 0$ $\tilde{T} = (\tilde{v}^{1/3} - 1)\tilde{v}^{4/3}$, which leads to

$$\tilde{v}^{\frac{1}{3}} - 1 = (\alpha T/3)(1+\alpha T) \qquad (2.32)$$

where $\alpha = \left(\frac{\partial \ln v}{\partial T} \right)_{p=o}$.

For binary mixtures, assuming mixing is random, the partition function may be written :

$$Z = Z_{comb} \, \Omega \exp(-E_o/kT) \qquad (2.33)$$

where Z_{comb} is the combinatory factor for mixing.

The Free Energy of mixing may be expressed as :

$$\Delta G_m = \Delta G_{comb} + G^R \qquad (2.34)$$

where $\Delta G_{comb} = -T\Delta S_{comb}$, and G^R is the 'residual' free energy from the equation of state part of the partition function $\Omega \exp(-E_o/kT)$.

If the segments are chosen to be of arbitrarily equal core volume, the partition function can be expressed as

$$Z = \text{const. } Z_{comb} (\tilde{v}^{1/3}-1)^{3\bar{r}N\bar{c}} \cdot \exp(-E_o/kT) \qquad (2.35)$$

where the total number of molecules $N = N_1 + N_2$, the mean segment ratio $\bar{r} = (r_1 N_1 + r_2 N_2)/N$, and the mean number of degrees of freedom

$$\bar{c} = (r_1 N_1 c_1 + r_2 N_2 c_2)/\bar{r}N$$

ϕ_1 and ϕ_2 expressed as segment fractions give

$$\phi_2 = 1 - \phi_2 = r_2 N_2/\bar{r}N \text{ and } \bar{c} = c_1\phi_1 + c_2\phi_2 \qquad (2.36)$$

The molar characteristic volume of species i is given by

$$V_i^* = r_i v^* \text{ and } r_2/r_1 = V_2^*/V_1^* \qquad (2.37)$$

($\tilde{v}_i = V_i/V_i^*$ and $V_i = r_i v$ is the molecular volume or molar volume)

Therefore

$$\phi_2 = N_2 V_2^* / (N_1 V_1^* + N_2 V_2^*) \qquad (2.38)$$

or

$$\phi_2 = m_2 v_{sp}^* / (m_1 v_{sp}^* + m_2 v_{sp}^*) \qquad (2.39)$$

where m is the mass of component i and v_{sp}^* is the characteristic volume per gram.

The energy E_o follows from previous arguments

$$-E_o = (A_{11}\eta_{11} + A_{22}\eta_{22} + A_{12}\eta_{12})/v \qquad (2.40)$$

where $A_{i,j}$ is the number of i, j contacts, each being characterised by the energy $-\eta_{ij}/v$, and this energy may be written

$$- E_o/\bar{r}N = [\theta_1\eta_{11} + \theta_2\eta_{22} - \theta_1\theta_2\Delta\eta]\ (S/2v) \qquad (2.41)$$

where $\Delta\eta = \eta_{11} + \eta_{22} - 2\eta_{12}$, θ_i are the site fractions, and

$$S = (S_1r_1N_1 + S_2r_2N_2)/\bar{r}N = \phi_1S_1 + \phi_2S_2$$

If E_o is expressed from the theory for pure components as

$$- E_o/\bar{r}N = p^*v^*/\tilde{v} \qquad (2.42)$$

then by comparison with the above expression (2.41),

$$p^* = \phi_1p_1^* + \phi_2p_2^* - \phi_1\theta_2X_{12} \qquad (2.43)$$

where $X_{12} = S_1\Delta\eta/2v^{*2}$ is a measure of the contact interaction energy and

$$1/T^* = (\phi_1p_1^*/T_1^* + \phi_2p_2^*/T_2^*)/p^* \qquad (2.44)$$

Both these expressions show the dependence of $\tilde{p} = p/p^*$ and $\tilde{T} = T/T^*$ on composition. The theory then suggests that the Enthalpy of Mixing can be approximated to the Energy of Mixing for a condensed system, such that

$$\Delta H_m = \bar{r}Nv^*[\phi_1p_1^*/\tilde{v}_1 + \phi_2p_2^*/\tilde{v}_2 - p^*/\tilde{v}] \qquad (2.45)$$

or

$$\Delta H_m = \bar{r}Nv^*[\phi_1p_1^*(v_1^{*-1}-\tilde{v}^{-1}) + \phi_2p_2^*(\tilde{v}_2^{-1}-\tilde{v}^{-1}) + \phi_1\theta_2X_{12}/\tilde{v}] \qquad (2.46)$$

and this is more complex than the expression $\Delta H_m = BN_1\phi_2$ from the simple theory, where B is a constant, independent of concentration.

Now B can be expressed in terms of the new theory

$$B = \lim_{\phi_2\to o}\left(\frac{\Delta H_m}{N_1\phi_2}\right) = \lim_{N_2\to o}\left(\frac{\Delta H_m}{N_2}\right)\left(\frac{V_1^*}{V_2^*}\right)$$

$$= \left(\frac{V_1^*}{\tilde{v}_1}\right)\left\{p_2^*\left[\frac{\tilde{v}_1}{\tilde{v}_2} - 1 - \alpha_1T\left(1 - \frac{\tilde{T}_2}{\tilde{T}_1}\right)\right] + (1+\alpha_1T)\left(\frac{S_2}{S_1}\right)X_{12}\right\} \qquad (2.47)$$

For $\alpha_1 > \alpha_2$ the equation of state contribution in square brackets will be negative, hence the enthalpy of mixing will be negative unless X_{12} is large enough to dominate.

The additive volume $\tilde{v}^0 = \phi_1\tilde{v}_1 + \phi_2\tilde{v}_2$, differs from the mixture volume $\tilde{v}$ by $\tilde{v}^E = \tilde{v} - \tilde{v}^0$ which is related to composition by T*.

From the partition function and the energy of mixing expression, the residual entropy due to differences between the pure components

$$S^R = -3(N_1p_1^*V_1^*/T_1^*)\ell n[(\tilde{v}_1^{1/3}-1)/(\tilde{v}^{1/3}-1)] - 3(N_2P_2^*V_2^*/T_2^*)\ell n[(\tilde{v}_2^{1/3}-1)/(\tilde{v}^{1/3}-1)] \quad (2.48)$$

The partial molar quantities of interest may be found

$$\bar{H}_1^R = \bar{H}_1 - H_1^0 = (\partial\Delta H_m/\partial N_1)_{T,p,N_1} = p_1^*V_1^*[(\tilde{v}_1^{-1}-\tilde{v}^{-1})+(\alpha T/\tilde{v})(\tilde{T}_1-\tilde{T})/\tilde{T})] + (V_1^*X_{12}/\tilde{v})(1+\alpha T)\theta_2^2 \quad (2.49)$$

$$TS^R = -p_1^*V_1^*\{3\tilde{T}_1\ell n[(\tilde{v}_1^{1/3}-1)/\tilde{v}^{1/3}-1)] - (\alpha T/\tilde{v})(\tilde{T}_1-\tilde{T})/\tilde{T}\} + \alpha T(V_1^*X_{12}/\tilde{v})\theta_2^2 \quad (2.50)$$

Combination of these yields

$$(\mu_1-\mu_1^0)^R = p_1V_1^*\{3\tilde{T}_1\ell n|(\tilde{v}_1^{1/3}-1)/\tilde{v}^{1/3}-1)| + (\tilde{v}_1^{-1}-\tilde{v}^{-1})\} + (V_1^*X_{12}/\tilde{v})\theta_2^2 \quad (2.51)$$

With this revision the original Flory-Huggins expression becomes

$$(\mu_1-\mu_1^0)/RT = \ell na_1 = \ell n(1-\phi_2) + (1-1/r)\phi_2 + [(\mu_1-\mu_1^0)^R/RT\phi_2^2]\phi_2^2 \quad (2.52)$$

where χ is now called the reduced residual chemical potential

$$\equiv (\mu_1-\mu_1^0)^R/RT\phi_2^2 \quad (2.53)$$

and is often represented as χ^*.

The advantage of this theory has been well shown by the work of McMaster[28] which demonstrates the importance of thermal expansion and thermal pressure coefficients, and indicates that the L.C.S.T. should be normal behaviour for polymer mixtures. This work shows that spinodal decomposition might be a common phenomenon for polymers, which diffuse more slowly than metals or glasses for which the original postulate was made[31].

An explanation for McMaster's findings can be found in the contribution of the free volume of mixing to both the enthalpy and entropy of mixing. Indeed the free volume change may be caused by either a specific interaction or merely by favourable packing arrangements associated with the expansion coefficients. This would mean that ΔH_m would be negative, or at least small. At the same time ΔS_m must be negative, due to the ordering conferred on the system, so that although $\Delta G_m = \Delta H_m - T\Delta S_m$ is negative it may become positive as the temperature rises or $\left(\frac{\partial^2 \Delta G}{\partial \phi^2}\right)$ will become zero.

The object of this work was to establish whether two similar polymers with no specific interactions could show an L.C.S.T., and to establish the usefulness of phase diagrams in polymer technology.

2.2 Two phase polymers and Composites

2.2.1 History

The adhesion between particles is of fundamental importance in many industrial applications, and this has stimulated interest in this subject for many years. Early studies of colloids and surfaces were only really understood with the application of modern thermodynamics by Gibbs[32] in 1867. Further elaboration of these theories in the 1920's by Langmuir and Harkins and the systematic evaluation of adsorption isotherms, enabled access to new information on the free energy of adsorption for

different states of matter - solid-gas, solid-liquid, liquid-gas and liquid-liquid. However, the subject of solid-solid interactions derived its main advance from the work of Griffith[33] on fracture theory, in 1920.

As polymers developed in importance, different composites were prepared, which were essentially heterogeneous, such as natural rubber and carbon black, glass fibre and epoxy resin, and wood and adhesive laminates. Most theoretical treatments of these were on a continuum or empirical basis. The rigorous approach was developed from studies of adsorption isotherms, which were limited by the nature of the polymer and solvent, and competition between them for adsorption.

Such cases as those when the adsorption can be well characterised are limited to very dilute solutions by rapid multilayer formation. As Adamson explains[34], these do give a Langmuir isotherm, but the number of complications make explanations difficult.

Some advances were made in the 1950's when Zisman[35] developed a technique for the determination of the critical surface tension for spreading of liquids on solid substrates, which gave a measure of the surface free energy of solid polymers. However, the major advances came with the theoretical treatment of Silberberg[36] in 1962, which showed the adsorption process was essentially entropic in nature. When a polymer is adsorbed from solution onto a surface, the increase in entropy of the solvent molecules leaving the surface is greater than that the decrease in entropy of the polymer. The entropy of adsorption can dominate the free energy adsorption for non-polar polymers. This work showed that the adsorbed polymer existed as a series of contact points called 'trains', with large 'loops' extending from the surface, the nature of this adsorption state being determined by polymer-solvent-surface interactions. The use of solutions in adsorption studies is limited to temperatures below the solvent boiling points, and cross-linked polymers are excluded. It has been necessary to resort

to other techniques to measure surface interactions due to these problems. Direct evaluation of forces between solids at room temperature has been estimated and measured experimentally.

These forces were theoretically estimated from the additivity of London dispersion forces by Derjaguin[37] and Hamaker[38], and the estimates were not checked until the advent of direct measurements of surface forces by cleaving single crystals of mica[39]. In principle it should be possible to apply these findings to polymeric composites, but unfortunately, as stated in a recent paper by Israelachvili[40], the theory of deformable viscoelastic solids is not resolved. This paper also highlights the dichotomy in interface science between solutions studies and studies of the solid state.

Resolution of the difference between solution studies and direct measurement has been attempted here, using the technique of Inverse Phase Gas Chromatography (I.G.C.).

2.2.2 Theory of Adhesion and Interfaces

The free energy of adhesion for an interface between two unlike solids is given by[43]

$$\Delta G_{ADS} = \gamma_1 + \gamma_2 - \gamma_{12} = \text{Work of Adhesion} \qquad (2.54)$$

where γ_1 and γ_2 are the surface free energies of components 1 and 2, and γ_{12} is the interfacial free energy, so γ_{12} should be small for a large ΔG_{ADS}.

It is difficult to relate this to the continuum theories of composites, because a polymeric matrix is strengthened or stiffened by a particulate or fibrous second phase in a very complex manner. The second phase appears to restrict the mobility of the matrix by introducing a mechanical restraint, which depends on its size and spacing. The extent of this restraint also depends on the properties of the interface, such as the work of adhesion, and those of the matrix and of the incorporated phase[44].

Mechanical properties of composites are also influenced by the isotropy of the second phase. Fibres give a marked anisotropy in composites, whereas particulate fillers are less marked. Much of the theory of interfaces has been derived from fibre reinforced composites but the major concern here is for particulate fillers, either solids or elastomers.

The evidence of the influence of the filler on the matrix via the interface is the increase in the glass transition (T_g) as found by Nielsen et al[45]. They proposed a modified version of the important equation due to Einstein[46]

$$\ln\left(\frac{G_c}{G_p}\right) = 2.5\ v_f / \left[1 - \frac{v_f}{\phi_m}\right] \qquad (2.55)$$

where : G_c and G_p are the Shear Moduli for composite and polymer,

ϕ_m is the maximum packing fraction for a system of dispersed spherical particles,

and v_f is the filler volume fraction.

These continuum approaches are useful for most applications, but the subject has become restricted by the controversy over the role of the interface[44]. According to the protagonists, it is possible that for any interface with maximum contact, the site of failure will be within the matrix of the weaker component, in which case mechanical 'keying' on a microscopic scale is the only technique for improvement. Alternatively, the use of silane coupling agents has been shown to improve the mechanical properties of glass-epoxy resin composites, indicating the formation of covalent chemical bonds at the interface is significant.

Although the effect of fillers on the modulus is relatively clear, the consideration of their effect on Ultimate Tensile Strength and elongation to failure is less so.

Using a simple model, Nielsen[47] has sought to extend additivity predictions for

rigid fillers to include stress-strain behaviour for perfect adhesion and no adhesion, and gives the result shown in Fig. 2.5. Although this model lacks many details it illustrates the contradictory role of adhesion in increasing strength and decreasing ultimate strain (or toughness).

Since by definition the perfect interface between two solids must adhere, it is apparent that the testing of adhesion is frequently related to the techniques of obtaining good contact between solids.

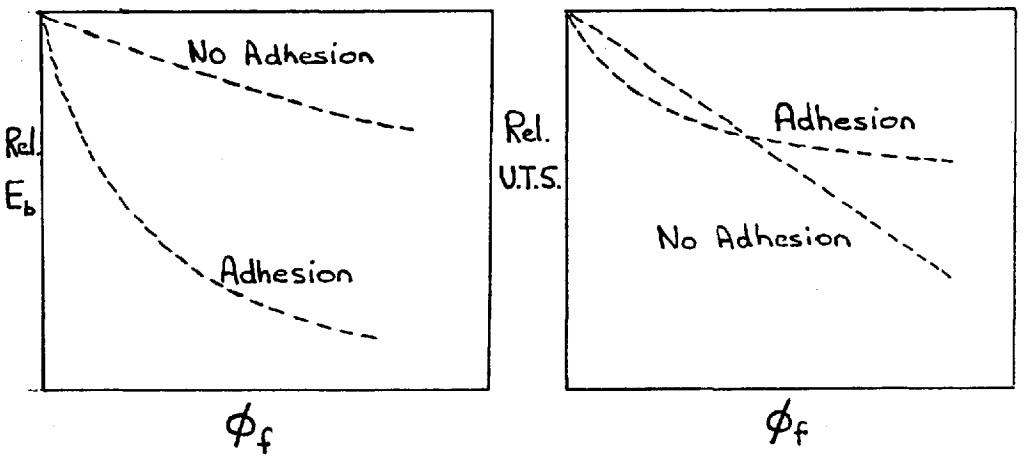

Fig. 2.5 The effect of adhesion on the mechanical properties of composites

In conclusion, it is obvious that there is a dilemma in the preparation of two phase filled polymers, in that increased adhesion can readily be achieved, but normally only with the loss of other highly desirable properties. The great advantage of elastomers over glassy fillers is that they promote craze formation and shear yielding and in order to understand this it is necessary to consider the theory of fracture mechanics.

2.2.3 Fracture Mechanics

Knowledge of the nature of the interfaces in composites may be obtained from microscopy, and this is a common technique for evaluating fracture surfaces. This is due to the Griffith Fracture Condition, that a crack will initiate when $G = G_c$,

where G = Energy per unit area of crack, and $G_c = 2\gamma$ where γ is the surface free energy of the solid. The fracture path should have the minimum area possible and microscopes can measure this. These conditions apply only to elastic solids, and visco-elastic losses cause complications which have not been solved[40].

The main measurement of interest at present is the Fracture Toughness. This is given by Williams[48] as:

$$K_I^2 = E\, G_I \qquad (2.56)$$

where E is the value of Young's modulus, and G_I is the energy release rate per unit area of crack and is often called 'fracture toughness'.

A critical value $K_{IC}^2 = E\, G_{IC}$ may be derived, which is called the Stress Intensity Factor.

From the Griffiths Condition it might be assumed that an absolute value of G_I (independent of test) might be obtained from the surface free energy γ which is $\sim 40\ mJ\ m^{-2}$ for P.V.C.[49], but this is not possible, since the energy absorbed by deformation at the tip of the crack may be several hundred times greater than the surface energy[50]. In fact, if one considers the work done in fracture as relating to a 5 Å separation in the atoms,

$$\text{Work} = \text{U.T.S.} \times 5 \times 10^{-8} = 2\gamma \qquad (2.57)$$

$$\text{i.e.} \quad \text{U.T.S.} \times 5 \times 10^{-10} = 2 \times 40 \times 10^{-3}\ (J\ m^{-2})$$

$$\text{so} \qquad \text{U.T.S.} = 160\ M\ N\ m^{-2}$$

and this is rather greater than that actually measured ($\sim 50\ M\ N/m^{-2}$).

This observed value of the strength which is usually almost ten times lower than that theoretically predicted must be explained by the presence of flaws or cracks in the solid which acts as 'stress-multipliers'. Such cracks can be considered as mechanisms which dissipate energy until a critical value is reached when failure occurs. The expression for an infinite plate containing a small crack is given as

$$K_{IC}^2 = \sigma^2 \pi a \qquad (2.58)$$

where 2a is the crack length and σ is the tensile strength.

$$G_{IC} = \delta_c * \sigma_c \qquad (2.59)$$

where δ_c is the critical crack opening displacement.

Bucknall[51] has pointed out some of the complications of the analysis of composites, particularly the effect of yielding at the crack tip, which makes Linear Elastic Fracture Mechanics (L.E.F.M.) invalid. This yielding phenomenon has been related by Good[43] to the free energy of adhesion, so that a high value will cause cohesive (bulk) failure and a low value adhesive or interfacial failure. Broutman[52] has also considered the phenomenon of yielding and the effect of the adhesive strength of an interface in determining the mode of energy dissipation for a propagating crack.

Recent work by Williams et al[48] has been instrumental in applying the theory of sharp crack failure to impact tests in order to obtain experimental values for the fracture toughness G_{IC}. In these results it is evident for systems such as A.B.S. or High Impact Polystyrene that contain a large interfacial area of low energy glass-elastomer interfaces, possess a mechanism for energy dissipation.

The object of this study was to investigate the interfaces formed between kaolin and the two polymers chosen, P.V.C. and S.C.P.E.

2.2.4 Reinforcing and Non-reinforcing Fillers

In the normal terminology of the industry reinforcing fillers are those which give properties greater than the sum of the two components. The best examples are carbon blacks and silicas in rubber, and fibre glass in polyester. In the case of 'reinforcing fillers', the idea of an interphase region has been promoted[53], implying that the effect of strong surface interactions extends into the bulk polymer. The

mechanisms are complex, but are thought to be associated with, respectively, pi bonding in the carbon surface, Si-OH groups in the silica, and with siloxane 'coupling agents' in the glass-polyester interface.

It is apparent that the hydroxy groups in the surfaces of silicas may be used to promote adhesion at the interface. One common group of minerals which have been shown also to possess active surface groups are the kaolin clays[8]. The interaction between kaolins and ionic polymers has been extensively reviewed because of the technological importance of these systems in oil recovery[54,55]. Little work has been carried out on their interaction with polar synthetic macromolecules, as this has shown adverse effects from the untreated kaolins, so the approach was to neutralise the surface to give a non-interacting, non-reinforcing filler[56].

It is evident that if an acidic filler like silica can be reinforcing for certain elastomers it is possible for other silicates to behave similarly. If an active filler particle could be surrounded by a thin layer of strongly adsorbed elastomer, and this could in turn be in contact with a compatible glassy polymer, the existence of two low energy interfaces should provide some possibilities for energy dissipation in crack propagation. This approach has been attempted with polyethylene as bulk polymer[57], but using high modulus polymer for encapsulation.

All these techniques indicate the importance of the interface in composites. It is necessary to understand the influence of the surface on the adsorbed phase in order to control their properties.[58]

CHAPTER 3

EXPERIMENTAL DETERMINATION OF THE PHASE DIAGRAM

3.1 Introduction

The techniques used to determine phase diagrams for amorphous polymers in the absence of solvent have only recently been developed[1]. Industrial researchers have used the term compatible when any two polymers have been mixed in the molten state and form a coherent blend[59]. The criterion applied is usually melt viscosity, tensile strength, and elongation at break, or impact strength.

The problem of mixing polymers at room temperature has normally been solved by the technique of solvent casting. Dilute solutions of the polymers are mixed in a common solvent, and a film is formed by evaporating the solution to dryness. This film can be considered 'single phase' if it is optically homogeneous and transparent, and has a single glass transition (T_g), generally midway between the T_g's of the component polymers.

These techniques have been found to be ambiguous because different solvents give different results, and because the residual solvent may reduce the T_g[60]. If the blend phase separates on heating this problem is more important, because attempts to remove residual solvent by heating under vacuum could cause phase separation, and give spurious results.

Patterson[61] has undertaken an extensive investigation of the effect of solvent on polymer compatibility. This has shown the limitations of the technique of solvent casting due to the interference of the solvent in the interactions between the two component polymers.

Methods for measuring phase diagrams based on T_g measurements are limited by the fact that the normal technique of T_g determination is itself temperature

dependent. Optical criteria for phase separation (cloudiness) are also limited to solvent free mixtures with an adequate refractive index, which sometimes makes them difficult to apply. The problem is therefore to establish tests which are isothermal and can be used to study events such as glass transitions and phase separations.

There are many different methods of determining T_g which have been developed because it is an important property of polymers. T_g measurements may be made using : dielectric relaxation, differential scanning calorimetry (D.S.C.), dilatometry, and dynamic mechanical spectroscopy. Those attempted are discussed in further detail where appropriate. Not all of these yield the same result due to the fact that the T_g value obtained depends on the heating rate of the experiment, the size of the sample and the thermal history of the sample. The glass transition is a pseudo second order transition due to these rate effects[62]. It is not a true thermodynamic transition.

The problems of investigating amorphous polymers are similar to those of other amorphous solids such as inorganic glasses. Techniques such as C^{13} n.m.r. and Wide Angle X-ray Scattering (W.A.X.S.) can determine only short range ordering[62,63].

'Long-range' phenomena can now be determined using pulsed n.m.r., small angle X-ray scattering (S.A.X.S.) and small angle neutron scattering (S.A.N.S.)[63]. These techniques enable some experimental results to be obtained on the nature of a 'single phase' blend. The solution of this problem would assist in resolving the shortcomings of the theories of polymer compatibility.

The main properties which should be controlled for polymer compatibility studies are the purity and the polydispersity of the materials. It is also preferable to prepare samples at ambient temperatures and ensure that they are in thermodynamic equilibrium at these temperatures.

Polymer mixtures were prepared by the following techniques :

(i) Solvent casting

(ii) 'In-situ' polymerisation

(iii) Mechanical mixing

These methods meet the stated criteria to different extents.

3.2 Sample Preparation

3.2.1 Materials

The polymers used were, Breon S/125/12, a suspension polymerised P.V.C. homopolymer supplied by B.P. Chemicals Int. Ltd., and Hypalon 48, a solution chlorinated polyethylene (S.C.P.E.) which contains 42% wt. chlorine and 1% sulfur as sulfonyl chloride groups[5] supplied by Du Pont (U.K.) Ltd.

Vinyl chloride monomer, when used, was supplied by B.P. Chemicals Int. Ltd. at Barry, Wales, and was used in their facilities. Analar grade (B.D.H.) solvents, such as butan-2-one (M.E.K.) were distilled from baked (450°C, 24 hr) type 5A molecular sieves, to remove water prior to use.

The polymers were dissolved in M.E.K. to 5% wt. concentration by warming to 50°C for 2 hours. These solutions were then centrifuged in stainless steel tubes at 10,000 r.p.m. for 2 hours, to remove insoluble impurities. The supernatant liquid was poured into petri dishes and slowly evaporated to dryness. The resultant films were dried in a vacuum oven at 50°C and 10^{-2} torr. for 24 hours. Polymers used to prepare blends by mechanical mixing were used as supplied.

All polymers were analysed by a Gel Permeation Chromatograph (G.P.C.) from Applied Chromatography Systems Ltd.

The polymers were made up as 1% wt. solutions in tetrahydrofuran (T.H.F.) and these were measured on elution by a refractive index analyser. A typical trace of the P.V.C. in T.H.F. is shown in Fig. (3.1).

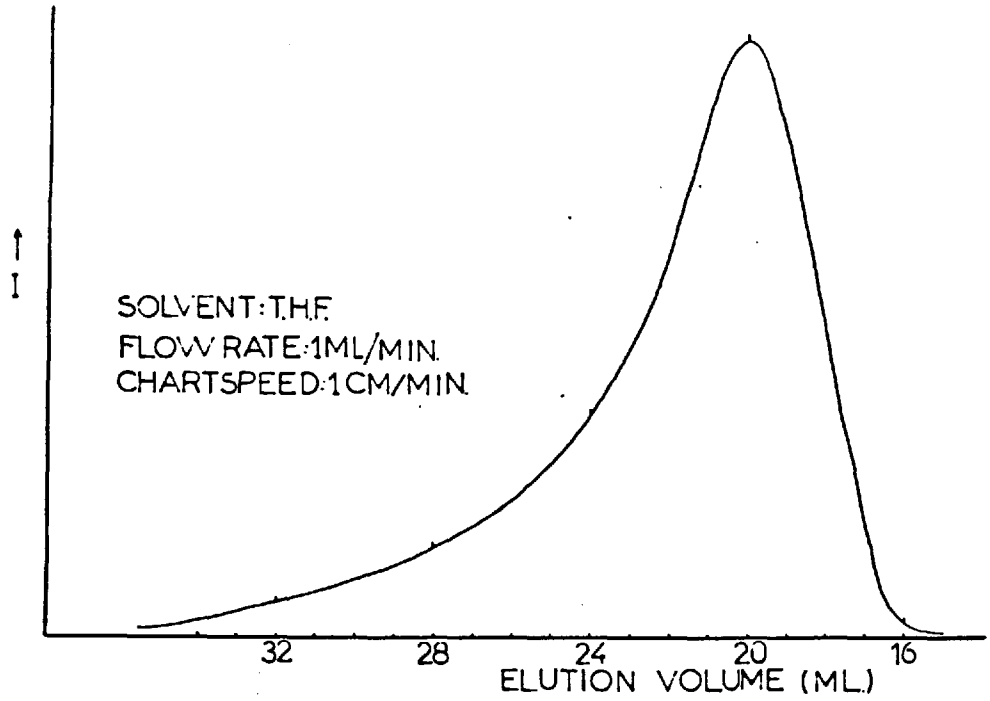

Fig. 3.1 A G.P.C. trace of P.V.C. polymerised by Co^{60} (γ) rays at 40°C

This was analysed to obtain the number average molecular weight $\bar{M}_n$, and the weight average molecular weight $\bar{M}_W$, relative to monodisperse polystyrene (P.S.) samples[64]. The expressions used were :

$$\bar{M}_n = \frac{\sum n_i M_i}{\sum n_i} \qquad 3.1$$

$$\bar{M}_W = \frac{\sum n_i M_i^2}{\sum n_i M_i} \qquad 3.2$$

where : n_i is the number of species i with molecular weight m_i and is measured from the intensity for points at 1 cm intervals. The molecular weight M_i for each point is obtained from a polystyrene calibration curve.

The overall rates of elution of the polymers in the G.P.C. are determined by the dimensions of the polymer coils. Values relative to polystyrene can be corrected by the use of the Mark-Houwink equation provided values of K and α are known for both polymers[65]. The values obtained are listed in Table 1.

Polymer	K value	α value	$\bar{M}_n \times 10^5$ (GPC)	$\bar{M}_N \times 10^5$ Corrected	$\bar{M}_W \times 10^5$ (GPC)	$\bar{M}_W \times 10^5$ Corrected	Polydispersity
P.V.C. (BP)	1.60	0.77	2.0	1.22	4.5	2.7	2.2
S.C.P.E.	N.A.	N.A.	1.4	-	3.1	–	2.3
P.V.C. (Y)	1.60	0.77	1.5	0.9	2.8	1.7	1.8
P.S. standard	1.17	0.725	0·1–10				1.01

Table 1 Molecular weights and polydispersity of polymers

These are high molecular weight polymers which have about the normal polydispersity for a free radical polymerisation.

The cast films were checked for residual solvent, using a Perkin-Elmer (P.E. 457) Infra red Grating Spectrometer. The spectra for films cast from M.E.K. show an absorption at 1712 cm^{-1} which is absent in the pure component polymers. This peak was not removed after heating to 80°C at 10^{-2} torr for one hour, suggesting the solvent is bound to the polymers in the blend. A study was made of the absorption wavelengths of 1% solutions of M.E.K. in a number of environments, and the results are listed in Table 2.

Composition	Absorption	Composition	Absorption
1% in Dichloromethane	1695 cm^{-1}	1% in P.V.C.	1700 cm^{-1}
1% in Chloroform	1720 cm^{-1}	1% in S.C.P.E.	1712 cm^{-1}
1% in Water	1722 cm^{-1}	1 : 1 Blend	1712 cm^{-1}
1% in Cyclohexane	1712 cm^{-1}		

Table 2. A list of I.R. absorption frequencies for the carbonyl group in M.E.K.

These results show the effect of hydrogen bonding on the carbonyl absorption frequency compared with bulk M.E.K. (1715 cm^{-1}). In highly polar molecules such as water and chloroform, the absorption (1720 cm^{-1}) is shifted to higher energies and a similar shift occurs for non-polar cyclohexane (1712 cm^{-1}), possibly due to self-association of the M.E.K. If the protons on the solvent are capable of weak hydrogen bonding such as those on dichloromethane (D.C.M.), the absorption energy is reduced (1695 cm^{-1}). In this context the solvent carbonyl group appears to undergo greater bonding with S.C.P.E. (1712 cm^{-1}) than P.V.C. (1700 cm^{-1}). A solvent such as

D.C.M. would not hydrogen bond to the polymers, but it would not be readily detectable, so M.E.K. was retained as the solvent for film casting.

In order to determine the concentration of residual solvent, two liquid cells were fitted with low density polyethylene (L.D.P.E.) windows, as L.D.P.E. has no strong absorptions in the wavelengths of interest and is insoluble in most solvents. The cells were balanced and a 2% solution of the film in D.C.M. was run against pure D.C.M. as shown in Fig. (3.2).

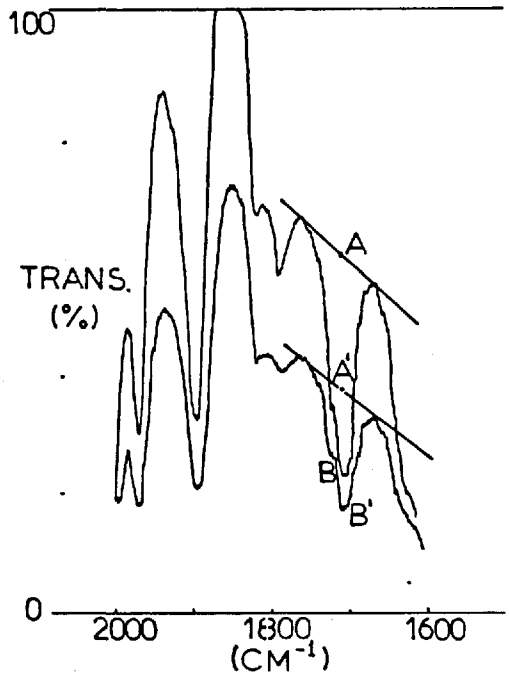

Fig. 3.2 I.R. analysis of residual solvent in cast polymer films

These results were analysed using the Beer-Lambert law according to the method given by Haslam[66]. This result was checked by measuring the weight loss on heating a film to 120°C for 30 minutes. In both cases the answer was 1% w/w approximately.

3.2.2 Solvent Casting and 'In-Situ' Polymerisation

P.V.C. is noted for its resistance to solvents and the normally accepted solvents are M.E.K., T.H.F., 1,1 dichloromethane (D.C.M.) and 1,2 dichloroethane (D.C.E.)[65]. All of these are also solvents for S.C.P.E. Since compatibility is

generally most critical at $\phi_2 = 0.5$, the blends were prepared by dissolving 0.5g of each purified polymer in 50 cc dried and distilled solvent at 50°C. The clear solutions were then mixed and evaporated slowly in petri dishes. The films were then removed and dried as before until constant weight was obtained.

When solvent casting is used as a technique it is necessary to check the temperature of the cloud point for polymer/solvent, to ensure that it is well above the experimental temperature. Apparatus described by Yip[67] was used, and the results in Fig. (3.3) show the cloud points. These are well above the temperatures normally used, so the solutions should not phase separate. It is important to note the decrease of the cloud point with increasing polymer concentration.

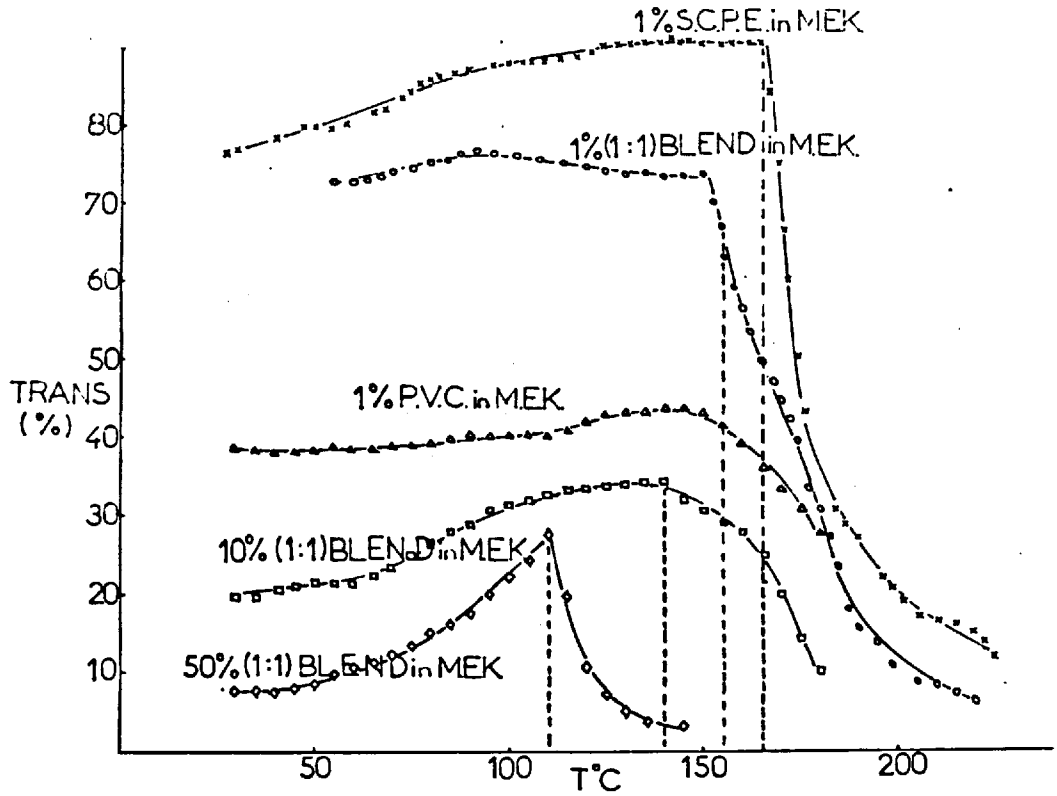

Fig. 3.3 Cloud point curves for polymer solutions of different compositions

Due to the problems encountered with residual solvent detailed in 3.2.1, a new method for preparing solvent free blends was developed. 'Interstitial' blends[68] and 'Interpenetrating Networks'[53] have been prepared by swelling one polymer with the monomer of a second, and polymerising this after equilibrium swelling has been

reached. Vinyl chloride is ideal as a swelling monomer due to its high volatility (b.p.t. - 14°C)[65] which makes residual monomer easy to remove. The polymensation of vinyl chloride is dependent only upon temperature, so the molecular weight and distribution are readily controlled[69].

In order to prepare the required blends, vinylchloride was distilled into the cold finger of the vacuum line shown in Fig. (3.4). This was cooled by dry ice/ methanol (-78°C).

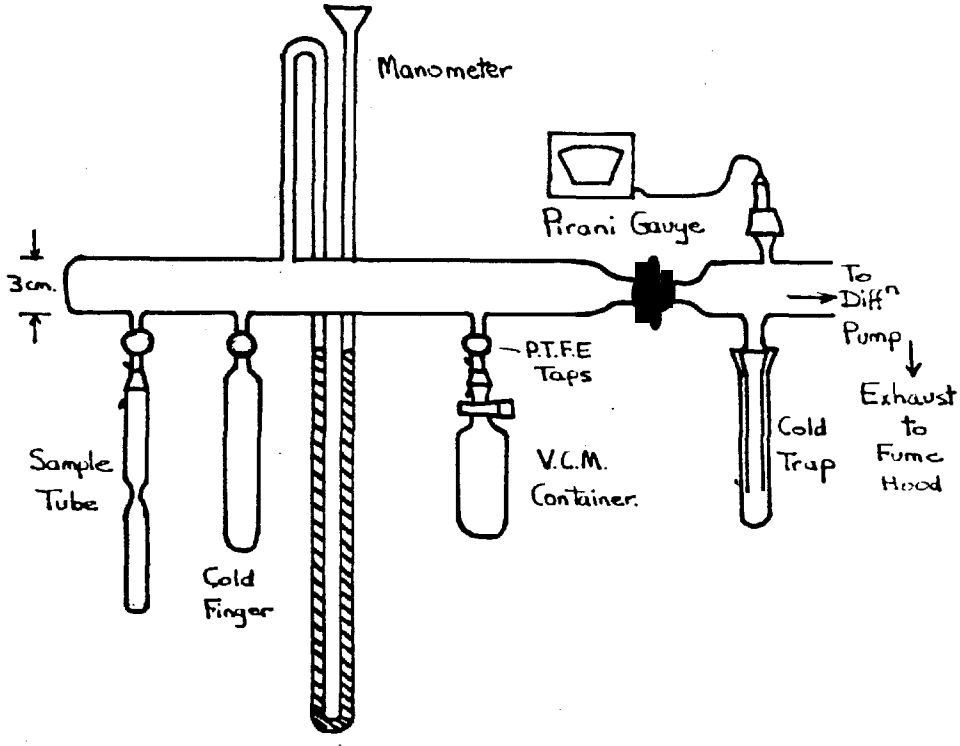

Fig. 3.4

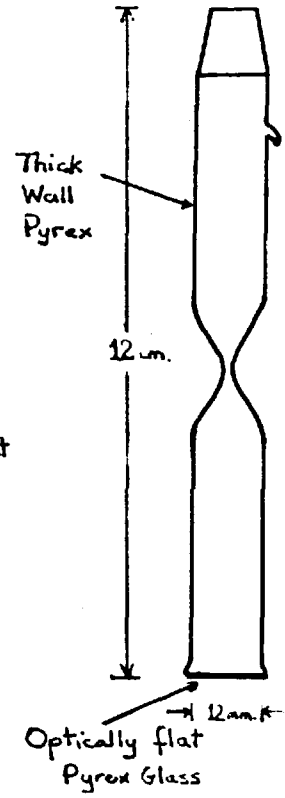

Fig. 3.5

Fig. 3.4 A diagram of the vacuum line for loading ampoules

Fig. 3.5 The reactor tube for the preparation of samples as discs for neutron scattering experiments

The reactor tubes were loaded in advance with the desired quantity of S.C.P.E.

If appropriate, a chemical initiator, (BIS (4-t-butylcyclohexyl) peroxydicarbonate) dissolved in methanol was added as 0.1% wt. of monomer. The tube was then drawn down as shown in Fig. (3.5), and evacuated for one hour. After the tube was dried it was attached to the vacuum line and further degassed until the pressure reached 10^{-3} torr on the Pirani gauge. The line was isolated from the pumps and the vinyl chloride was let in to fill the 3 cm arm at a known pressure. Since the 3 cm arm had been previously calibrated using D.C.M., the quantity of vinyl chloride in the line could be calculated. In this way the desired quantity of monomer could be condensed into the reactor tube by cooling it with the dry ice/methanol. This polymer/monomer mixture was then frozen to - 186°C using liquid nitrogen and evacuated. After thawing the monomer with the tube isolated to remove dissolved gases, the mixture was again frozen to - 186°C and evacuated to 10^{-2} torr. The reactor tube was isolated under vacuum and the lower section removed using an oxygen-gas torch. This ampoule was then allowed to equilibrate for 12 hours at 20°C.

Usually these ampoules were prepared free of chemical initiator and polymerised by ^{60}Co (γ) rays.

The conditions used were 0.1 Mrad hr^{-1} for 5 hours at 40°C, followed by post polymerisation at 60°C for 5 hours. This gave conversions greater than 99% measured by weighing the ampoule before and after fracture.

Samples for neutron scattering experiments for radius of gyration measurements were prepared by similar techniques. Deutero (d^3) vinyl chloride monomer (Merck, Sharpe and Dohme Ltd. of Canada) was polymerised by the same conditions of irradiation as before. This polymer was dissolved in 1,2 dichlonoethane (D.C.E.) to 5% wt/v. concentration. S.C.P.E. films which had been cut into discs of the appropriate dimensions and weights were placed in the reactor tubes. An aliquot

of the solution of d P.V.C. was added to the S.C.P.E., such that the deuterated polymer would be 2% of the total sample weight. This was allowed to equilibrate for 12 hours and then dried under vacuum. The reactor tubes were then constricted as in Fig. 3.5 and connected to the vacuum line for evacuation to 10^{-3} torr. Known quantities of vinyl chloride were then condensed into each tube from the vacuum line as required. The constriction was then sealed under vacuum while the mixture was frozen to - 186°C. All the ampoules were then allowed to equilibrate for 24 hours, after which the mixtures were polymerised as before. The ampoules were then carefully broken and the discs of polymer removed and weighed. Some of these blends were dissolved in T.H.F. and the gel fraction was measured to be 0%.

It was found that the vinyl chloride would only swell S.C.P.E. by ∿ 300% at 20°C. This meant that compositions with more than 75% P.V.C. were made by a two stage process, as shown in Fig. 3.6.

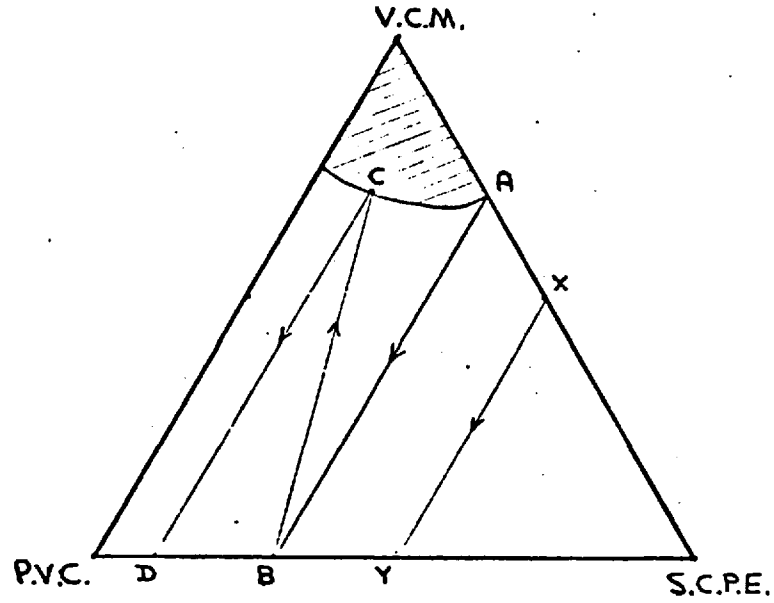

Fig. 3.6 The limit of swelling for vinyl chloride in P.V.C. and S.C.P.E.

The route ABCD indicates the path for a two-stage preparation

The limit of swelling for vinyl chloride in P.V.C. is 250%, even though the polymer is almost totally insoluble in the monomer[69]. In the two stage process, the

result of the polymerisation of S.C.P.E. saturated with monomer (75% P.V.C.) is itself divided and reswollen with monomer. The second polymerisation at 40°C yields a blend with 88% P.V.C.

3.2.3 Mechanical Mixing

This was initially carried out using a Brabender Plastograph 30 c.c. Twin Sigmoidal Rotor Mixing Head, as in Fig. (3.7). Polymer mixtures were prepared in the appropriate ratios with 1% wt calcium stearate as lubricant, and 1% dibutyltin-dilaurate or barium/cadmium carboxylates as stabiliser.

Further work was undertaken using a 2 kg batch Banbury intensive internal mixing. This is similar to Fig. (3.7). Normally, the elastomer was added to the mixer at 120°C, then stabilisers, and the P.V.C. added last. Shear heat resulted in a temperature increase to 180°C in 12 minutes. At this point the mixture was released onto a two roll mill at 175 - 180°C and milled for 10 minutes. In some cases a sample including heterogeneously chlorinated polyethylene (H.C.P.E.), which has a high level of surface chlorination[5] was added for comparison.

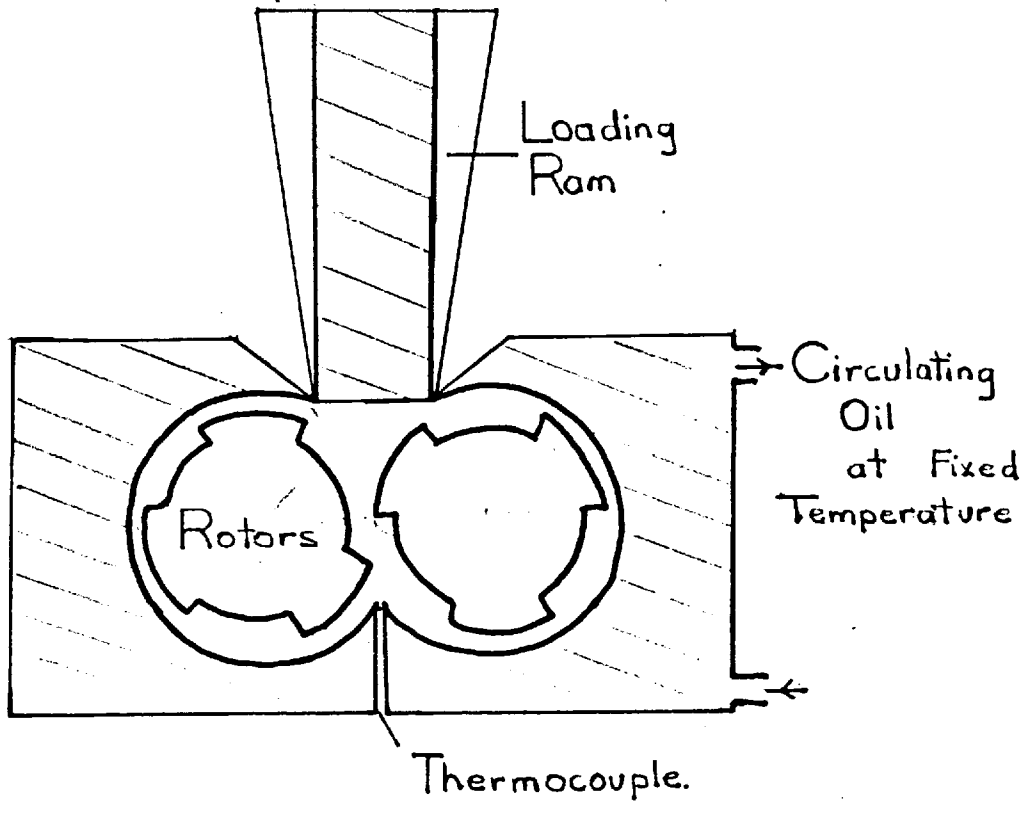

Fig. 3.7 A diagram of a twin rotor internal mixer

3.3 Dynamic Mechanical Spectra

3.3.1 Theory

The viscoelastic properties of polymers such as creep (constant stress) and stress relaxation (constant strain) describe the time-dependent behaviour of the mechanical response of polymers[70]. In order to provide information over a wide range of conditions, it is possible to apply to a sample a sinusoidal strain with a frequency ω in cycles/sec and determine the stress response resulting. Generally, the applied deformation and the resulting stress both vary sinusoidally with time.

Such experiments measure the elastic modulus of the material and its mechanical damping or energy dissipation characteristics. These quantities may be measured as a function of frequency or as a function of temperature. Due to the time-temperature superposition principle, a temperature range of 100° may correspond to several decades of frequencies[71]. Measurements of dynamic mechanical and dielectric properties of polymers are closely analogous. In many experiments using these techniques, the energy dissipation within the material can be measured and interpreted in molecular terms. This subject has been well reviewed[71], and the essential theory is as follows :

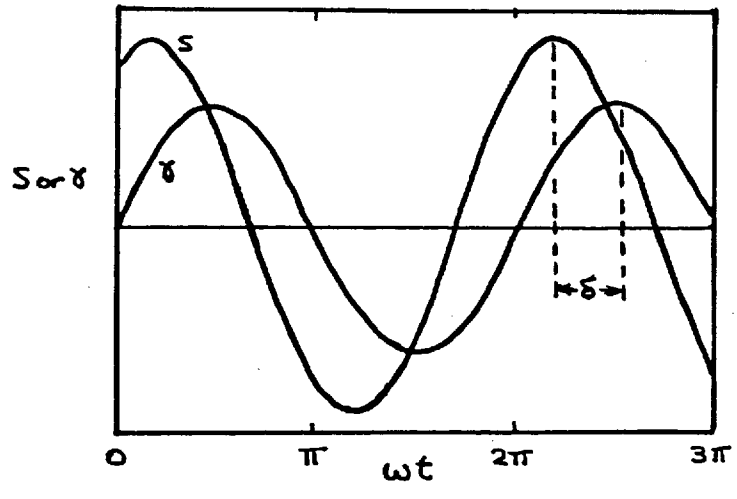

Fig. 3.8 The application of a sinusoidal shear to a viscoelastic specimen

If a sinusoidal elongation is applied to a viscoelastic specimen at a frequency ω and with a small amplitude, the stress also acts sinusoidally, but is out of phase with the strain by a phase angle δ.

This can be described by the equations :

$$\gamma = \gamma_0 \sin wt \qquad 3.3$$

$$s = s_0 \sin (wt + \delta) \qquad 3.4$$

where γ is the strain and γ_0 the peak strain, and s is the stress, and s_0 the peak stress respectively.

The latter can be expanded to give :

$$s = s_0 \sin wt \cos\delta + s_0 \cos wt \sin \delta \qquad 3.5$$

so the peak stress can be resolved into two components; $(s_0 \cos \delta)$ which is in phase with the strain and related to the stored elastic energy, and $(s_0 \sin \delta)$ which is out of phase with the strain, and related to the viscous loss of energy. Two moduli can be defined :

$$E' = \left(\frac{s_0}{\gamma_0}\right) \cos \delta \qquad 3.6$$

$$E'' = \left(\frac{s_0}{\gamma_0}\right) \sin \delta \qquad 3.7$$

where E' is the storage modulus and E" is the loss modulus.

These may also be expressed in the complex form :

$$E^* = E' + iE'' \qquad 3.8$$

where E^* is the complex modulus.

The ratio of the two moduli may also be determined :

$$\frac{E''}{E'} = \frac{\sin \delta}{\cos \delta} = \tan \delta \qquad 3.9$$

where tan δ is the loss factor.

Since the glass transition (T_g) is defined as the temperature which corresponds to the onset of molecular motion, a plot of E', E" or tan δ vs temperature will show this point.

3.3.2 Experimental

There are a number of machines which have been developed to measure T_g, and two typical examples are the Torsion Pendulum and the Rheovibron (Toyo Sangamo Ltd.). The former requires large (100 x 4 x 2 mm) samples of adequate modulus, which can stand freely. It provides very accurate measurements of the Shear Moduli, but due to the poor heat transfer of the sample, is very slow to operate. The latter instrument was designed to overcome these problems and requires only very small samples (20 x 5 x 0.1 mm) and operates over a range of frequencies. The values of tan δ are reliable for low modulus samples, but the machine cannot be used with rigid samples, and the values of the moduli obtained are not reliable.

One other experimental difficulty with the Rheovibron is that it is operated in two modes - one above room temperature, using resistance heating, and one below, using liquid nitrogen cooling. This means it is difficult to sequentially observe the peaks due to different components of a blend.

Samples were annealed prior to testing when appropriate, and each run was made in duplicate.

3.3.3 Results and Analysis

Fig. (3.9) shows an example of the equivalence of using tan δ and Storage or Loss Modulus to determine the T_g. After this the criterion used to determine T_g was the point of onset of the loss peak found by extrapolating values of tan δ . In this respect, Fig. (3.10) has the results for the two component polymers, with examples of the variation of T_g for different degrees of chlorination in S.C.P.E., and with the

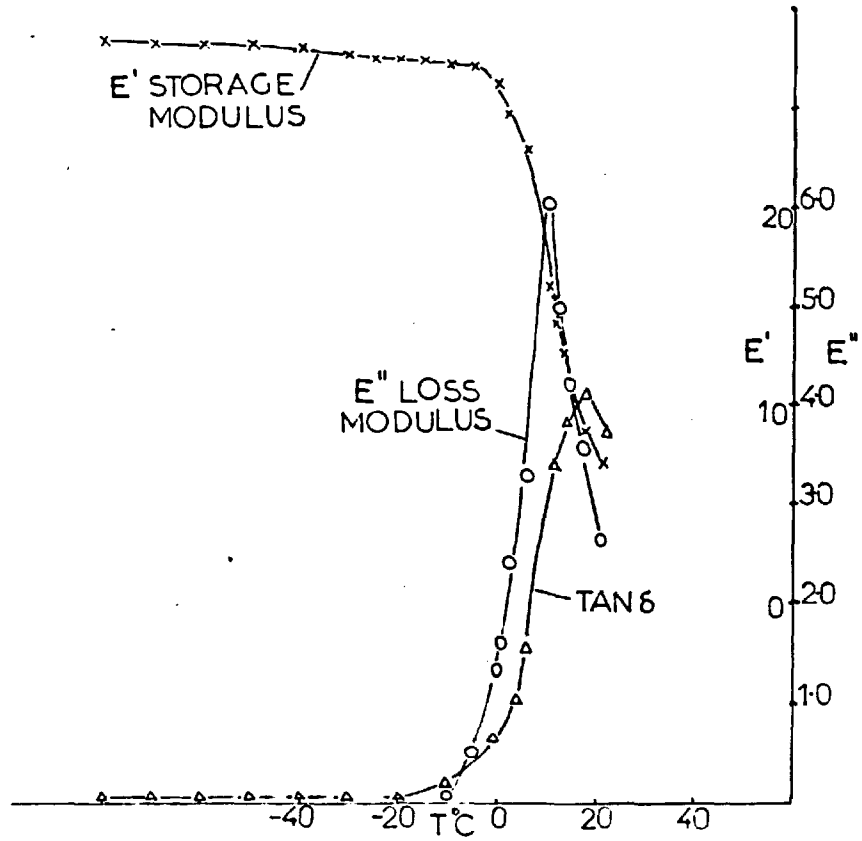

Fig. (3.9) A comparison of the use of loss factor, storage or loss modulus to determine T_g

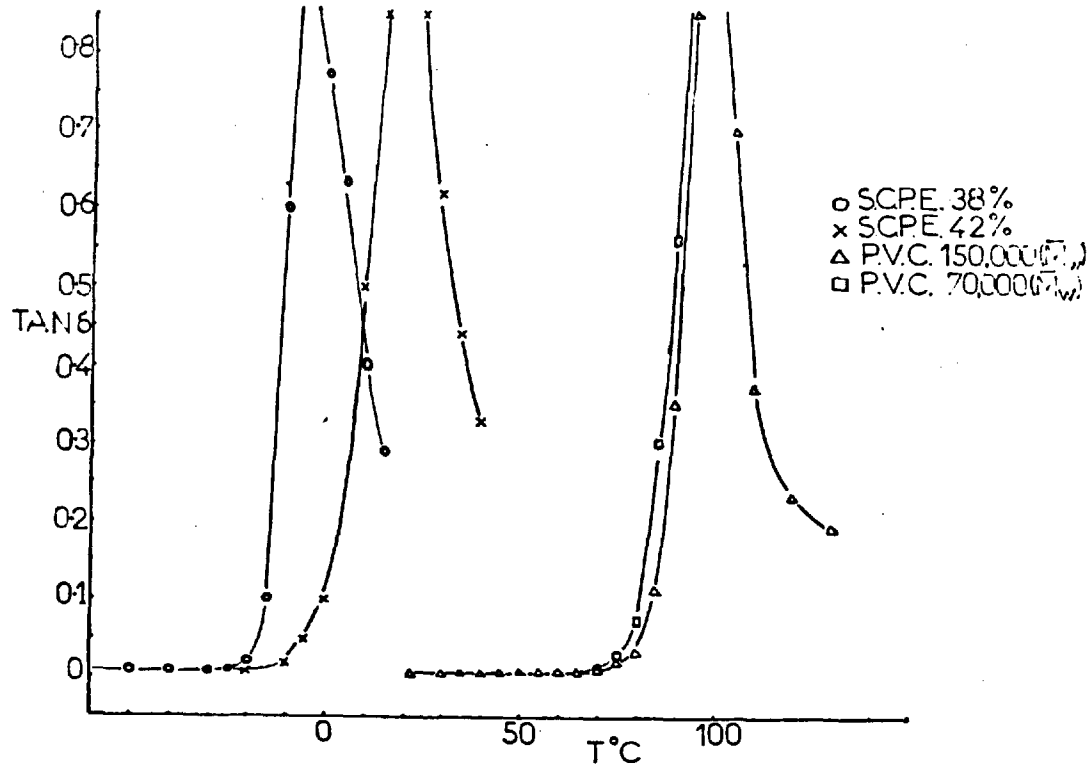

Fig. (3.10) The variation of tan δ with temperature for the component polymers, P.V.C. and S.C.P.E.

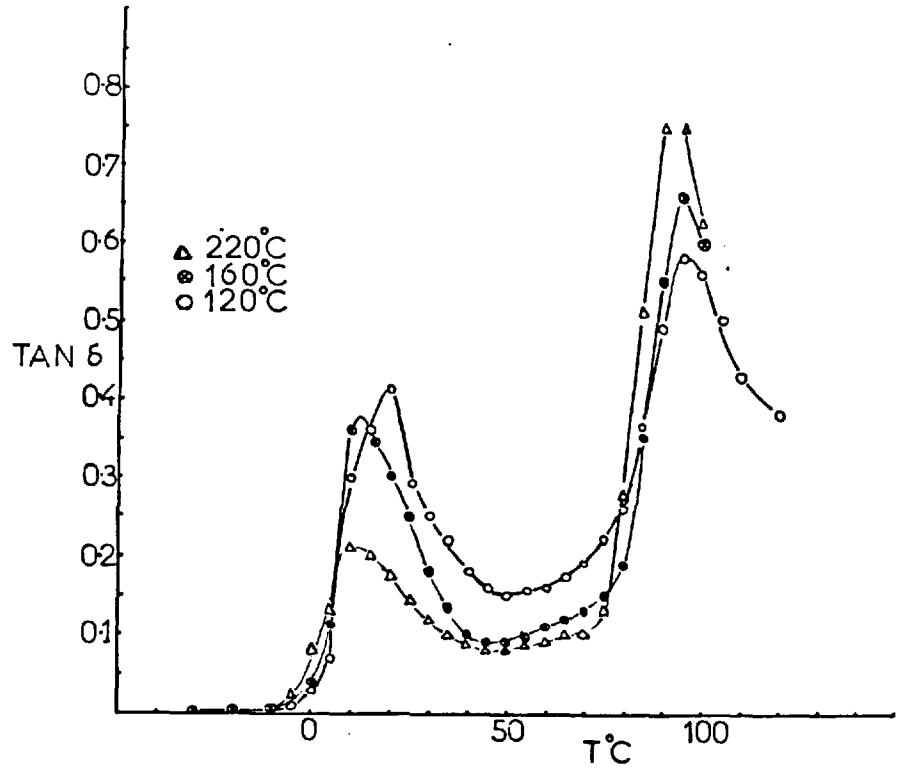

Fig. (3.11) The effect of temperature on the compatibility of mechanically mixed 50% P.V.C. : S.C.P.E. blends

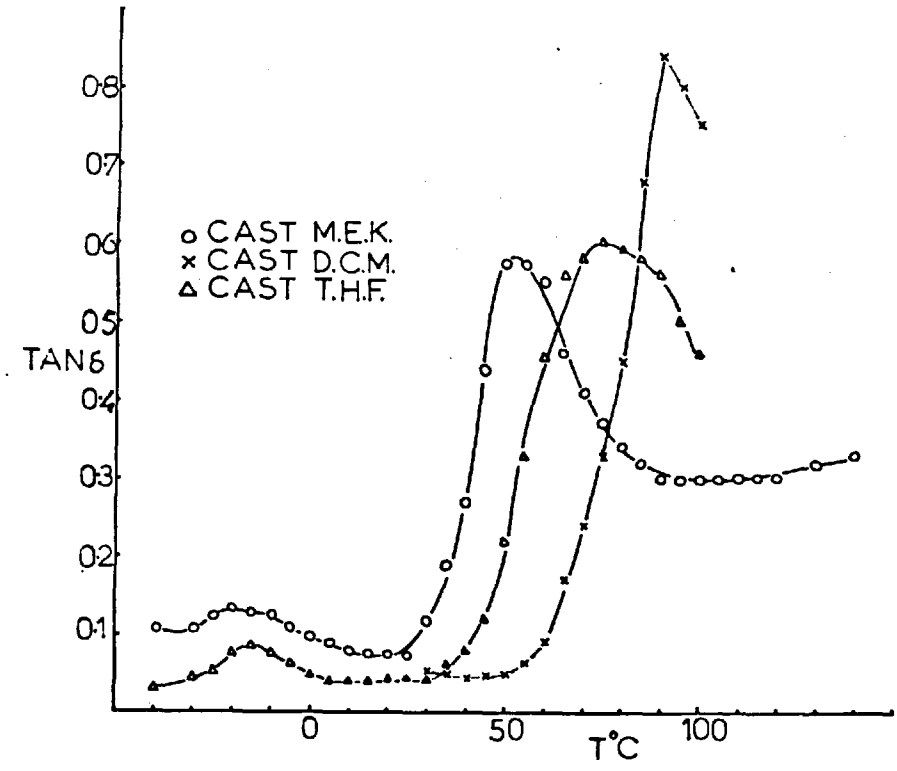

Fig. (3.12) The effect of solvent on the compatibility of 50% P.V.C. : S.C.P.E. solvent cast films as shown by mechanical spectra

degree of polymerisation in P.V.C.

When the two component polymers are shear mixed in the molten state, the T_g values remain approximately as for the two components in a compatible blend, although in Fig. (3.11) there is some change of the two T_g's. This could be interpreted as an indication of partial miscibility. However, the absence of any strong dependence on the temperature of mixing contradicts this. One would expect much greater variations in the T_gs of blends where the compatibility varied with temperature.

However, if two polymers are cast from a common solvent such as M.E.K. at room temperature, as in Fig. (3.12), there is only one T_g at an intermediate temperature between the original T_g's. If D.C.M. is used as the solvent, the result shows incompatibility. It is difficult to conclude definitely that the polymers are compatible because it is not possible to remove residual solvents, such as M.E.K. or T.H.F. without heating. Since these are capable of hydrogen bonding they may reduce the polymer T_g to give spurious results.

This result was confirmed by the behaviour of blends prepared by 'in situ' polymerisation, as shown in Fig. (3.13). The values of T_g obtained from these blends are slightly higher than those in Fig. (3.12), and this could be evidence of the effect of residual solvent. It is evident that the blend separates into two components at higher temperatures, but it is difficult to determine the temperature of phase separation by this method. The samples must be heated to a certain temperature for a set time, cooled to room temperature, and then tested.

This gives ambiguous results, as one cannot assume the structure of the sample at room temperature is the same as that at the temperature of interest. However, this is strong evidence for the existence of a lower critical solution temperature (L.C.S.T.).

Some other compositions were prepared by the melt mixing procedure and showed the normal incompatibility, except 90% P.V.C. : 10% S.C.P.E. The results from this are shown in Fig. (3.14) and these show a slight decrease in T_g. These also show some

Composition	Preparation	T_g °C	Composition	Preparation	T_g °C
S.C.P.E. 42	Pressed 160°C	- 20	50% PVC : SCPE	Cast + 120° 5 min	62
S.C.P.E. 36	Pressed 160°C	- 10	50% PVC : SCPE	Cast + 180° 5 min	78
P.V.C.	Pressed 160°C	82	50% PVC : SCPE	Cast + 220° 5 min	80
50% PVC : SCPE 42	Mixed 120°C	78	50% PVC : SCPE	Cast at 0°	45
50% PVC: SCPE 42	Mixed 160°C	79	50% PVC : SCPE	'In-situ'	42
50% PVC: SCPE 42	Mixed 220°C	79		In-situ + 120°/5 min	46
50% PVC: SCPE 42	Cast 20°C M.E.K.	32		In-situ + 140°/5 min	55
50% PVC: SCPE 42	Cast 20°C Evacuated	35	90% PVC : 10% SCPE	Mixed 160°C	80
50% PVC: SCPE 42	Cast 20° Heat to 80°	65			
50% PVC: SCPE 42	Cast 20, D.C.M.	70			
	Cast 20, T.H.F.	42			

Table 3 A list of T_gs for various blend compositions

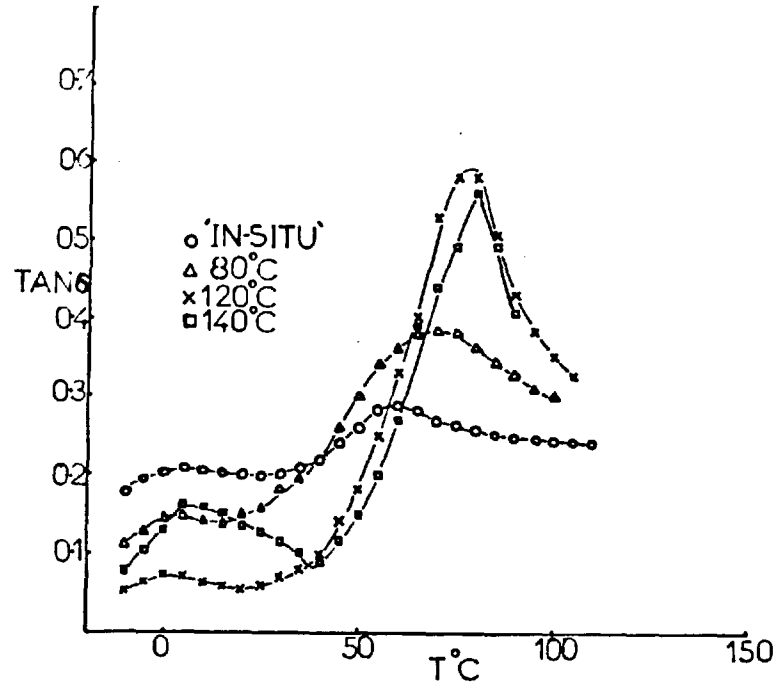

Fig. (3.13) The effect of temperature on 50% P.V.C. : S.C.P.E. mixtures prepared by 'in situ' polymerisation, as shown by mechanical spectra.

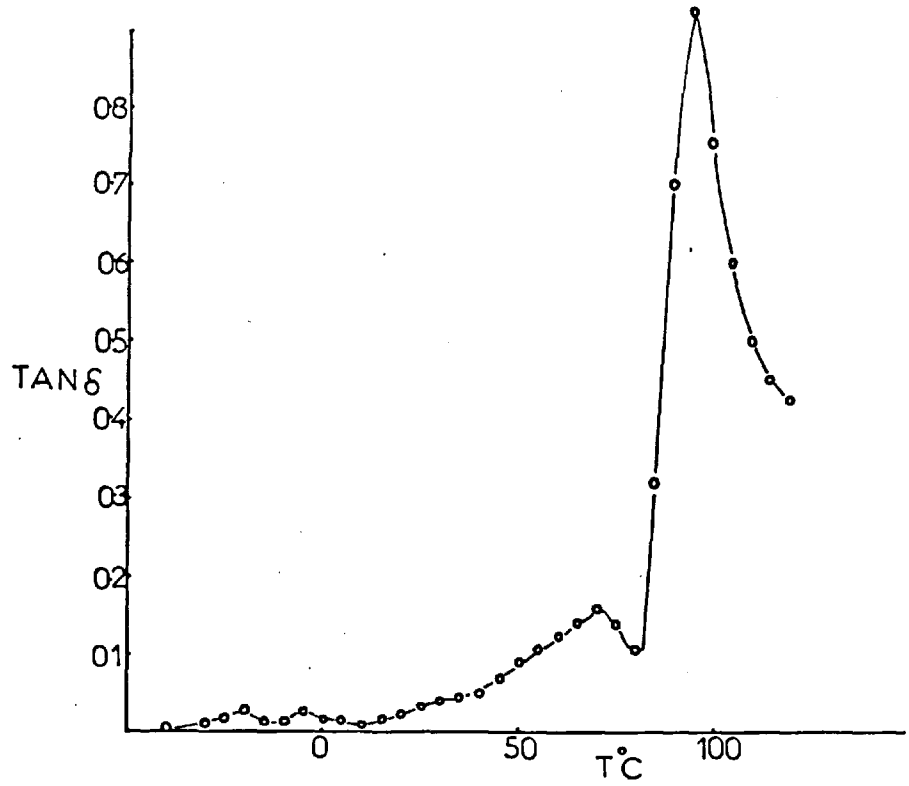

Fig. (3.14) The variation of tan δ with temperature for a 90% P.V.C. : 10% S.C.P.E. sample mechanically mixed at 160°C.

evidence of an intermediate phase. Measurements on this system were repeated several times, and the results confirmed. This is consistent with the L.C.S.T. behaviour, since the phase boundary is at a higher temperature at these compositions.

Extrapolated values of T_g for different compositions and conditions of preparation are listed in Table 3.

3.4 Dielectric Relaxation

3.4.1 Theory

At the glass transition there are pronounced changes in the various electrical properties of polymers which have their origins in the reorientation of the dipole groups on the polymer chain. Examples of two macroscopic parameters which can be used to observe this are the dielectric constant relating to electronic interactions, and the nuclear magnetic longitudinal relaxation time T_1. The former can be studied by measuring the change in the dielectric constant ε' and the dielectric loss ε'' as they pass through a temperature or frequency range, as appropriate. The latter can be measured using a nuclear magnetic resonance (n.m.r.) spectrometer with a thermostatted cavity. However, since T_1 relies on large differences in the chemical environment of the protons of each component, and as the two polymers used here are chemically similar, the technique was not attempted.

Both these techniques have the advantage that they can be used in isothermal studies and provide quantitative data. McCrum , Read and Williams[71] review this subject in detail.

In a similar fashion to 3.31, a complex dielectric constant ε^* may be defined as :

$$\varepsilon^* = \varepsilon' - i\varepsilon'' \qquad 3.10$$

where ε' is the storage dielectric constant, and ε'' the loss dielectric constant

and the loss tangent by :

$$\tan \delta = \frac{\varepsilon''}{\varepsilon'} \qquad 3.11$$

By using a series of bridges with different frequency ranges it is possible to detect slight movements of the broad peaks in the frequency spectrum.

3.4.2 Experimental

The apparatus used was a General Radio 1621 Precision Capacitance Measuring System which incorporates a Radio frequency bridge as shown in Fig. (3.15).

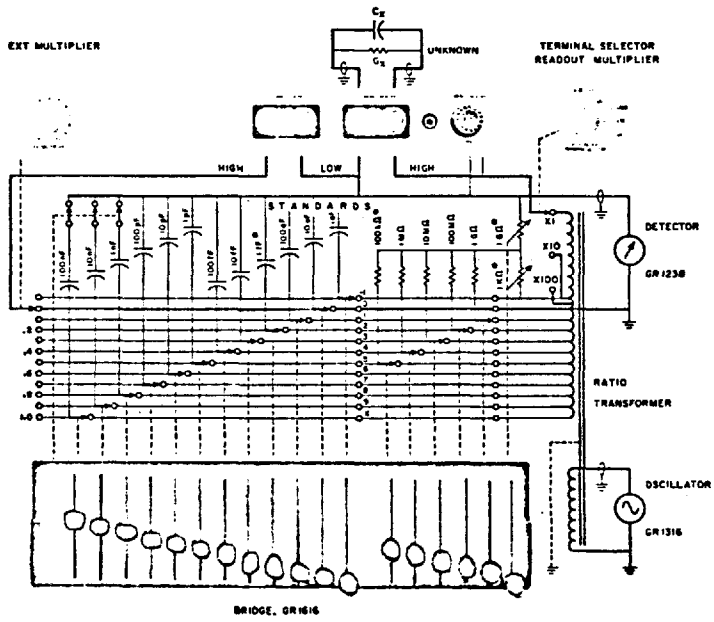

Fig. (3.15) The circuit diagram for a radio frequency bridge

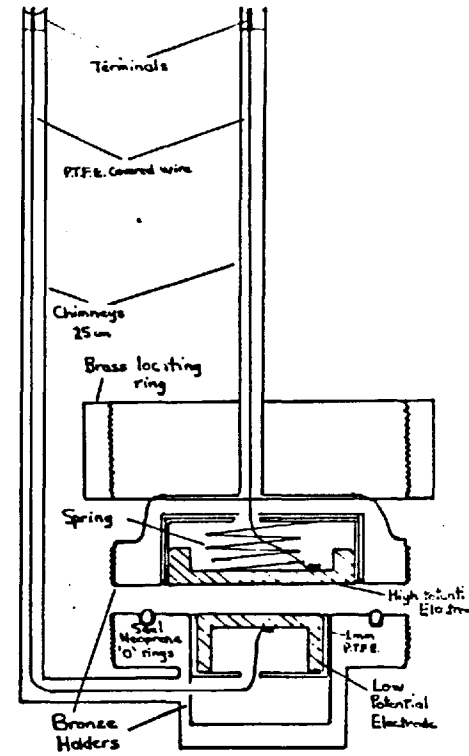

Fig. (3.16) The cell for dielectric studies

The cell drawn schematically in Fig. (3.16) which was designed for isothermal operations was used in conjunction with the bridge. In order to calculate the loss tangent the theory given by McCrum , Read and Williams[63] was used :

$$\varepsilon' = \frac{C_x}{C_0} \qquad \text{and} \qquad \varepsilon'' = \frac{G_x}{\omega C_0} \qquad 3.12$$

where C_x is the capacitance of the sample

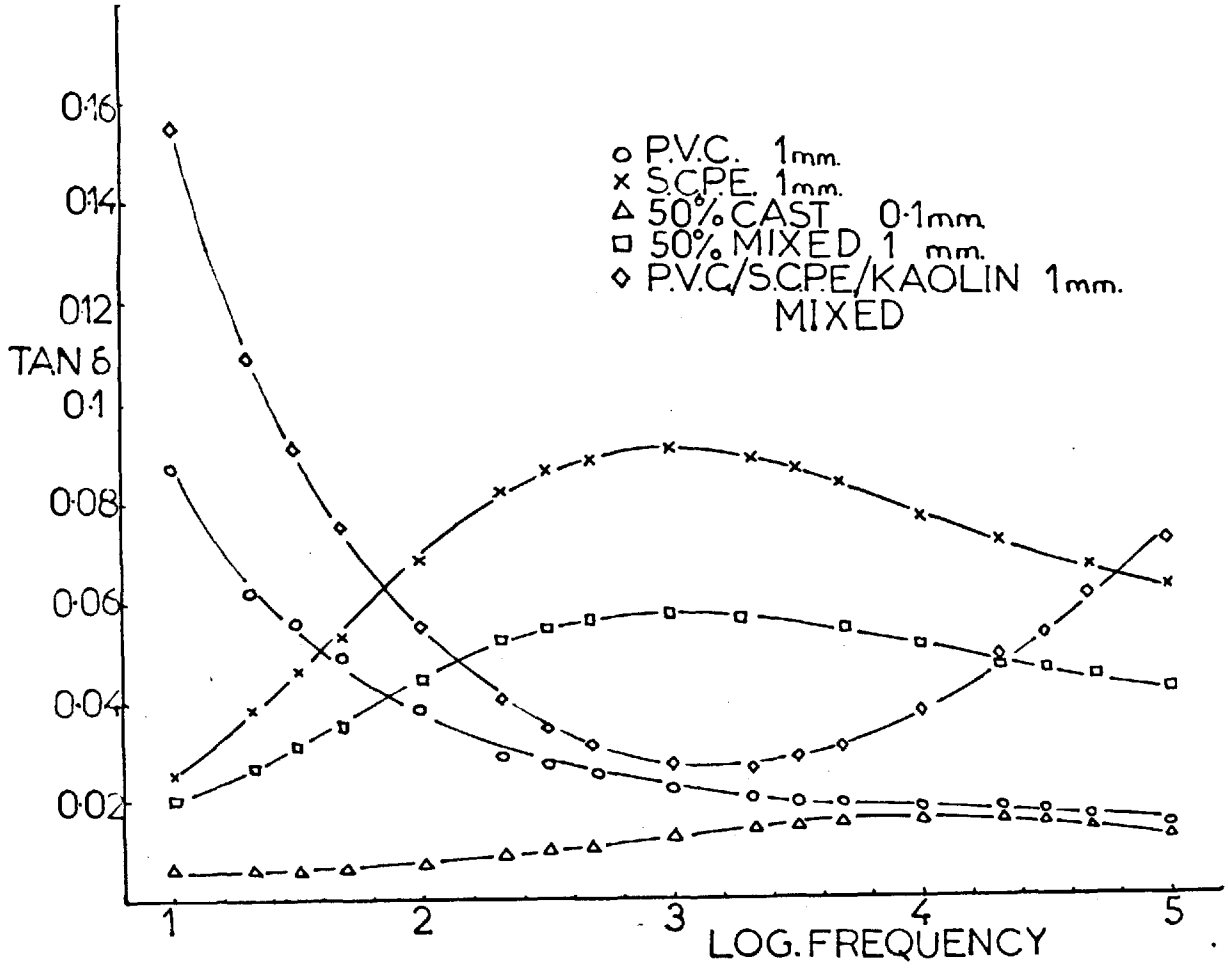

Fig. (3.17) A plot of dielectric loss factor against frequency for various blends

G_x is the conductance of the sample

C_o is the capacitance for air

$\omega = 2\pi\nu$ and ν is the frequency

$$\tan \delta = \frac{\varepsilon''}{\varepsilon'} = \frac{G_x}{\omega C_o} \times \frac{C_o}{C_x} = \frac{G_x}{\omega C_x} \qquad 3.13$$

3.4.3 Results

In order to establish that there is a signal which can be observed over a range of temperatures, the two component polymers were first measured, and then the blend. Results in Fig. (3.17) were made at 20°C and are not normalised to unit thickness. The thicknesses are indicated, and it is evident that the peaks in the time domain are broad and are difficult to interpret. Several more decades of frequencies would be required to observe the entire range of peaks, and these could not be expected to remain observable during a series of experiments at increasing temperatures[72]. Also, the 'single phase' blend does not show a peak at intermediate frequencies to the two components. It appears at higher frequencies corresponding to lower T_g. The 'two-phase' blend exhibits only the peak due to the elastomer. The blend incorporating Kaolin shows the P.V.C. peak and another at higher frequencies. This type of result could be explained by water vapour in the cell causing spurious circumstances, but the exact reason has not been determined. Due to the complexity of these results, the technique would not be suitable for measuring phase separations of blends.

3.5 Microscopy

3.5.1 Interference Phase Contrast Microscopy

Sections from the blends were initially investigated on a normal high magnification microscope (Beck, London), and no structure could be ascertained for either mechanically mixed or solvent cast blends. Some consideration of the optics of micro-

scopes[73] indicates there must be a significant refractive index difference between the two phases for an image to be resolved.

Refractive indices were determined by using a Zeiss Epival Microscope in the shearing mode. Fringes generated in the microscope were displaced due to the optical path difference between the phases. These were measured when the section of each polymer was immersed sequentially in two different reference liquids with widely different refractive indices. The result was then calculated from the theory of Zernike[74]:

$$n_3 = \frac{n_1\Delta_1 - n_2\Delta_2}{\Delta_1 - \Delta_2} \qquad 3.14$$

where n_3 is the refractive index of the polymer,

n_2 is the refractive index of reference liquid z,

n_1 is the refractive index of reference liquid 1,

and Δ_1 and Δ_2 are the number of fringes displaced when the sample was immersed in liquids 1 and 2 respectively.

The result was n = 1.54 for P.V.C. and n = 1.52 for S.C.P.E. with an error of $\pm$ 0.01. This difference is smaller than that required for contrast[75].

The Zeiss Epival microscope may also be used as an interference phase contrast microscope which means phases with similar refractive indices can be resolved. Also, the microscope can be equipped with a specimen heating stage to enable the observation of features as the temperature is changed. The advantage of this technique is that it avoids the possibility of artefacts due to staining, and limits artefacts due to the use of a number of sections heated to different temperatures.

The principle of interference phase contrast is the diffracted and undiffracted beams emitted from the specimen may be recombined by an interferometer to give phase

information. This causes changes in the optical path length due to refractive index difference to be manifested as colour changes.

In this way objects which have a different geometrical path length, such as dust, will have the same colour as their fringe, but will be different in intensity. Features which cause a change in the optical path length will appear as the same colour as an adjacent fringe. This is shown in Fig. (3.18).

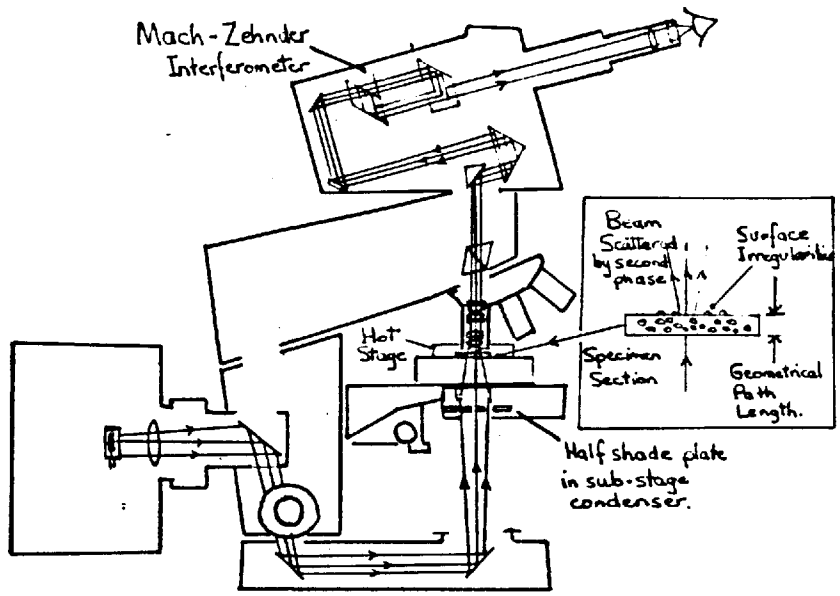

Fig. (3.18) A schematic representation of the Zeiss 'Epival' Microscope

A series of photographs were taken from 20°- 120°C over increments of 10°C after 30 minutes. These are in colour and some are shown in Fig. (3.19). This experiment was repeated for 50% P.V.C. : S.C.P.E. films cast from M.E.K. and 'in-situ' polymerised samples. In both cases the sections showed a distinct change in image at 120°C after exhibiting a steady image at all previous temperatures.

The problem of the limit of resolution of optical microscopes led to the experiment being repeated in the electron microscope.

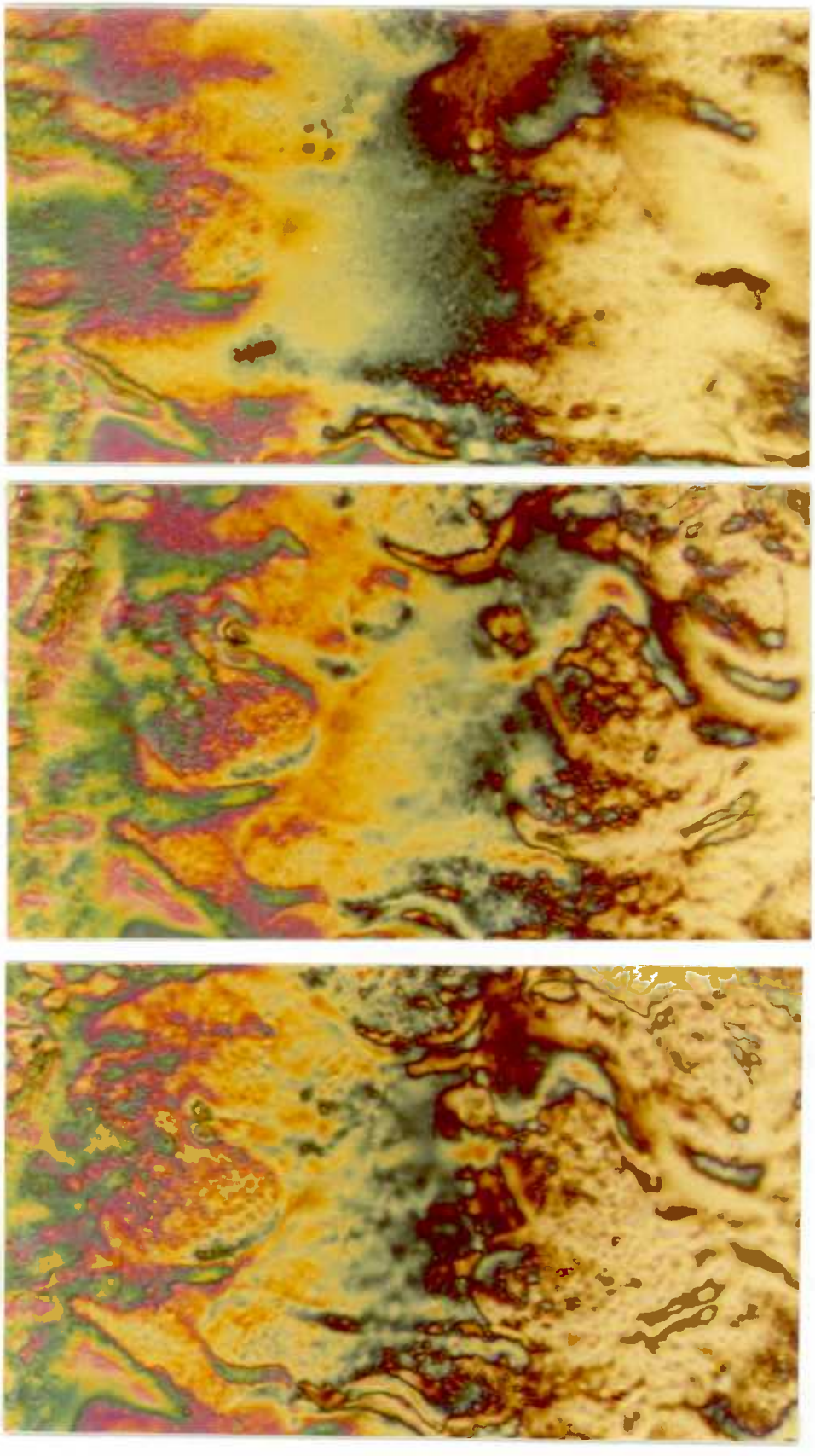

Fig. (3.19) Phase separation observed in the Zeiss. The first photograph of the section at 90°C shows a relatively homogeneous region surrounded by various irregularities. Vertical fringes from the left are yellow to brown. The next photograph at 110°C shows the development of some second colour within the fringes, and the third shows this more strongly.

3.5.2 Specimen Preparation for Electron Microscopy

Kay[76] gives details of the considerations for sample preparation. In this case an Ultramicrotome equipped with a liquid nitrogen cooled cold chamber was used (L.K.B., Sweden). Glass knives were freshly prepared for each section, using the L.K.B. 'Knifemaker'. Samples were clamped and trimmed by hand, using liquid nitrogen to cool if the T_g was below room temperature. The sample temperature was set to 50°C below its T_g, and the knife temperature set to 30°C below the sample T_g. This is the principle of 'Hot Knife through Butter' and means the knife can be used with only a thin film of iso-propanol (M. Pt. - 80°C), so called 'Dry Sectioning'. The sections were made by setting the specimen advance control to 1000Å, which causes the specimen mounting arm to extend by small increments due to resistance heating, and cannot be considered as an accurate guide for thickness. However, this gave regular sequences of sections which had adequate transmission, provided the specimen was well aligned.

Sections retained in the viscous iso-propanol could be recovered either by capilliary rise on a copper grid, or by washing with distilled water into a Petri dish and floating onto the grid. The grids were dried in an air stream prior to insertion in the sample chamber of the electron microscope.

Some experiments with gold decoration were made using an Edwards Evaporator, where the gold is evaporated from a boat upward to the specimen to prevent large particles being deposited. The same machine was used to make carbon supports on the grids by direct evaporation. These carbon films were too brittle to be used routinely.

3.5.3 Transmission Electron Microscopy

The limitation of optical microscopy is set by the resolving power of the objective lens and the wavelength of light. A change in the wavelength from $\sim$ 5000Å to $\sim$ 0.04Å, from visible light to an electron beam, indicates resolution of atomic dimensions as

possible. However, contrast in the electron microscope image arises primarily from differential loss of electrons by scattering at object-details of varying elementary composition or thickness[77]. A small aperture in the objective admits the central part of the electron beam that has passed through the specimen, but traps all electrons that have suffered a deviation greater than the critical angle for optimum resolution determined by spherical aberration and wavelength. Such a contrast aperture will admit a large proportion of the inelastically scattered electrons, but stop most scattered ones at higher angles.

For elements of high atomic number, such as gold, the elastic scattering cross section is greater than inelastic. Since the critical thickness for elastic scattering is small, a thin layer of heavy metal will scatter efficiently and give high contrast images. Carbon, however, has a smaller elastic scattering cross-section than inelastic, so that contrast due to elastic scattering will be small. This means that very thin $<1000\,\text{Å}$ sections will show poor contrast whilst thicker will show poor resolution.

The best way to overcome this problem is to use an objective aperture of smaller diameter than the critical value by trapping more of the inelastically scattered electrons. Contrast may also be improved by the use of lenses to screen the inelastic electrons, or by using lower voltages to increase the proportion of elastic scattering. Complete assessment of the above facts leads to the rule that resolution is limited to one tenth of the thickness of the specimen, such as 100Å from 1000Å.

Electron microscopes are certainly limited by the sample preparation and properties, but they do give increased information on the microstructure of solids.

A Japan Electron Optics Laboratories J.E.M. 100 B, 100 kV Transmission Electron Microscope (T.E.M.) of guaranteed resolution (3.5Å) was used to investigate the structure of the polymers. A simpler T.E.M. from the same company, the JEM7, equipped with a resistance heating specimen stage, was used to check the phase

separation seen on the optical microscope.

The details of a modern T.E.M are given in Kay[76]. Principal considerations for their use are the preparation of the specimen, the determination of the scattering contrast, and the assessment of changes due to irradiation.

It is well known that polymers may undergo cission or crosslinking reactions during irradiation by an electron beam[78]. Both polymers used are of the type which should undergo crosslinking[79], but in all cases beam exposure was kept to a minimum and samples repeated to vary the time before recording the image. These images were recorded on archive grade Silver Iodide photographic glass plates, and enlarged on a Durst enlarger.

Images formed in the T.E.M. have their origin in the electron scattering contrast of the specimen. This is measured by the electron density or concentration of atoms with similar atomic numbers[80]. Two polymers with approximately 57% wt. and 42% wt. chlorine might not be expected to show adequate contrast, so a known two phase 50% wt. mechanical mixture was sectioned and decorated with $\sim$ 10 Å gold to enhance contrast, as in Fig. (3.20). There is a possibility that the section can relax after preparation below T_g, and this may give an uneven surface as the elastomer contracts on warming. Such a topographical phenomenon would explain why the gold decoration corresponds to the interstitial region between the spheres which one would expect to be the more electron rich P.V.C. and hence darker. (This is confirmed by later surface studies). In fact, the same sample mixed at a different temperature gave the image in Fig. (3.21) without decoration, confirming the Au decoration was topographical and that scattering contrast was adequate without treatment in this case.

The other important result from these micrographs is the change in size distribution of the P.V.C. particles from 1 - 5μ in the 50/50 mixture sample mechanically mixed at 120°C, as shown in Fig. (3.20) to 0.1 - 1μ in the sample mixed at 160°C, as shown in

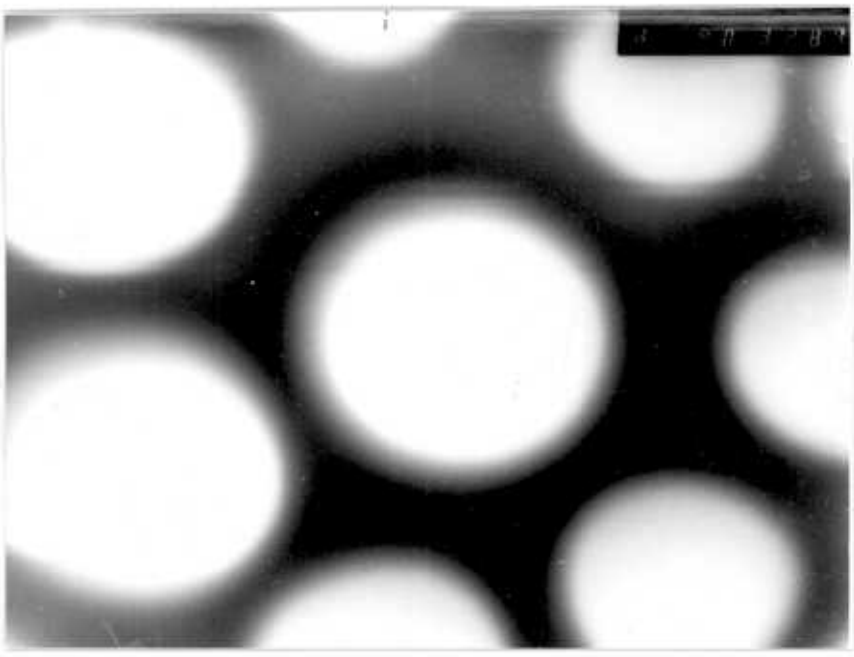

Fig. (3.20) An electron micrograph of a gold decorated section from a 50% P.V.C. : 50% SCPE blend mechanically mixed at 120°C. This shows the distinct two phase structure.

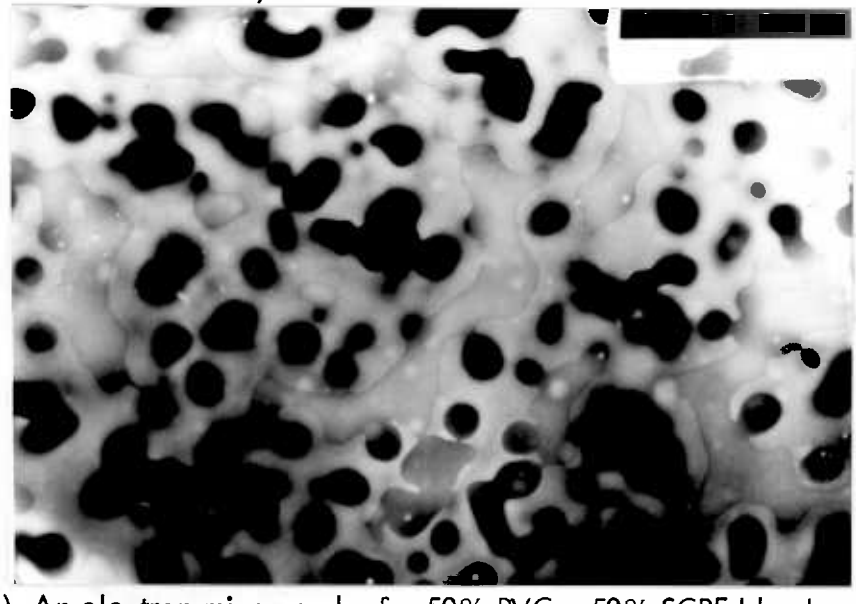

Fig. (3.21) An electron micrograph of a 50% PVC : 50% SCPE blend mechanically mixed at 160°C. The darker particles have been shown to be PVC and are smaller than those in Fig. (3.20)

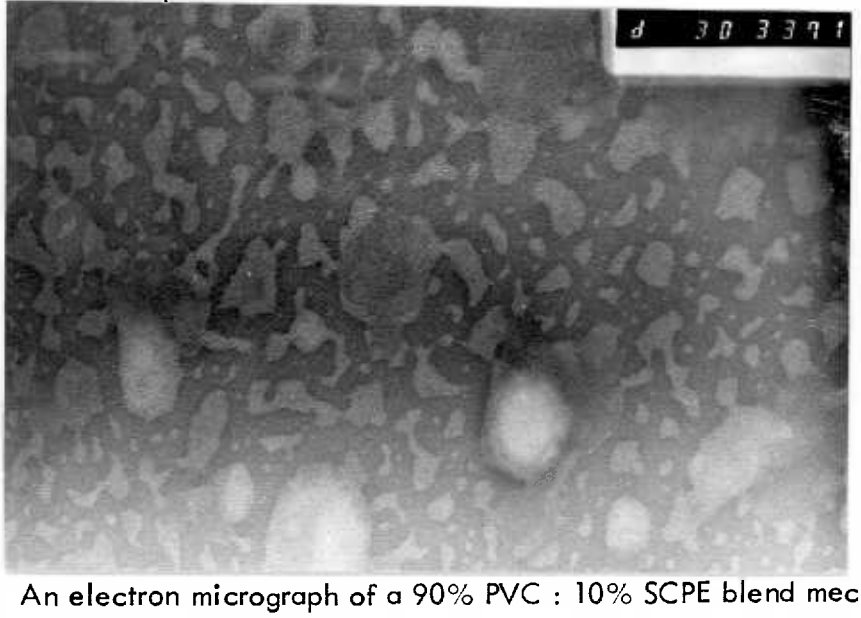

Fig. (3.22) An electron micrograph of a 90% PVC : 10% SCPE blend mechanically mixed at 160°C. This shows a highly dispersed structure with features at ~100Å and ~ 500Å. It is not understood why the 100Å features can occur in the 500Å.

Fig. (3.21). This shows the effect of temperature in dispersing the original P.V.C. resin particles, which are initially 20 - 100μ in size[81].

Since high resolution T.E.M. has some unresolved problems due to focussing and astigmatism[82], and since one object of this investigation was to ascertain the structure of the 'single T_g' blends, recourse to staining or decoration would destroy more information than was gained. Unfortunately, this limited the specimens to low thicknesses as the minimum objective lens aperture was necessary to obtain contrast. Irradiation was kept to a minimum for these thin sections.

Using the 'natural contrast', blends containing 75% and 25% P.V.C. showed similar features to the 50% blend, but at 10% S.C.P.E. the features were different, as shown in Fig. (3.22). One observes a dispersed two-phase structure with two levels of heterogeneity. Since this blend contained a tin stabiliser it is difficult to assign the two phases to either polymer. The general features are those of an interconnected dark network with quasi-spherical inclusions of the order of 200 - 2000Å, and an underlying structure of < 100Å, which suggests some compatibility.

Fig. (3.23) is a micrograph of a 'single-phase' 50% P.V.C., 50% S.C.P.E. film cast from M.E.K. and decorated with $\sim$ 10 Å of gold. The filamentous structures observed are less than 0.1 μm in size, and it is difficult to consider these similarly to Fig. (3.20). The basic gold particles produced by this technique are given by Kay as 10 - 20 Å diameter.

An example of the images which can be obtained from untreated different films cast on glass are shown in Fig. (3.24). The contrast gives details which would be obscured by decoration. The features are of diffuse particles of $\sim$ 0.1 μ together with the same type of fine-structure observed in Fig. (3.22). This would explain Fig. (3.23) if the decoration was condensing on the phase boundaries. A high magnification photo-

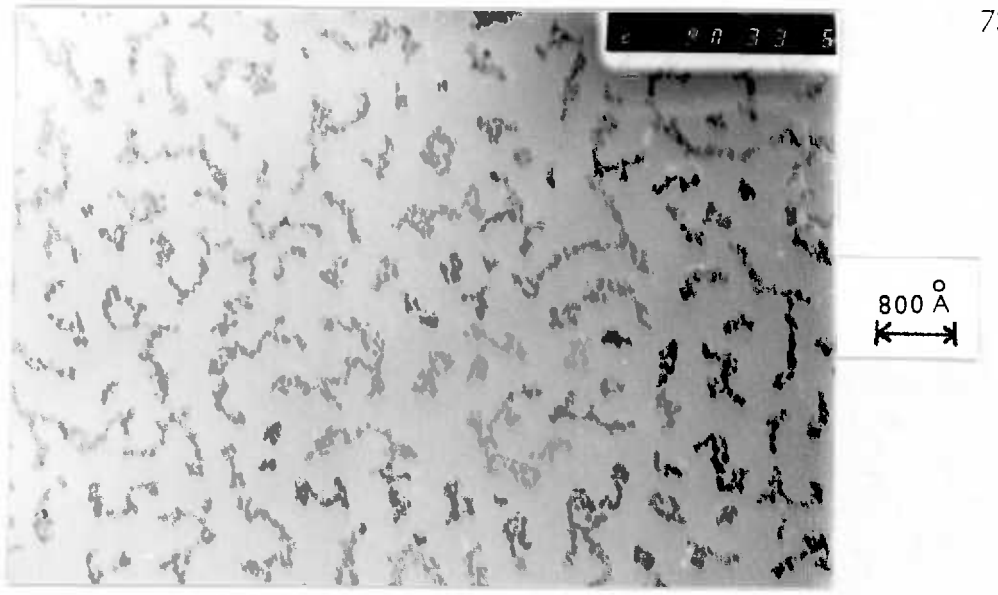

Fig. (3.23) A high resolution micrograph of a section of 'single phase' 50% PVC : 50% SCPE cast from M.E.K. Decorated with ~ 10 Å gold.

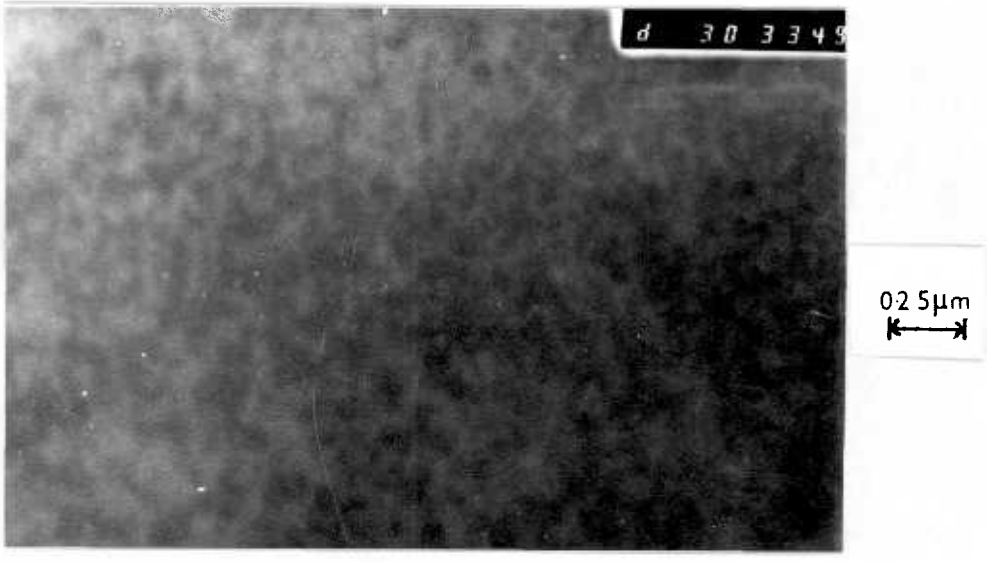

Fig. (3.24) An electron micrograph of a section of 'single phase' 50% PVC : 50% SCPE cast from M.E.K. The contrast features explain how the gold decoration features were formed.

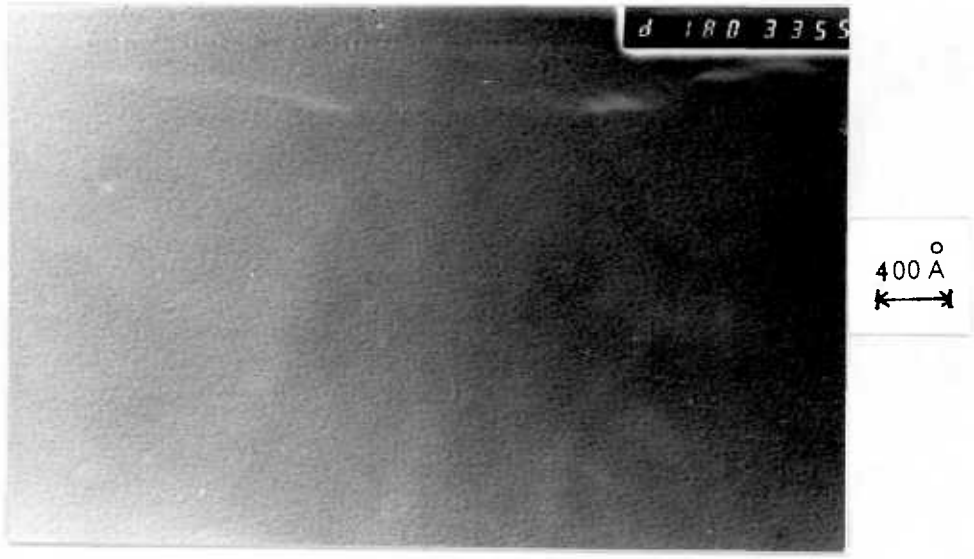

Fig. (3.25) A high resolution micrograph of the fine structure in Fig. (3.24). There appears to be contrast between regions ~ 50 Å apart, but it is not possible to check the focussing of this micrograph.

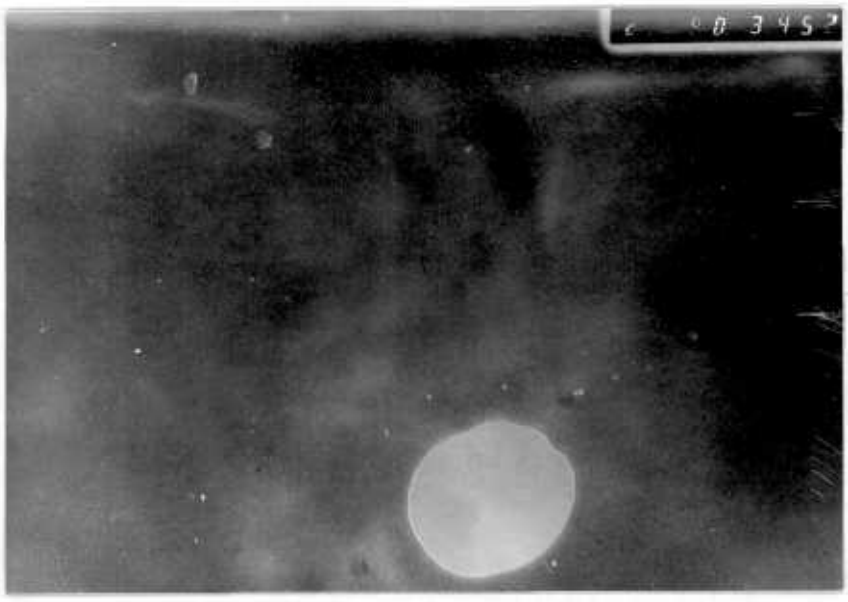

Fig. (3.26) A high resolution electron micrograph of the fine structure in Fig. (3.24) using the hole to check focus by Fresnel fringes.

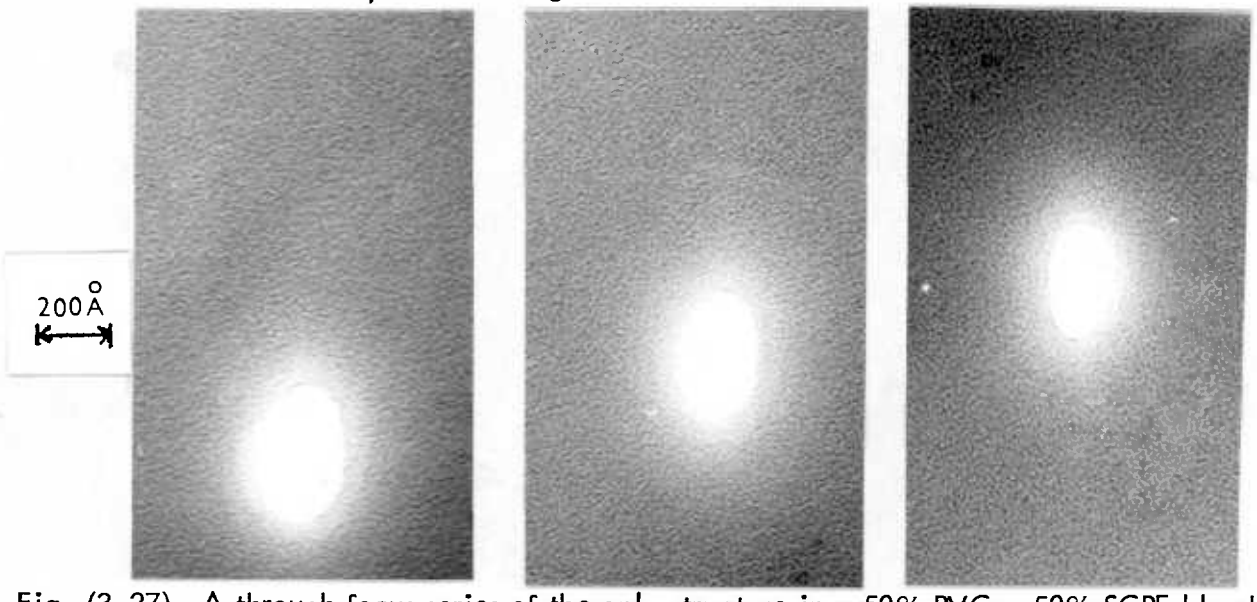

Fig. (3.27) A through focus series of the only structure in a 50% PVC : 50% SCPE blend prepared by 'in-situ' polymerisation. The hole was used to check for astigmatism by the appearance of asymmetric Fresnel fringes.

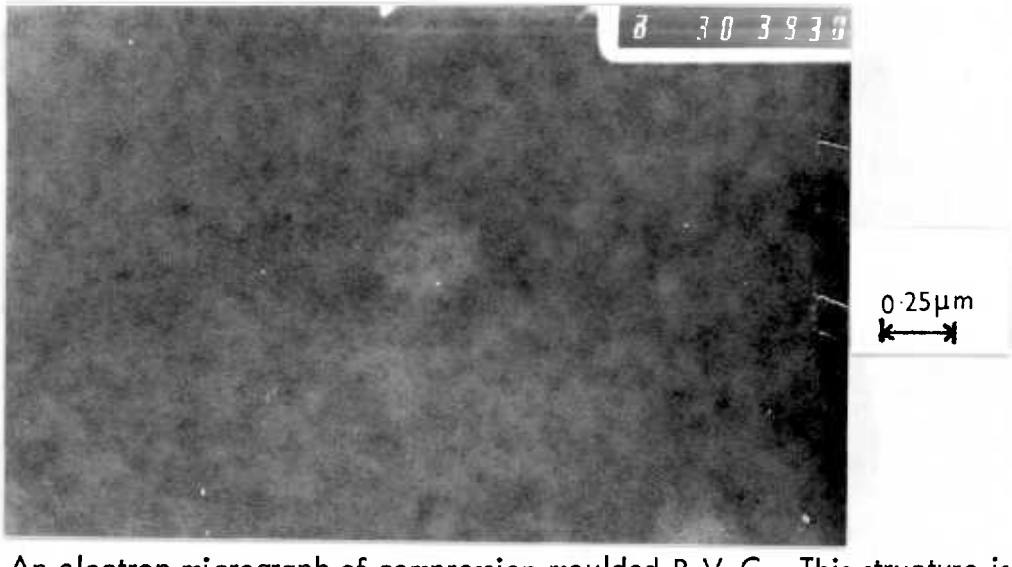

Fig. (3.28). An electron micrograph of compression moulded P.V.C. This structure is very similar to that from solution cast films. Fig. (3.24)

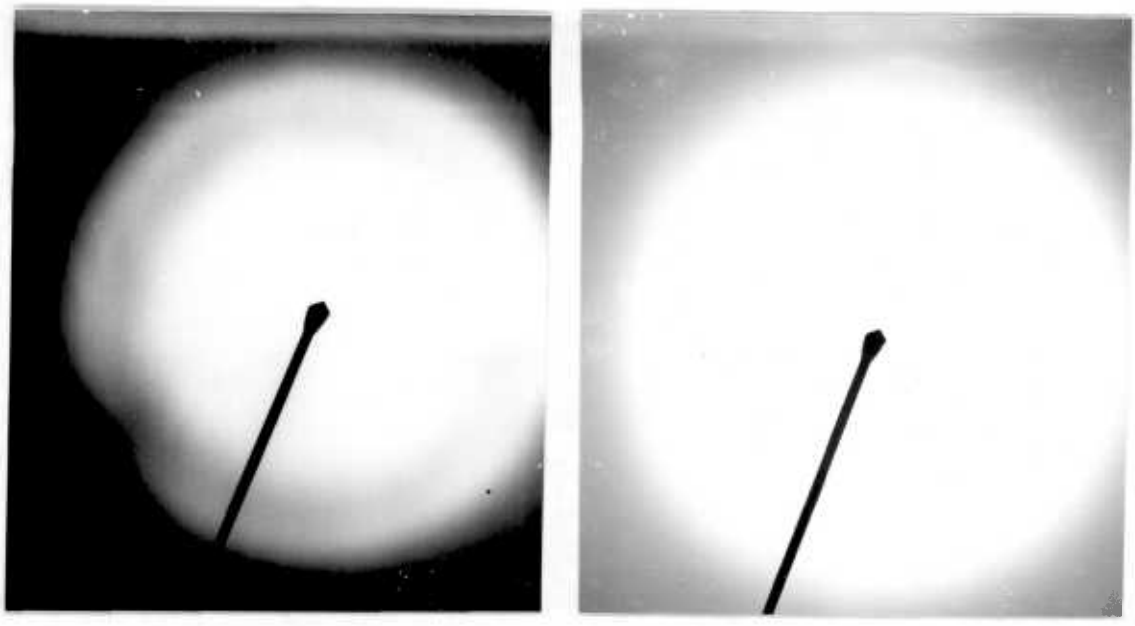

Fig. (3.29) Electron diffraction photographs of P.V.C. and S.C.P.E. These show only the diffuse halo characteristic of amorphous solids.

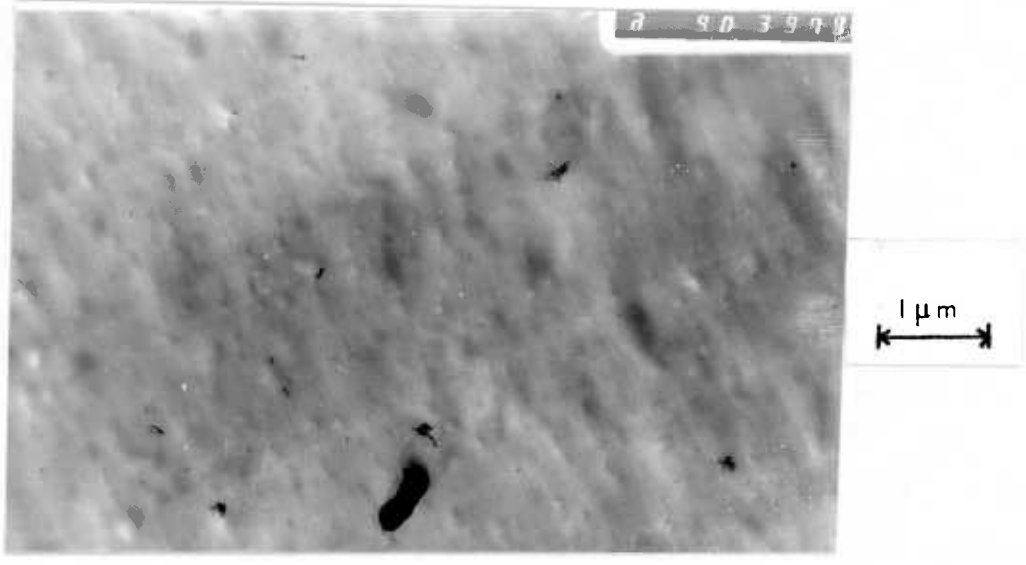

Fig. (3.30) An electron micrograph of a 90% P.V.C. : 10% S.C.P.E. blend mechanically mixed on a large scale (2 kg) at 180°C. This differs from Fig. (3.22).

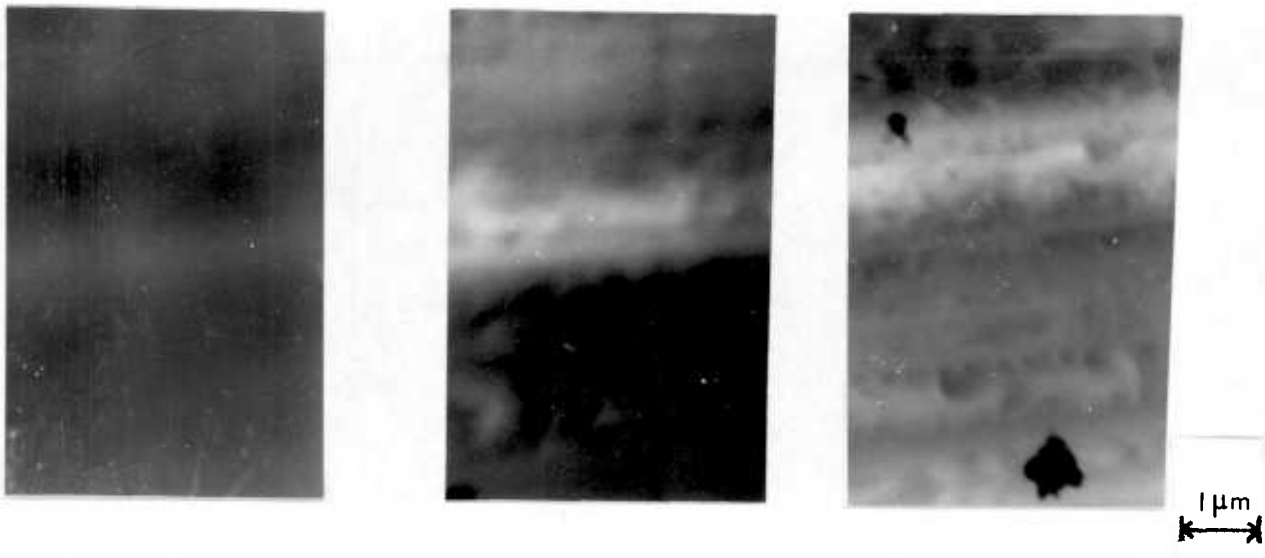

Fig. (3.31) Phase separation of a 50% P.V.C. : 50% S.C.P.E. blend prepared by 'in-situ' polymerisation. The straight features running left to right are knife marks. The dark diffuse features developed slowly at 120°C ± 5°C.

graph of this structure was taken (Fig. 3.25), but it becomes very difficult to determine the position of focus at high magnification. From Figs. (3.23) and (3.24) it is obvious that the specimen morphology is dependent on film preparation. The technique of 'in-situ' polymerisation should produce specimens reproducibly and free from artefacts. It is possible to 'foam' the samples by breaking the ampoules at 90% conversion, so the decrease in pressure causes the formation of many bubbles which are useful in focussing. Micrographs in Fig. (3.26) show this feature and the reproducible 'single-phase' fine-structure. There is a contrast of ~50 Å, but the rule of Coslett[77] states the resolution is only one tenth of the specimen thickness. So the thickness must be controlled.

The fine structure in 'single phase' blends was investigated more rigorously, using a 1000 Å thick specimen from a sample, which was 'foamed' by rapid degassing of the residual monomer, then sectioned. After thorough alignment and checking of the JEM 100B, a through focus series was taken over the area surrounding the hole, so that focus and astigmatism could be checked. These are shown in Fig. (3.27), where it is evident that there is contrast between regions approximately 50 Å apart.

Since the blends show fine structure it is necessary to consider the microstructure of P.V.C. itself. Fig. (3.28) is a micrograph of compression moulded P.V.C. which shows both diffuse particles of approximately 500 Å 'diameter' and fine structure below 100 Å. The structure of P.V.C. has been investigated in some detail[81], and the diffuse particles could be associated with the so-called 'Primary Particles' of P.V.C.. Fine structure of the order of 100Å could be an artefact of the machine, according to the results of Uhlman et al[83] or could have its origins in the scattering contrast mechanism relating to the electron density, i.e. molecular distribution. High dispersion diffraction experiments which would detect any Bragg peaks due to an ordered morphology revealed only the normal diffuse halos for both component polymers in Fig. (3.29).

The blends which were prepared on a larger scale in the Banbury/2 roll-mill system were also photographed and the results in Fig. (3.30) are consistent with those of Figs. (3.21) but not (3.22) from the Brabender blends.

The phase separation experiment using the Zeiss Interphako Optical Microscope was repeated using the JEM 7B T.E.M. For this experiment the magnification was set at x 10,000, using the minimum objective aperture, and the specimen stage temperature was monitored by a Fe-Cr thermocouple attached to a digital voltmeter. At 10°C intervals after ten minutes the section was imaged by the electron beam, and a photograph recorded. Results shown in Fig. (3.31) contain the development of contrast independent of the knife marks present, at 120°C. The final diffuse and discontinuous structure has dimensions of approximately 1 μm, which is significant when one considers the rate of diffusion of polymers[1].

3.5.4 Scanning/Analytical Electron Microscopy

Transmission Electron Microscopes (T.E.M.) have attained very high resolutions, however they are often unable to resolve anomalous and ambiguous results. New complex microscopes such as the JEM 100C have been developed, which can image the transmitted electrons in normal transmission (T.E.M.) or in scanning transmission (S.T.E.M.). These can also image the secondary emitted electrons from inelastic scattering at the surface of the specimen by scanning (S.E.M.), and can image or analyse the X-ray signal which may also come from inelastic scattering.

There is a limit to the resolution possible with this technique which is determined by the minimum spot size of the scanning beam which theoretically may be 30Å, but for many practical reasons is usually limited to 100Å.

Initially the mechanically mixed blends of Figs. (3.20) and (3.21) were investigated. Fig. (3.32) is an area analysis of the specimen by X-ray energy dispersion (E.D.A.X.) where the X-rays are separated by a solid state detector that produces a

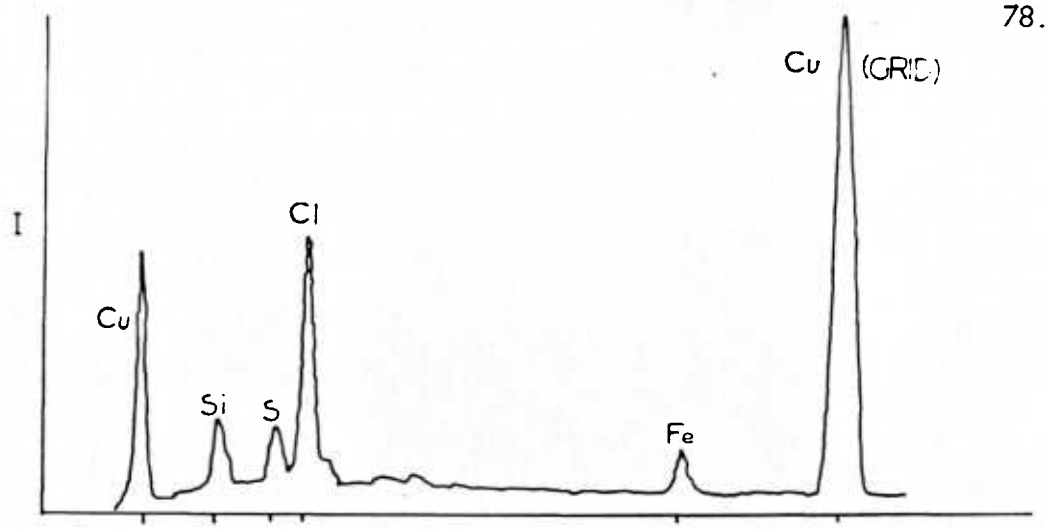

Fig. (3.32) Area analysis of a 50% P.V.C. : 50% S.C.P.E. blend mechanically mixed at 160°C, using the J.E.M. 100 C E.D.A.X. analyser.

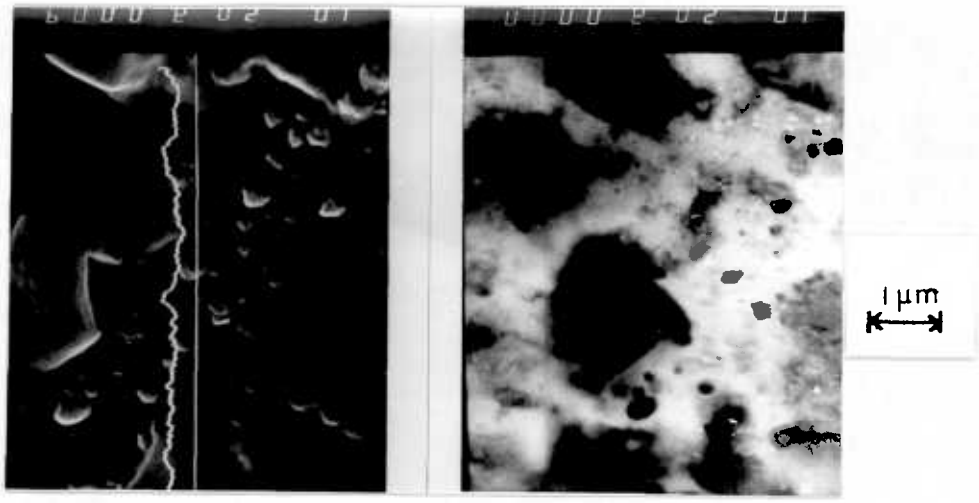

Fig. (3.33) A comparison of surface (left) and transmission (right) images for the two phase blend in Fig. (3.21).

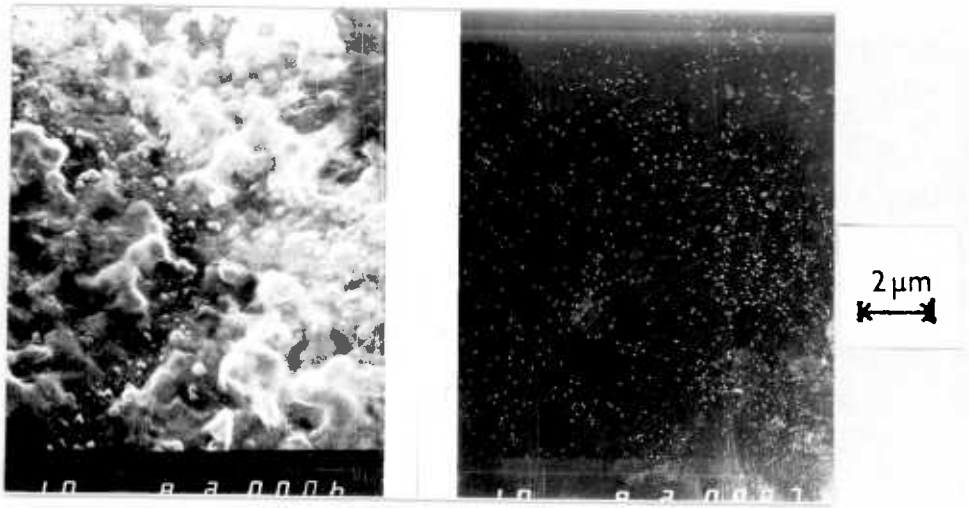

Fig. (3.34) A comparison of the surface image (left) and an X-ray 'map' (right) for the sample in Fig. (3.33).

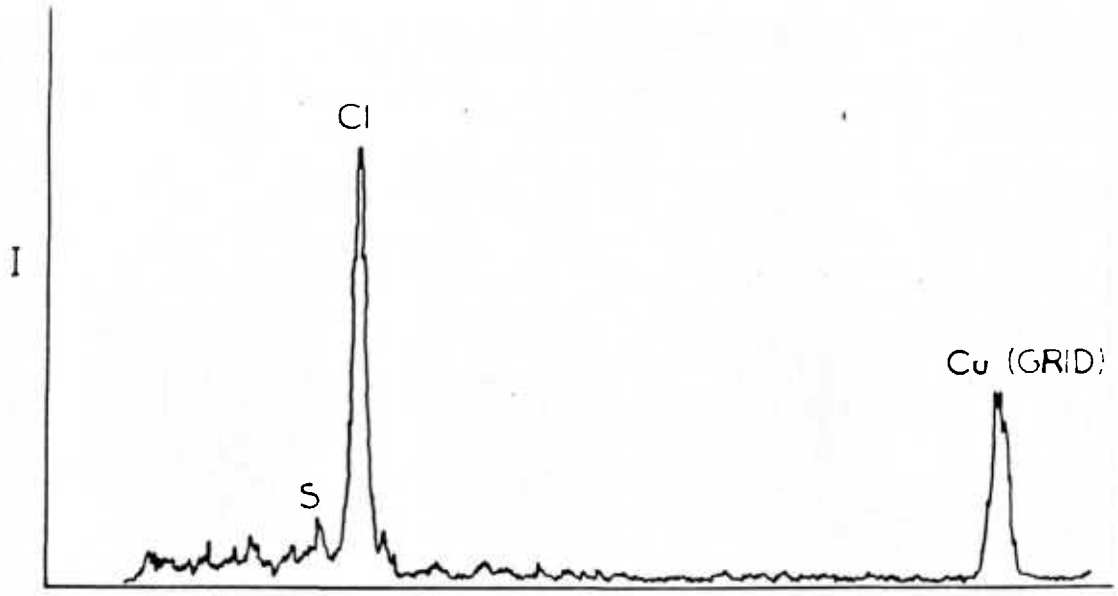

Fig. (3.35) Area analysis of a 50% P.V.C. : 50% S.C.P.E. blend prepared by 'in-situ' polymerisation, using the JEM 100C E.D.A.X. analyser.

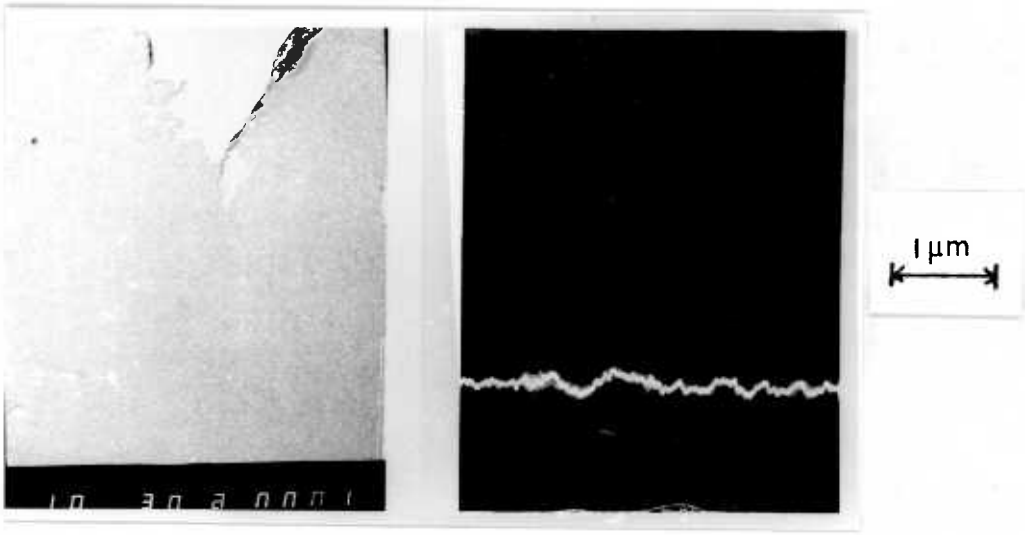

Fig. (3.36) A comparison of the surface image and line analysis of the sample in Fig. (3.35).

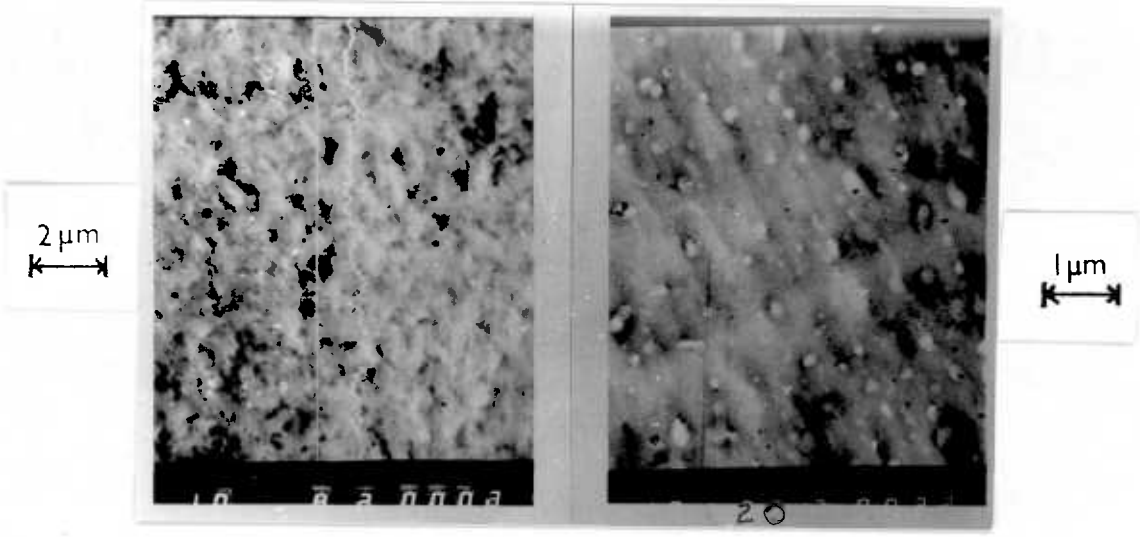

Fig. (3.37) A comparison of the scanning transmission images for two different elastomers as 10% blends with 90% P.V.C.

voltage pulse proportional in energy to the energy of the incident photon. This enables the identification of elements down to Na = 11. The peak for iron is significant, and this demonstrates the problem of iron contamination in industrial P.V.C.

Fig. (3.33) has different aspects of the technique, showing the transmission image of the blend at left and the surface image with line analysis at right. The surface image at left in Fig. (3.34) and the X-ray map for chlorine at right give the correlation for light areas on the surface image being chlorine rich. These light areas in S.E.M. correspond with the dark areas in S.T.E.M.., so these may also be considered chlorine rich. This means the light/dark contrast in T.E.M. can be considered as the difference in chlorine densities of the regions. This result also confirms the topographical nature of the surface.

Fig. (3.35) is the area analysis of the pure 'in-situ' blend with no spurious elements present. The flat image obtained for a 'single-phase' blend is shown at left in Fig. (3.36), together with, at right, the line analysis for chlorine which was an attempt to obtain periodic fluctuations corresponding to the T.E.M. image (Fig. 3.27). The signal to noise ratio was too low for the correlation to be made, and this instrument could not overcome the problem.

Since the images obtained in T.E.M. for the blends prepared in the Banbury mixer were not clear, they were repeated in S.T.E.M., as shown in Fig. (3.37). Despite the difference in magnification the S.C.P.E. exists obviously as a discrete phase, whereas the H.C.P.E. exhibits a more complex morphology.

This result illustrates the approach of Bucknall and others[51] that the surface area of contact is most important. The particle size of S.C.P.E. is smaller (0.2 μ cf 0.5 μ),so the surface area should be greater, but the complex shape of the H.C.P.E. increases the area of contact.

The experiment which was carried out in place in the JEM 7 was repeated, but using sections which were separately heated for 10 minutes at appropriate temperatures. Fig. (3.38) shows the influence of diffusion rates, where the micrograph on the left is of the 'single phase' blend heated to 150°C, and that on the right at 180°C which has undergone phase separation. The structure is similar to Fig. (3.31) in dimensions and features, as the phases appear anisotropic ($\sim$ 1 μm × 0.1 μm) with a wide distribution of sizes. It is not the structure resulting from a nucleation and growth mechanism, which requires the formation of discrete particles in a continuous matrix. The alternative is that it could be the structure resulting from spinodal decomposition described by Cahn[31], which consists of two highly interconnected phases.

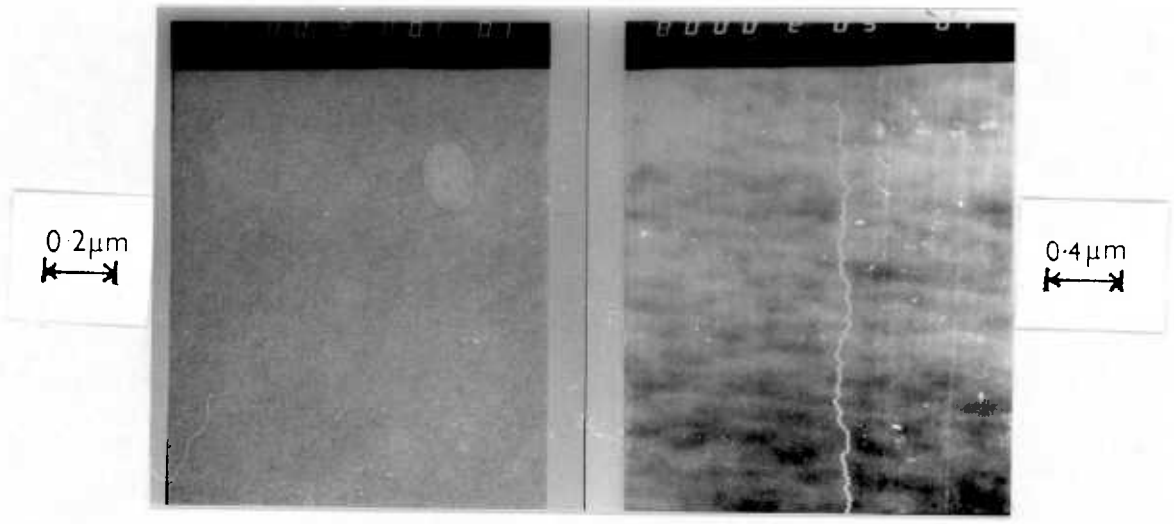

Fig. (3.38) A comparison of the scanning transmission images for the sample in Fig. (3.35) when heated to 150°C and 180°C

These results show how the sequence of microscopical investigations made can give some images or models of the microstructure. However, it is necessary to resort to other techniques to confirm these.

Techniques such as small angle X-ray scattering may give data which can be

analysed and averaged for the whole sample. The following sections contain the details of other attempts to elucidate the structure and properties of these P.V.C./ S.C.P.E. blends.

3.6 Differential Scanning Calorimetry

3.6.1 Introduction

The measurement of the Heat of Mixing (ΔH_m) for polymer pairs is restricted by problems of high viscosity and slow rates of diffusion. Most estimates have been made by indirect methods such as Hess's Law[84] or by using oligomers[85]. However, if a compatible polymer pair which exhibit an L.C.S.T. can be prepared at equilibrium, any heat of demixing will be observed at phase separation. Since the blend does not phase separate into the pure components, the heat of demixing is not exactly equal and opposite to the heat of mixing. This heat of demixing can, however, give information regarding the sign and size of the heat of mixing.

Data for such a system may be obtained directly from differential scanning calorimetry (D.S.C.). In this technique the temperatures of the sample and a standard reference are maintained at an equal level, as they are increased. The variation in power required to maintain this level during a transition is monitored and fed to an X-Y recorder. Fluctuations in the signal may be measured relative to standards in absolute energy units. A great advantage of this technique is the very small sample size required.

The theory has been reviewed in detail[86], but the more relevant aspects are presented here to show the quantitative nature of the technique.

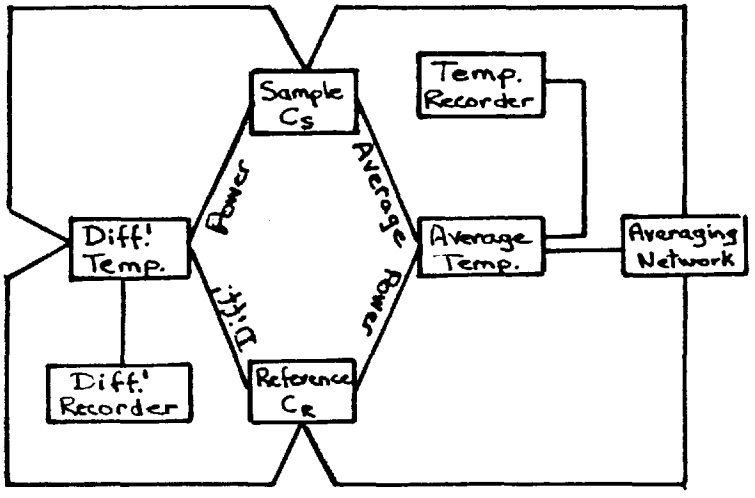

Fig.(3.39) A diagram of the D.S.C.

The schematic representation of the D.S.C. in Fig. (3.39) shows two junctions, one for the sample and one for a reference sample, monitored by platinum resistance thermometers. The system is divided into two loops, one for average temperature control, and one for differential temperature control. In the former the signal is proportional to the average desired temperatures, whilst in the latter the differential between the two is monitored and the power required to maintain equilibrium is recorded.

If the sample is at T_s with a heat capacity C_s, and the reference at T_R has a heat capacity C_R it can be shown that[86]:

$$\frac{dH}{dt} = -\frac{dq}{dt} + (C_s - C_r)\left(\frac{dT_r}{dt}\right) - RC_s\left(\frac{dq^2}{dt^2}\right) \qquad 3.15$$

where ; $\frac{dH}{dt}$ is the nett rate of energy generation, $\frac{dq}{dt}$ is the rate of heat generation, and R is a machine constant.

This contains the important result that the area under the curve f(t) is a direct measure of ΔH.

3.6.2 Experimental

A Perkin-Elmer D.S.C.-2 machine at a sensitivity of 0.5 m cal/sec was used with 20 mg of samples in crimped aluminium pans.

Initially P.V.C. and S.C.P.E. were run separately, and there was only the slight change in baseline expected at T_g[86]. Results from cast films were confused due to the presence of large exotherms caused by the presence of residual solvent (Fig. (3.40)).

The result for 50% P.V.C. : S.C.P.E. mixture prepared by 'in-situ' polymerisation is shown in Fig. (3.41). This trace contains an endotherm, the onset of which corresponds to the temperature of phase separation observed by other techniques. This

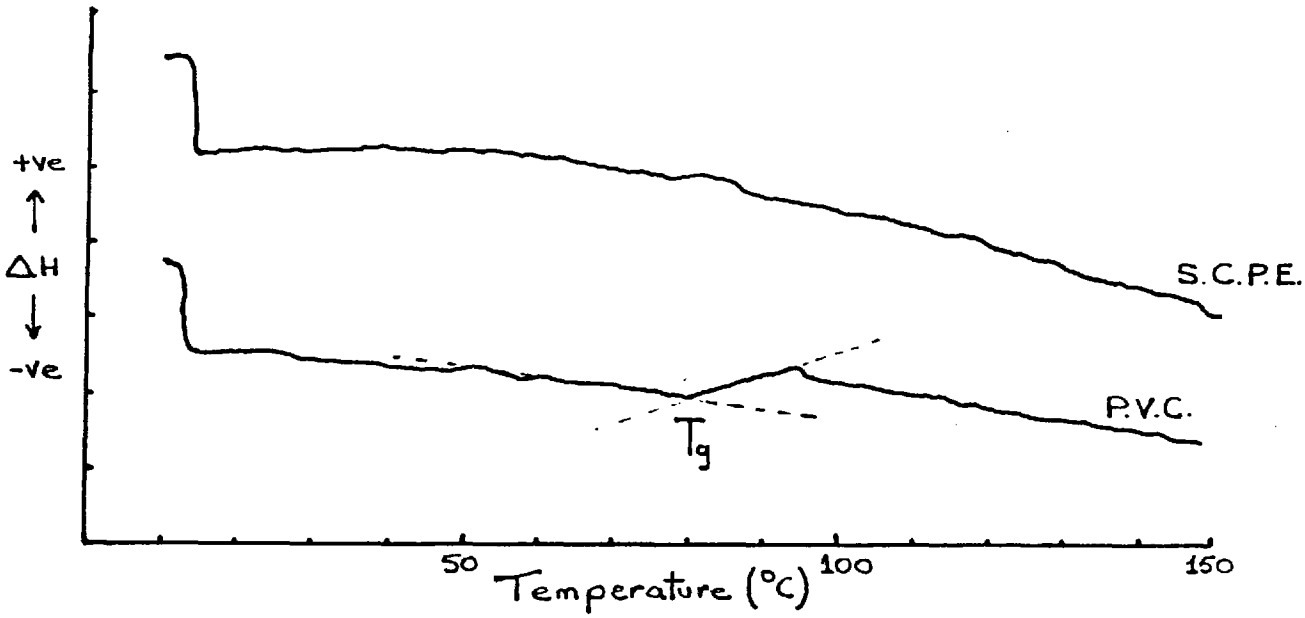

Fig. (3.40) D.S.C. traces for the component polymers

peak was attributed to the heat of demixing and taking a simplistic approach was assumed to be approximately equal and opposite to the heat of mixing, i.e. $(-\Delta H_m)$.

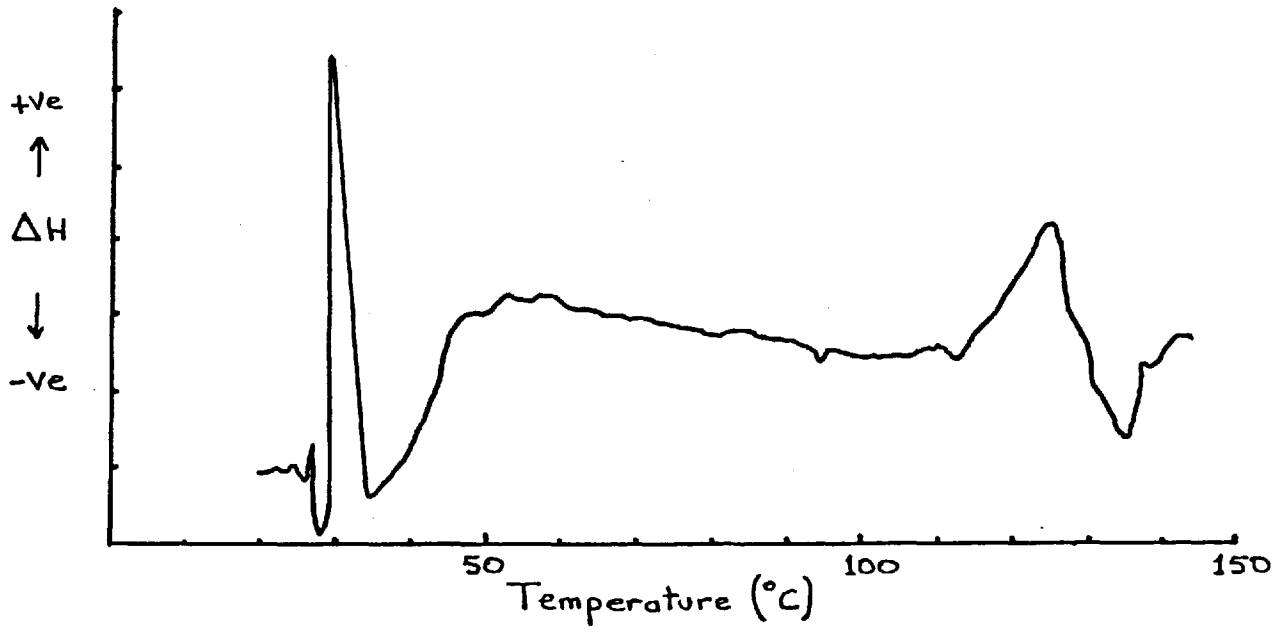

Fig. (3.41) The D.S.C. trace for a 50% P.V.C. : S.C.P.E. mixture prepared by 'in-situ' polymerisation, showing the peak of the heat of demixing

Experiments were carried out at other compositions. The simple theory predicts

the heat of mixing should not vary greatly with composition. This is due to the $\phi_1\phi_2$ term of equation (2.7) where the product of the volume fractions is 0.25 at 50%, 0.19 at 25%, and 0.09 at 10%. However, the temperature of demixing would be higher and it was difficult to clearly assign the small signals which were observed. This indicates the limitations of the technique.

Annealing the 50% mixture at 1°C/min after phase separation resulted in a broad exotherm which did not appear on cooling at 10°C/min. This was interpreted as evidence for the separation being reversible, but only on annealing.

Peaks obtained were integrated using a planimeter, and the value of the area compared with that obtained for the known heat of fusion for a standard Indium sample.

This gave an average value of

$$\Delta H_m = -0.15 \text{ cal gm}^{-1}$$

Further analysis was done also on a simplistic approach.

Assuming at phase separation $\Delta G_m = 0$,

$$T\Delta S_m = \Delta H_m$$

$$\therefore 393 \times \Delta S_m = -0.15 \text{ cal gm}^{-1}$$

$$\therefore \Delta S_m = -0.0004 \text{ cal gm}^{-1} {}^{\circ}K$$

These are very small values and are consistent with the low values of ΔH_m obtained in the absence of a specific interaction, such as hydrogen bonds. The Equation-of-State theory indicates the change in free volume (ΔV_m) may contribute to both the ΔH_m and ΔS_m terms, and this was investigated.

3.7 Density Measurements

There is some debate regarding the appropriate values to use for the specific gravity of glassy polymers[62]. This relates to the Volume-Temperature diagram, which refers to the glass as a supercooled liquid, with 'frozen-in' microvoids.

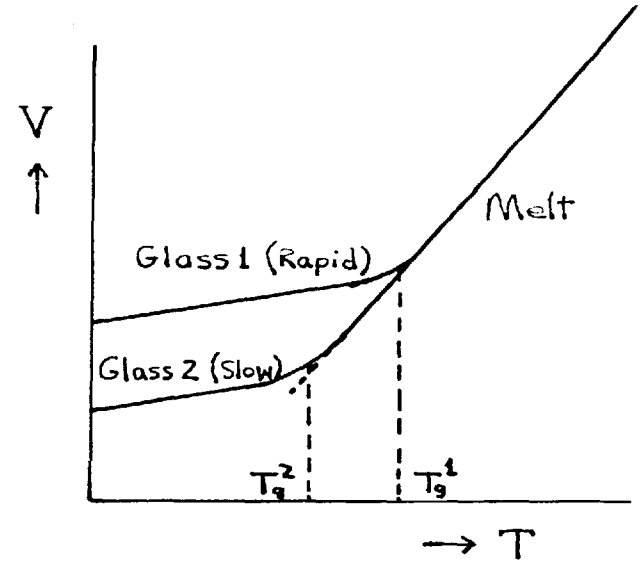

Volume–Temp. Relations for amorphous polymers

Fig. (3.42)

Rehage[87] has extensively studied this subject for macromolecules, and it is evident that the frozen-in volume due to glass formation is responsible for much of the heat of mixing and volume of mixing, so this could be a significant driving force in the formation of single phase mixtures.(Fig. 3.42)

Normal techniques for Specific Gravity determinations such as pyknometry have inadequate accuracy for these measurements, and the very accurate density gradient column is in the wrong density range. Graduated cylinders of 500 cc may be used to prepare columns of appropriate densities, using concentrated sodium and potassium bromide solutions in distilled water[88].

40% wt Na Br	D_{20}^{20}	1.4163
30% wt K Br	D_{20}^{20}	1.2615
36% wt K Br	D_{20}^{20}	1.3287

These solutions cover the ranges required and were used at room temperature $\sim 20^{\circ}C$ in conjunction with Standard Glass Hydrometers, each accurate to $\pm$ 0.001. Each hydrometer acted as an internal standard for the solutions when they were concentrated in the floatation experiment.

Specimens of the materials were submerged in the solution, ensuring all entrapped air bubbles were removed and the concentration of the solution was adjusted so that the specimen remained submerged. Gradually a more concentrated solution was added until the specimen was just suspended. The reading on the hydrometer was then taken as the

S.G.

In practice it was necessary to use a number of specimens, because of the possibility of voids or microbubbles, and it was found that a drop of detergent could aid wetting to reduce these problems.

The specific volume values obtained were (in $cm^3\ g^{-1}$) :

(i) Annealed P.V.C. 0.712 ± 0.002

(ii) 'In-situ' 50% P.V.C. : S.C.P.E. 0.743 ± 0.002

(iii) S.C.P.E. 0.787 ± 0.002

(iv) Mechanically mixed 50% P.V.C. : S.C.P.E. 0.750 ± 0.002

The value of ΔV_m so obtained is $\Delta V_m = -0.007 \pm 0.003$, which must reflect increased association of the two components when mixed in a single phase mixture, compared with that which could be expected, i.e. the arithmetic mean of the densities.

3.8 X-ray Analysis

3.8.1 Theory

It is convenient to discuss the X-ray measurements at large and small angles separately[95] : Wide Angle X-ray Scattering (W.A.X.S.), which measures structures between 1 and 20 Å and Small Angle X-ray Scattering (S.A.X.S.) which measures structures of 50 - 1000Å.

The theory of these experiments has been discussed in detail[89,90], so only the pertinent features will be considered here.

Apparatus for measurements using the Laue technique is shown in Fig. 49. This is normally used for the detection of short range order by W.A.X.S., i.e. between one atom and up to its fifth neighbour, which may be manifested as diffraction peaks according to Braggs Law :

$$n\lambda = 2d \sin \theta \qquad 3.16$$

where λ is the incident wavelength,

θ is half the diffraction angle, and

d is the 'spacing' between scattering centres

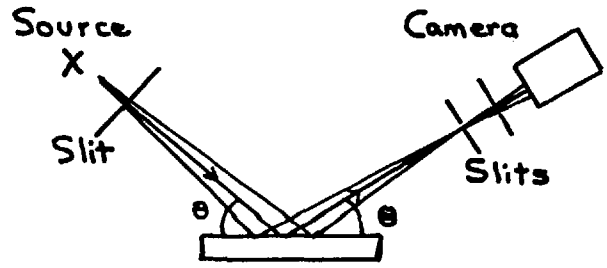

Fig.(3.43) W.A.X.S. Apparatus

The scattering mechanism for X-rays is similar to that for fast electrons noted previously[76], but the important difference is the wavelength of X-rays at ~ 1 Å is much longer than that of the fast electrons, ~ 0.004 Å. In all scattering measurements, there is a reciprocal relationship between scattering angle and real space dimensions.

W.A.X.S. relies on the retention of phase information in the scattering vector :

$$s = \frac{2 \sin \theta}{\lambda} \quad \text{or} \quad k = 2\pi s \qquad 3.17$$

where s and k are scattering vectors and other terms are as in eqn. (3.16),such that constructive influence in the scattered waves results in the Bragg Peaks. In the case of amorphous materials, the scattering is determined by the effective atomic packing density only since no order is present, and the scattered waves appear as a diffuse peak or 'halo'.

In the case of S.A.X.S. or scattering below angles of $\sim 2\theta = 2^{\circ}$, great care is required to obtain accurate data. Recent work has led to the development of apparatus capable of such measurements, such as that shown in Fig. (3.44).

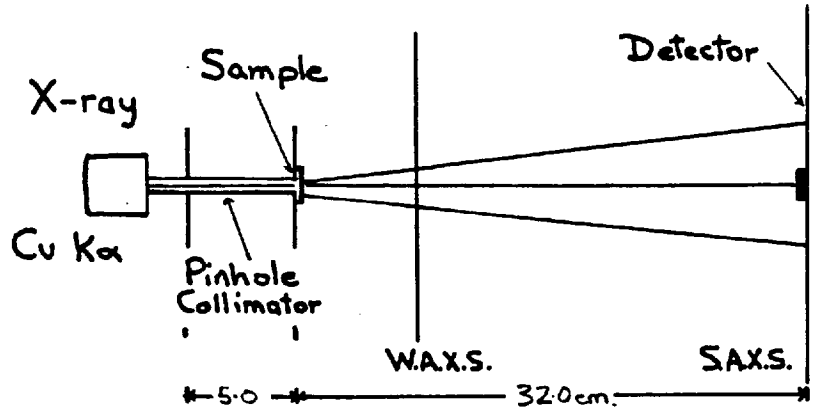

Fig.(3.44) S.A.X.S. Apparatus

The high intensity source must be capable of a uniform distribution of intensity along its length, and for accurate measurements monochromatisation is necessary.

The overall characterisation of any polymer system is given from the volume fraction of the phases which make up the system and their electron densities. This is expressed in the Debye equation for a pinhole aperture as :

$$Q = \int_0^\infty s^2 \, I(s) \, ds \qquad 3.18$$

and for a slit aperture as :

$$\tilde{Q} = \int_0^\infty s \, \tilde{I}(s) \, ds \qquad 3.19$$

where ; I (s) is the relative intensity, Q is a quantity invariant for pinhole and slit collimation, S is the scattering factor and $\tilde{Q}$ equals 2Q.

For a two phase system the scattering power is given by :

$$\langle(\rho - \bar{\rho})^2\rangle = \langle(\rho_1 - \rho_2)^2\rangle \, w_1 w_2 \qquad 3.20$$

where ; w_1 and w_2 are the weight fractions of components 1 and 2 respectively, and $\rho_1 \rho_2$ the electron density of components 1 and 2 respectively.

S.A.X.S. from composites can be described by the theory of Debye and co-workers[91] where a spatial correlation function is given as :

$$\gamma(r) = \frac{\langle \eta_A \eta_B \rangle}{\langle \eta^2 \rangle} \qquad 3.21$$

where ; η_A and η_B are fluctuations in the electron density,

$\langle \eta_A \eta_B \rangle$ represents the average product for all pairs of points at a distance r apart, and $\langle \eta^2 \rangle$ is the mean square deviation over all points.

For an isotropic composite the scattering intensity i(h) per unit volume of scatter is given by :

$$\frac{i(h)}{I_o} = 4\pi k \langle \eta^2 \rangle \int_{i=o}^{\infty} \gamma(r) r^2 \frac{\sin hr}{hr} \, dr \qquad 3.22$$

where ; I_o is the incident intensity, K is a proportionality factor which is constant for all values of θ , h is $4\pi/\lambda \sin \theta$, λ is the wavelength radiation, and 2θ is the total angle of scatter.

For a random two phase structure $\gamma(r)$ should take the form of a simple exponential $e^{-r/a}$ where a is a characteristic correlation length.

So that :

$$\frac{i(h)}{I_o} = \frac{8 \pi K a^3 \langle \eta \rangle^2}{(1+h^2a^2)^2} \qquad 3.23$$

and a plot of $i^{-\frac{1}{2}}$ vs h^2 should give a straight line whose ratio of slope to intercept is a^2.

In this way the average distance between scattering centres can be estimated.

3.8.2 Experimental and Results

Preliminary W.A.X.S. diffraction studies were carried out in the Laue mode on the 'single phase' blend in order to observe any preferential short range ordering.

Specimens 5 mm thick were examined, using 40 kV Copper K^{α} X-rays for 18 hours with a Unicam 525 camera of radius 30 mm. In this camera the Bragg angles of 5 - 20° could be analysed.

Experiments on annealed P.V.C., S.C.P.E. and the 50% 'in-situ' blend gave results shown in Fig. (3.45).

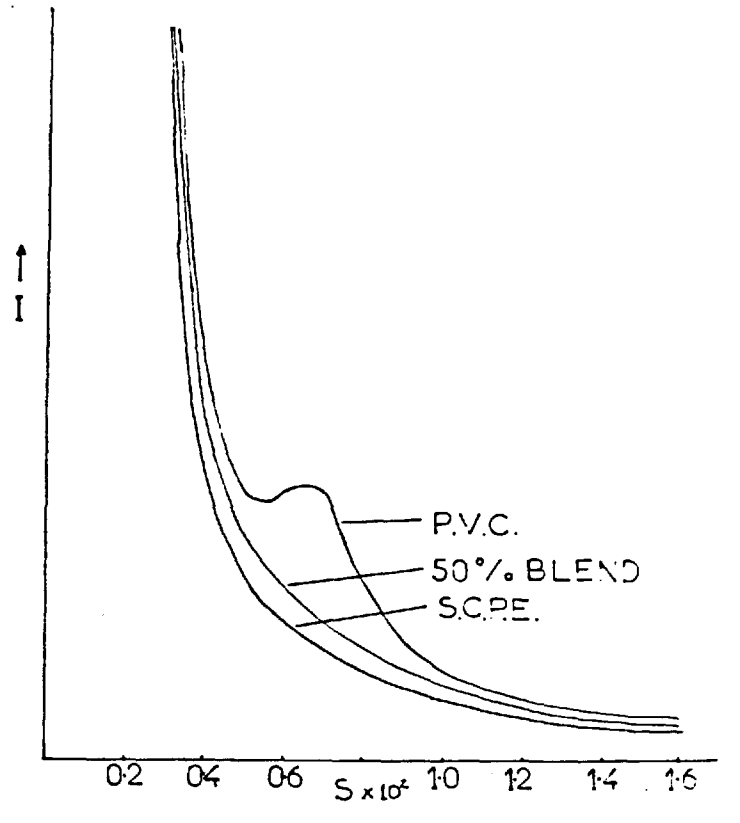

Fig. (3.45) S.A.X.S. for P.V.C., S.C.P.E. and the 50% P.V.C. 'in-situ' blend

W.A.X.S. showed a small difference between S.C.P.E. and P.V.C. ($2\theta = 24^{\circ}$ and 28° maximum respectively) and these were little different from the blend ($2\theta = 24^{\circ}$ maximum). However, none of these diffraction photographs showed any evidence of preferential short range ordering. There was only the diffuse peak associated with amorphous solids.

The results were not interpreted in terms of the Bragg equation because the peaks were not sharp. It was possible to use a 'modified' Bragg equation and the result suggested random correlations between atoms $\sim 4\text{Å}$ apart[92].

S.A.X.S. experiments were carried out on a Siemens/Kratky apparatus, equipped with an automated camera. The result for P.V.C. is a peak at an angle of $2\theta \simeq 1^{\circ}$, which corresponds to a distance in real space for a paracrystalline substance of 100-

200 Å. The result obtained is shown in Fig. (3.45) together with that obtained for the 50% P.V.C. 'in-situ' blend.

Recently the S.A.X.S. of commercial P.V.C. has been investigated by Wenig[93] who established a correlation between the degree of crystallinity, the Bragg spacing, and the molecular weight of the polymer. This work also suggested that there is a correlation between the so-called 'primary particles' and the 'para crystallites' present as 15% wt. of the matrix.

The scattering contrast in this experiment is given from the difference in electron density of the crystalline and amorphous polymer. From equation 3.20 :

$$= \frac{\text{Number of electrons}}{\text{molecule}} \times \frac{1}{\text{M. Wt.}} \times \text{Density} \quad \frac{\text{electrons}}{\text{Angstroms}} \qquad (3.24)$$

$$= \frac{\text{Number of electrons}}{\text{mole}} \times \frac{\text{mole}}{\text{gram M. Wt.}} \times \frac{\text{Density}}{} \times \frac{\text{Avagadro's Number}}{}$$

Using appropriate data[65] the value for crystalline P.V.C. is 0.440, and the value for amorphous P.V.C. is 0.422. Hence the contrast is :

$$(0.440 - 0.422)^2 \times \frac{0.15}{1.44} \times \frac{0.85}{1.38}$$

$$= 0.4 \times 10^{-4}$$

and this is adequate to produce a strong signal.

For S.C.P.E. the electron density is 0.397 (e/Å^3) and a 50% blend should be approximately 0.410 if the density is taken as the mean of the component densities.

For 5% 'paracrystallites' in a 50% blend the contrast would be :

$$(0.440 - 0.410)^2 \times \frac{0.05}{1.44} \times \frac{0.95}{1.34}$$

$$= 0.36 \times 10^{-4}$$

This result implies that 'crystallites' should be detectable to limits of 5% wt. concentration. The intensity for 15% 'crystallites' should be greater in a 50% blend,

but in fact no signal is observed.

The result suggests there may be a significant volume change in the blend which reduces the contrast or alternatively that there are no 'paracrystallites' present. It was not possible to improve the result without recourse to 'heavy-atom' labelling which has been mentioned as a technique which may give spurious results[62]. The only other technique available to resolve the structure of the 'single phase' blend was neutron scattering.

3.9 Neutron Scattering

3.9.1 Introduction

The neutron has a mass of 1 atomic unit, no charge, and has a spin of $I = \frac{1}{2}$. The wavelength distribution of thermal neutrons produced from reactors has a Maxwellian peak at 1.8 Å. At these wavelengths the kinetic energy is such that neutrons have ideal characteristics for investigating the properties of the solid state[94,95]. Using a suitable moderator, thermal neutrons with wavelengths of 1 - 20 Å and energies of 400 - 0.4 J/mol may be produced. These wavelengths are almost those of interatomic spacings, whereas the energies are of the order of molecular vibrational energies.

In thermal neutron scattering the magnitude of the interaction does not follow any simple rules such as those for X-rays, where the interaction is proportional to the number of electrons in the target. In neutron scattering the magnitude of the interaction is within a narrow range for all atoms. However, because the interaction is with the nucleus, the magnitude is different for different isotopes of the same element, and this can be very useful in obtaining 'contrast'.

For any particular atom the variation in interaction gives rise to incoherent scattering, whereas the mean value of the interaction gives rise to coherent scattering.

Table 4 lists the Nuclear Scattering Cross-Sections for low energy neutrons (in barns).

Atom	Spin (I)	$\sigma_{coherent}$	$\sigma_{incoherent}$	$b \times 10^{12}$(cm)
^{1}H	$\frac{1}{2}$	1.8	79.7	- 0.374
^{2}H	1	5.6	2.0	0.667
^{12}C	0	5.6	-	0.665
^{14}N	1	11.6	0.3	0.94
^{16}O	0	4.2	-	0.58
^{28}Si	0	2.0	-	0.42
$^{*}Cl$	3/2	11.58	19.5	0.96

* Natural Isotopic Ratio. (σ - Barns)

Table 4 A list of neutron scattering data for important atoms

The large difference in cross- section of ^{1}H and ^{2}H enables the use of deuterium to replace hydrogen in order to provide contrast for all scattering experiments.

For an elastic collision, the scattering factor Q is given by :

$$Q = \frac{4\pi}{\lambda} \sin \frac{\theta}{2} \qquad (3.25)$$

$$\equiv \quad k \text{ in X-rays}$$

where other symbols have the normal meaning of the Bragg Equation.

The interaction between neutron and nucleus is exceedingly short range $\sim 10^{-15}$m, and therefore is very small compared with the wavelength of the neutron (~ 1 Å $= 10^{-10}$m). The amplitude of the scattered wave, f, which is isotropic, is equal to - b, where b is called the scattering length. From consideration of geometry it can be shown that :

$$\left(\frac{d\sigma}{d\Omega}\right)_{coherent} = \overline{b}^2 \left| \sum_{L} \exp (iQR_L \right|^2 \qquad (3.26)$$

and

$$\left(\frac{d\sigma}{d\Omega}\right)_{incoherent} = N\left[\overline{b^2} - \overline{b}^2\right] = N\left[b - \overline{b}\right]^2 \qquad (3.27)$$

where the atomic cross section of N atoms is σ, Ω the solid angle, R_L the position vector of the L^{th} nuclei of scattering length b.

The total scattering cross section can now be written as :

$$\sigma_T = \sigma_{coh} + \sigma_{inc} = 4\pi\bar{b}^2 + 4\pi(\overline{b^2} - \bar{b}^2) \qquad 3.28$$

A scattering law S (Q) can be derived from the above expressions for elastic collisions, such that :

$$\frac{d\sigma}{d\Omega} = (b_{1\,coh} - b_{2\,coh}\,\bar{V}_1/\bar{V}_2)^2\, S_{1\,coh}(Q) + N_1 b^2_{1\,inc} + N_2 b^2_{2\,inc} \qquad 3.29$$

for N_1 molecules of substance 1 dissolved in N_2 of substance 2, where $b_{i\,coh}$ is the sum of the nuclear coherent scattering lengths in the molecule and $b_{i\,inc}$ is the sum of the nuclear 'incoherent scattering lengths' in the molecule. V_1 and V_2 are the partial molar volumes of substances 1 and 2 respectively. $\left(b_{1\,coh} - b_{2\,coh}\, V_1/V_2 \right)^2$ is the contrast factor K, and the larger this value, the more intense the scattering.

If the incoherent background scattering is subtracted from $\frac{d\sigma}{d\Omega}$ the excess scattering $\left(\frac{d\sigma}{d\Omega}\right)_{Ex}$ contains all the information about the structure of the scattering material since :

$$\left(\frac{d\sigma}{d\Omega}\right)_{Ex} = (b_{1\,coh} - b_{2\,coh}\,\bar{V}_1/\bar{V}_2)^2\, S_{1\,coh}(Q) = K\, S_{1\,coh}(Q) \qquad 3.30$$

In terms of polymer chain dimensions the coherent scattering law can be written as :

$$S_{1\,coh}(Q) = N_1{}^2 2/Q^2\langle s^2\rangle^2 \times \left[\mathrm{Exp}(-Q^2\langle s^2\rangle) - 1 + Q^2\langle s^2\rangle\right] \qquad 3.31$$

where N_1 is the number of segments in a chain whose mean square radius of gyration is $\langle s^2\rangle$.

For a polymer of molecular weight M and concentration c (wt/vol), then the intensity of scattering per unit volume :

$$I(Q) = \left(\frac{d\sigma}{d\Omega}\right)_{Ex} \frac{C}{M} N_a = \frac{K_c}{M} N_A N_1{}^2 2/(Q^2\langle s^2\rangle \times \left[\exp(-Q^2\langle s^2\rangle) - 1 + Q^2\langle s^2\rangle\right] \qquad 3.32$$

where N_A is Avagadros Number.

Now $N_1 = M/m$ where m is the segment molecular weight, so

$$\frac{KcN_A}{M} N_1^2 = \frac{KcN_A}{M} \frac{M^2}{m^2} = K^*cM \qquad 3.33$$

where $K^* = \frac{KN_A}{m^2}$ so that :

$$I(Q) = \frac{K^*cM2}{Q^2\langle s^2\rangle^2} \left[\exp(-Q^2\langle s^2\rangle) - 1 + Q^2\langle s^2\rangle\right] \qquad 3.34$$

Therefore,

$$\frac{K^*c}{I(Q)} = M^{-1}\left[\frac{2}{Q^2\langle s^2\rangle^2} \times \left[\exp(-Q^2\langle s^2\rangle) - 1 + Q^2\langle s^2\rangle\right]\right]^{-1} \qquad 3.35$$

The analysis of this expression depends on the value of Q compared to the molecular parameter of the polymer chain, and four regions may be discerned[90].

(i) $Q < \langle s^2\rangle^{-\frac{1}{2}}$ is the Guinier Range

$$\frac{K^*c}{I(Q)} = M^{-1}\left(1 + \frac{Q^2\langle s^2\rangle^2}{3}\right) \qquad 3.36$$

from which the Molecular Weight and Radius of Gyration are easily obtained.

(ii) $\langle s^2\rangle^{-\frac{1}{2}} < Q < a^{-1}$ where a is the persistence length of the polymer chain

$$\frac{K^*c}{I(Q)} = M^{-1}\, Q^2\langle s^2\rangle/2 \qquad 3.37$$

(iii) $a^{-1} < Q < \ell^{-1}$ where l is the statistical step length of the polymer.

Scattering intensity is characteristic of a rod of length nl where n is the number of statistical units in the chain

$$\frac{K^*c}{I(Q)} = \frac{M^{-1}\, nl\, Q}{\pi} \qquad 3.38$$

(iv) $\ell^{-1} < Q$

where the scattering intensity is governed by the structure of the segments forming the chain, which is the normal wide angle region.

If the contrast factor K is evaluated for d. P.V.C. and S.C.P.E. from[94]

$$K = \left[\sum \sigma_{dPVC} - \frac{\nu_{dPVC}}{\nu_{CPE}} \sum \sigma_{SCPE}\right]^2 = \left[4.5 - \frac{63}{1.4} \times \frac{1.27}{52} \times 0.9\right]^2$$
$$= 12.25 \times 10^{-24} \text{ cm}^2$$

for P.V.C. - S.C.P.E.

$$K = \left[1.35 - \frac{63}{1.4} \times \frac{1.27}{52} \times 0.9\right]^2$$
$$= .09 \times 10^{-24} \text{ cm}^2$$

Experimentally it has been found that K should be at least 10 for an adequate signal, so it is obvious that the use of deutero P.V.C. is necessary to enhance the signal. The assumption is made that d P.V.C. is equivalent to P.V.C.

3.9.2 Experimental

The apparatus used was the D 11 small angle neutron scattering spectrometer at the Institut Laue-Langevin, Grenoble, France. This facility is shown schematically in Fig. (3.46).

The liquid hydrogen cold source C produces long wavelength neutrons which then pass through a curved guide G. The guide reduces the amount of γ -rays and fast neutrons in the beam. The required wavelength in the range 5 Å to 12 Å and distribution

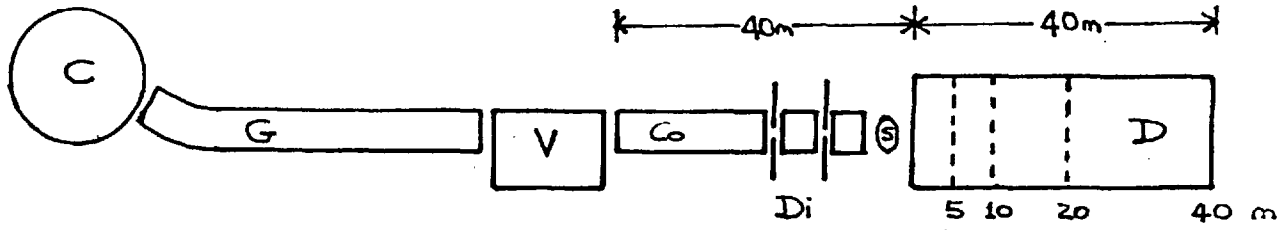

Fig. (3.46). The Small Angle Neutron Scattering Spectrometer at the Institut Lauë-Langevin

are determined by a helical slot velocity selector V. After the selector the beam is collimated by use of the diaphragms D_i, and neutron guides C_o, which can be moved out of the beam so as to produce the apparent neutron source at different distances from the sample.

Samples were prepared as in Section 3.2.2, except for 2% d P.V.C. in P.V.C., which was prepared by solvent casting from D.C.E. The size and thickness of the sample are determined by the beam which is 1 cm. diameter. Thickness is related to the scattering cross-section σ by the Beer-Lambert law :

$$I = I_0 \exp(-n\sigma L) \qquad 3.39$$

where I_o is the incident flux, I is the transmitted flux, n is the number of atoms per unit area and L is the thickness of the sample.

In Small Angle Neutron Scattering (S.A.N.S.) the samples are normally 1 mm thick.

On the other side of the sample there is a large evacuated tube into which the position sensitive detector can be placed at different positions to vary the range of Q. Experiments consist of the measurement of the intensity of the scattered beam from $\theta = 5^{\circ}$ to 0.15°.

The detector consists of a matrix of 64 x 64 1 cm^2 cells, which are connected

on-line to a PDP 11 computor, which records and displays the results on a visual display unit.

This data is retrieved and subjected to two computor programs for refinement[96]. The first, RNILS, where the number of counts in the detector is printed as a function of their average value of Q. The second, SPOLLY, is a more complex treatment of the signal in which all signals are normalised to unit incident flux. Signals from the sample holder are subtracted from the main signal, and the signal is normalised relative to the standard background

$$\text{i.e.} \qquad \frac{d\sigma}{d\Omega} = S_f = \frac{S'}{V_f} \frac{T_{V+VB}}{T_{S+SB}} \frac{N_V}{N_S} \frac{d\sigma_V}{d\Omega} \qquad 3.40$$

where S' is the difference between sample and sample holder,

T_V is the transmission for the (water) standard

T_S is the transmission for the sample

N_V No. of atoms in (water)

N_S No. of atoms in sample

V_f is the detector correction

$\frac{d\sigma_V}{d\Omega}$ is the cross-section of (water)

These programs may be visualised using a PLOTTING program on a Visual Display Unit (V.D.U.) and these may be recorded on TEKTRONIX V.D.U. Machines. Typical examples of small angle neutron scattering (S.A.N.S.) results are shown in processed form from the Tektronix in Figs. (3.47) and (3.48).

3.9.3 Radii of Gyration

Normally, these are measured by the use of the expression in the 'Guinier Range'[90] (equation 3.36), which means a plot of $\frac{C}{I(Q)}$ vs Q^2 (so-called 'Zimm Plot') will have an intercept of 1/M and a slope which can be related to $\langle s^2 \rangle$. This gives an independent check of the polymer $\bar{M}_W$ values and a simple calculation to obtain $\langle s^2 \rangle$.

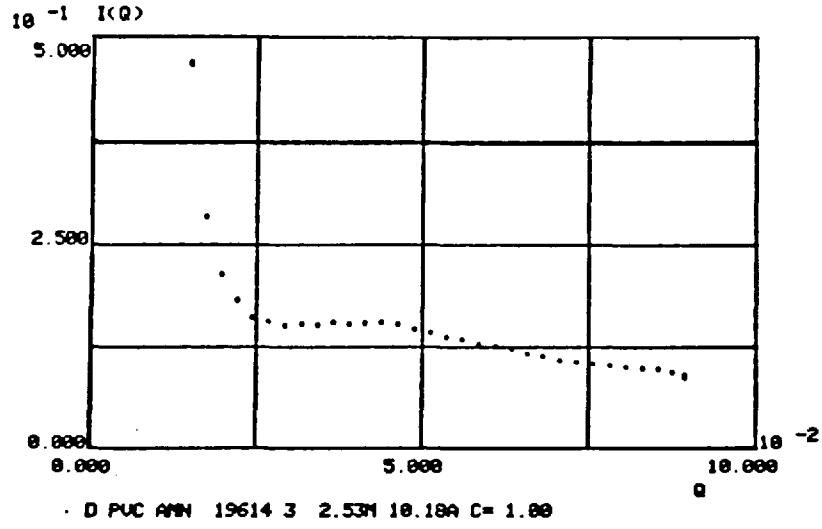

Fig. (3.47) The S.A.N.S. radial distribution function for d P.V.C. showing the 'Bragg' peak.

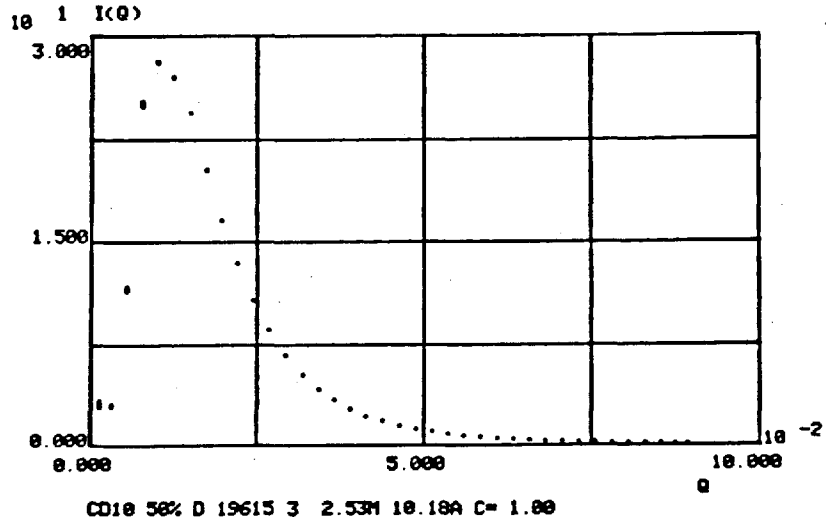

Fig. (3.48) The S.A.N.S. radial distribution function for 50% d P.V.C. : S.C.P.E. prepared by 'in-situ' polymerisation, showing small angle scattering only.

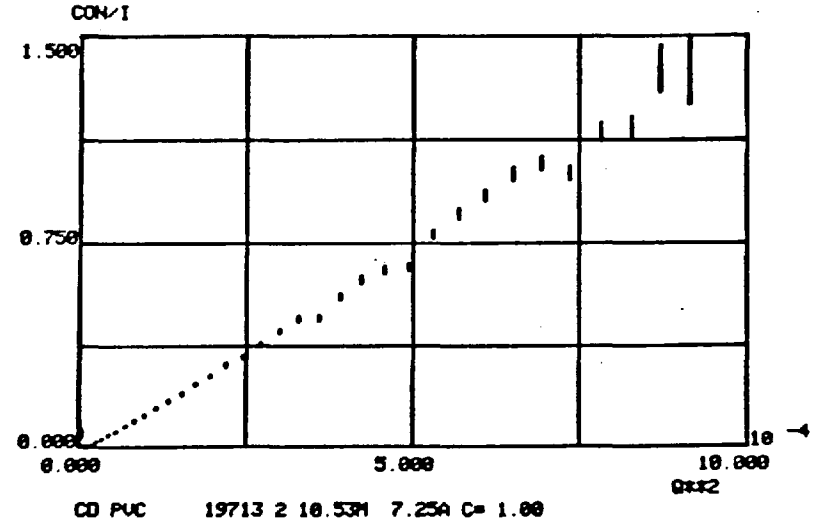

Fig. (3.49) A 'Zimm' plot for the S.A.N.S. from 2% d P.V.C. in P.V.C. after subtracting the S.A.N.S. from an identical specimen of P.V.C.

However, it is necessary to fulfil the condition $Q < \langle s^2 \rangle^{-\frac{1}{2}}$ for the Guinier Range, which anticipates some knowledge of $\langle s^2 \rangle$ in order to set the detector for the appropriate Q region. As the intensity decreases with the square of the solid angle (Ω) it is not always desirable to work with the detector set for such low values of Q.

In the Kratky region the conditions are that $\langle s^2 \rangle^{\frac{1}{2}} < Q < a^{-1}$ where a is the persistence length of the polymer chain, and the expression for this region, equation 3.37 means the values of $\langle s^2 \rangle$ can be easily obtained, but using a value of $\bar{M}_W$ measured elsewhere. According to Kratky a plot of $Q^2 I(Q)$ vs Q should give a straight line of slope zero when in the 'Kratky Range'.

The results from the 'Zimm plots' are shown in Fig. (3.49). These plots assume a zero value for the second virial coefficient, independent of concentration, so the values for the blends may be higher than the correct values. The value for the homopolymer should be correct. Results in Fig. (3.49) where the slope changes systematically with change in composition suggest strongly this is the Kratky region, as the negative intercept could be due to a change in slope as the Guinier region is entered. Fig. (3.50) is the plot which tests the Kratky condition for P.V.C. The plot is horizontal at higher Q but there is a different signal at low Q.

There are assumptions in the experiment which may explain this. It is assumed that the difference in signal between the 2% deuterated and non-deuterated samples is entirely due to the deuterated chains. However, there may be an underlying small angle signal due to the structure of the samples which may include a diffuse peak, and these may not subtract exactly.

It is necessary to correct the values obtained for I from SPOLLY computations using the expression[94,96]:

$$I_{ABS} = I_{SPOLLY} \times \frac{(1 - TRW)\, g}{TRS \times 4\pi \times t} \qquad 3.41$$

where TRS is the transmission of the sample, TRW is the transmission of the water standard, t is the sample thickness to express I per unit volume, and g is a factor which corrects for small inelastic scattering in water. $g = 1/[1-e^{-(0.6\lambda^{\frac{1}{2}})}]$. This expression has a value of 0.64 for samples 1 mm thick in this case.

$\bar{M}_w \times 10^5$	Composition	$K^* \times 10^2$	Slope	$\langle s^2 \rangle^{\frac{1}{2}}$	Thickness (mm)
1.70	P.V.C.	0.15	35.0	134 Å	0.75
1.70	75% P.V.C.	0.157	26.9	119 Å	0.65
1.70	50% P.V.C.	0.166	20.9	109 Å	0.55

Table 5 The radii of gyration of d P.V.C. in various P.V.C. : S.C.P.E. blends

From the results in Fig. (3.49) the values of $\langle s^2 \rangle^{\frac{1}{2}}$ were calculated from the Kratky expression. Errors in these measurements include errors from the measurement of : Sample Thickness 1%, Sample Transmission 0.5%, K* for blends 1.0%, $\bar{M}_W$ 5% and Concentration 5%. The square root term reduces the error to $\pm$ 5% overall.

The results in Table 5 show that the P.V.C. molecules are collapsing down in dimensions with increasing concentration of S.C.P.E. in the blend. Such a result is consistent with the S.C.P.E. being a 'poor solvent' for d P.V.C.

3.9.4 Analysis of Molecular Structure

The most significant result is the 'Bragg' peak in d P.V.C. like those in S.A.X.S. although in many cases the radial distribution functions of the samples also show small angle scattering (Fig. 3.48). These signals can be analysed by the same technique as those in S.A.X.S.. A plot of $I^{-\frac{1}{2}}$ vs Q^2 should give a straight line of intercept I and

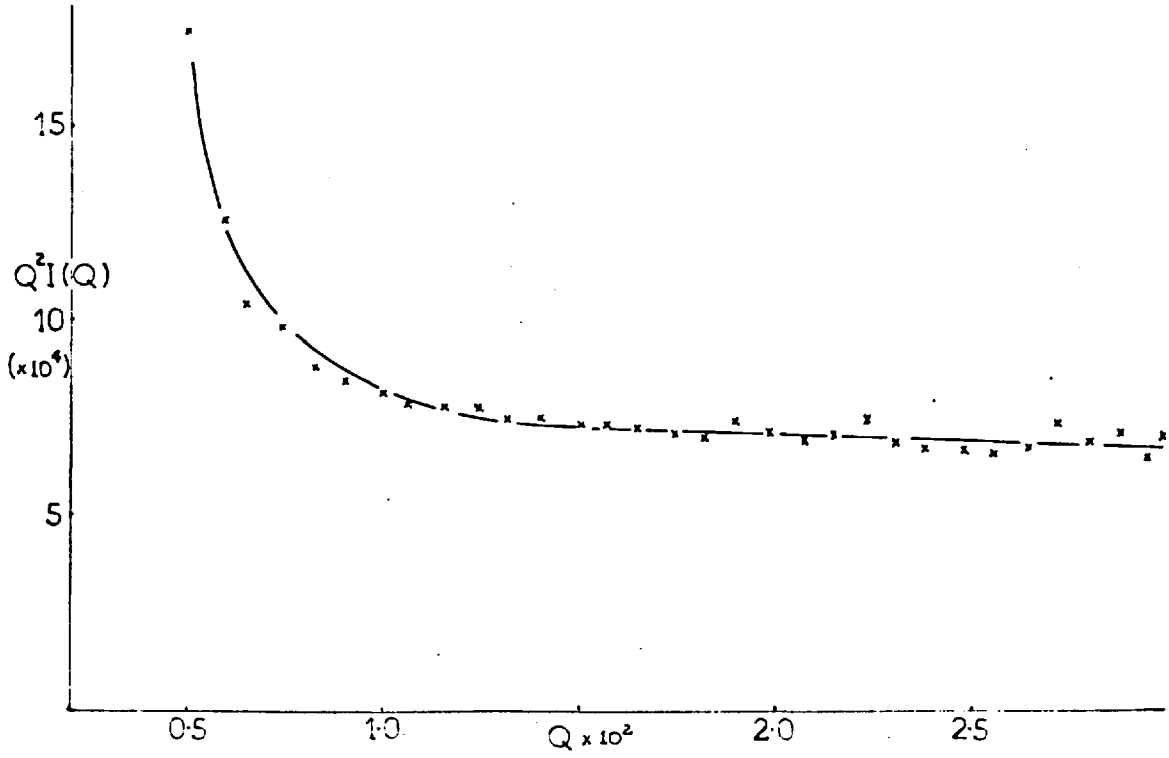

Fig. (3.50) A plot of Q^2 I (Q) vs Q to check the Kratky condition

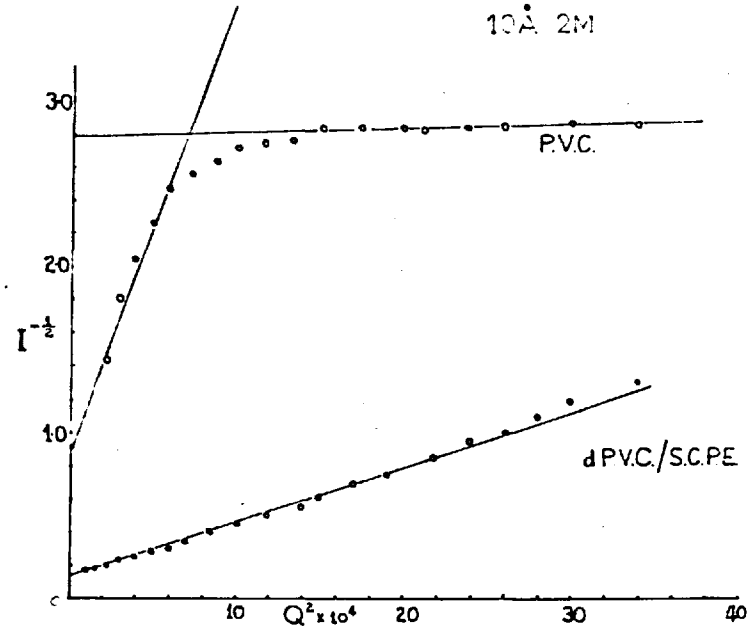

Fig. (3.51) A 'Debye-Bueche' plot for P.V.C. and for 50% P.V.C. : S.C.P.E. prepared by 'in-situ' polymerisation

The results are listed in Table 6

slope S such that $S/I = a^2$ where a is a characteristic correlation length, which is a measure of the average distance between scattering centres. I must be the absolute intensity. Some examples of these plots are shown in Fig. (3.51) and whilst some plots give straight lines, others give more complex behaviour, some of which could be two or more straight lines. In these cases, measurements are made on the basis of the best fit of two lines.

P.V.C. gives a small angle signal which can be related to density fluctuations over an order of 50 Å, as well as those over 5 Å which correlate with W.A.X.S. results.

The 'Bragg' peaks which occur in annealed d P.V.C. have the same d spacing as those from S.A.X.S. of 142 Å. This result confirms the results of other workers[97] which show there is inadequate scattering contrast between 'crystalline' hydrogenous P.V.C. and amorphous hydrogenous P.V.C., but adequate if the polymer is deuterated. If the polymer is studied 'as polymerised', the micro-morphology of the matrix gives rise to a small angle signal which obscures the 'Bragg' peak.

One important result is that a 'single-phase' blend of 50% d P.V.C. and 50% S.C.P.E. does not show any 'Bragg' peaks, but it does have a small angle signal, as in Fig. (3.48). The contrast factor for this system is such that any 'crystalline' regions should give a higher intensity signal than they would in pure d P.V.C. This result confirms that from S.A.X.S. studies and it can be concluded that there are no ordered regions in these 'single-phase' blends. However, there is some amorphous 'structure' which gives rise to a small angle signal and the correlation length for this is less than that for P.V.C.

This spacing is seen to decrease with increasing temperature, but there is no strong evidence of a change in structure after passing through the phase boundary.

The results for d P.V.C. 'as polymerised' indicate a slow diffusion rate for this

Composition	Correlation Length (Å)	Q Range (Å^{-1})	Temperature (°C)
d PVC (As Poly^{md})	1000	0.024 - 0.074	20°
d PVC (As Poly^{md})	1000	0.024 - 0.074	55
d PVC (As Poly^{md})	1000	0.024 - 0.074	92
d PVC (As Poly^{md})	1000	0.024 - 0.074	132
d PVC (As Poly^{md})	500	0.011 - 0.033	158
d PVC (Annealed)	15	0.011 - 0.033	20
50%d PVC (In situ)	6,46	0.05 - 0.15	20
50%d PVC (In situ)	48	0.024 - 0.074	20
50%d PVC (In situ)	48	0.024 - 0.074	55
50%d PVC (In situ)	45	0.024 - 0.074	92
50%d PVC (In situ)	40	0.024 - 0.074	132
50%d PVC (In situ)	40	0.024 - 0.074	158
P.V.C. (Annealed)	4	0.5 - 0.15	20
P.V.C. (Annealed)	9 and 57	0.024 - 0.074	20
P.V.C. (Annealed)	58 and 180	0.008 - 0.024	20
75% PVC (In situ)	42	0.024 - 0.074	20
75% PVC (In situ)			20
50% PVC (In situ)	49	0.024 - 0.074	20
50% PVC (In situ)			20
25% PVC (In situ)	36	0.024 - 0.074	20

Table 6. A list of correlation lengths for all blend compositions

polymer as no change in the correlation length is seen until well over the T_g.

3.10 Inverse Gas Chromatography

3.10.1 Introduction

Chromatography is based on the partition of a solute by a stationary phase. In Gas Liquid Chromatography the volatile solute is partitioned by a stationary liquid after being introduced at the column inlet as a plug of vapour. If the volatile solute is well characterised and a polymer substituted for the liquid stationary phase the polymer-solvent interaction can be studied. This technique is called Inverse Phase Gas Chromatography (I.G.C.)[42].

Normally the interaction is measured from the nett retention volume, given by :

$$V_N = (t_s - t_A)\, Q\, j \qquad 3.42$$

where t_s is the solvent peak elution time,

t_A is the non-interaction (usually air) peak elution time,

Q is the Carrier gas flow rate,

j is the Correction for Gas Compressibility

measured as $\frac{3}{2} \frac{\left[\left(\frac{P_1}{P_0}\right)^2 - 1\right]}{\left[\left(\frac{P_1}{P_0}\right)^3 - 1\right]}$

where P_i is the inlet pressure

and P_o is the outlet pressure

This quantity V_N can be considered to be :

$$V_N = K_L W_L + K_s A_s \qquad 3.43$$

where K_L is the Partition Coefficient for liquid phase,

W_L is the Weight of liquid phase,

K_s is the Partition Coefficient for surface adsorption,

and V_s is the Surface Area of stationary phase.

Guillet and Smidsrød have shown[98] that the activity coefficients can be measured for a polymer-solvent system only when the polymer is above its glass transition temperature (T_g).

In order to ensure that peak retention volumes are measured at equilibrium the values are extrapolated to zero flow rate. At this value :

$$V_g^o = \frac{V_N}{W_L} \times \frac{273.2}{T_E} \qquad 3.44$$

where V_g^o is the Retention Volume per gram of stationary phase corrected to 0^oC at zero flow rate,

T_E is the Experimental Temperature (^oK), and

W_L is the Stationary phase weight

Substituting Eqn. 3.43 in Eqn. 3.44 gives at constant temperature :

$$V_g = \frac{V_N}{W_L}\frac{273}{T_E} = K_L \frac{273}{T_E} + K_a\left(\frac{A_L}{W_L}\right)\frac{273}{T_E} \qquad 3.45$$

A plot of V_g^0 vs $1/\omega_L$ should give a straight line with an intercept of $K_L \times \frac{273}{T_E}$ which can be identified with V_g^0(Bulk) and so eliminate any surface contribution[99]. This also avoids any use of the Volume of Stationary Phase V_L which is subject to uncertainty.

Determination of the value of V_g^0 corresponding to bulk interaction means the polymer-solvent interaction parameter χ_{12} may be measured. If the coating consists of two compatible polymers, the polymer-polymer interaction parameter χ_{23} may be measured, provided χ_{12} and χ_{13} are known.

The relation between V_g^0 and the activity coefficient of the solvent is given by Young et al[100] as

$$\ln \gamma_1^{\infty} = \ln \left[\frac{(273.2\ R)}{(V_g^{o} p_1^{o} M_2)}\right] - \frac{p_1^{o}}{RT}(B_{11} - V_1) \qquad 3.46$$

where γ_1^{∞} is the mole fraction infinite dilution activity coefficient

p_1^{o} is the vapour pressure of the solvent

V_1 is the molar volume of the solvent

M_2 is the molecular weight of the stationary phase

and B_{11} is the second virial coefficient.

Problems associated with the use of M_2 lead to a treatment by Patterson[101] which introduces a weight fraction activity coefficient, such that :

$$\ln \left(\frac{a_1}{W_1}\right)^{\infty} = \ln \left[\frac{(273.2\ R)}{(V_g^{o} p_1^{o} M_1)}\right] - \frac{p_1^{o}}{RT}(B_{11} - V_1) \qquad 3.47$$

In this way the connection between experimental measurements and the interaction parameters is easily established, since from the Flory-Huggins theory :

$$\ln a_1 = [\ln \phi_1 + (1 - \frac{1}{r})\phi_2] + \chi_{12}\phi_2^{2} \qquad 3.48$$

since r is the ratio of the molar volume of the polydisperse polymer to the solute

$$r = \frac{(V_2)_n}{V_1} = \frac{(M_2)_n v_2}{V_1}$$

where $(V_2)_n$ is the number average molar volume

v_2 is the specific volume of the polymer

χ_{12} is the polymer-solvent interaction parameter and

ϕ is the volume fraction.

This leads to the result by combination of the above :

$$\chi_{12} = \ln \left(\frac{273.2\ R v_2}{V_g^{o}\ p_1^{o} V_1}\right) - \left(1 - \frac{V_1}{(M)_n v_2}\right) - \frac{p_1^{o}}{RT}(B_{11} - V_1) \qquad 3.49$$

Furthermore, the solution of the Flory-Huggins theory for three components by Scott[13] gives the expression :

$$\ln\left(\frac{a_1}{\phi_1}\right)^{\infty} = \left[1 - \frac{r_1}{r_2}\right]\phi_2 + \left[1 - \frac{r_1}{r_3}\right]\phi_3 \text{ (combinational)} +$$

$$\text{non-combinational } \left[\chi_{12}\phi_2 + \chi_{13}\phi_3 - r_1\left(\frac{\chi_{23}}{r_2}\right)\phi_2\phi_3\right] \equiv \chi_{1(23)} \qquad 3.50$$

which applies to a mixed column, where $\chi_{1(23)}$ is the interaction parameter between the solvent and a mixed column. Knowledge of χ_{12} and χ_{13} means that χ_{23}, the polymer-polymer interaction parameter, may be evaluated.

In this case, $r_i = \frac{V_i}{v}$, V_i and v being the molar volumes, and χ_{23} is expressed in terms of V_2 to avoid the arbitrary choice of polymer segment volume as favoured by Tompa[12]. Since :

$$\chi_{1(23)} = \left(\frac{\mu_1 - \mu_0}{RT}\right)_{\text{non combinational}} \qquad 3.51$$

Therefore :

$$\chi_{1(23)} = \left|\left(\frac{\chi_{12}}{V_1}\right)\phi_2 + \left(\frac{\chi_{13}}{V_1}\right)\phi_3 - \left(\frac{\chi_{23}}{V_2}\right)\phi_2\phi_3\right| V_1$$

$$= \ln\frac{273.2\ R(\omega_2 v_2 + \omega_3 v_3)}{p_1^0 V_g^0 V_1} - \left(1 - \frac{V_1}{V_2}\right)\phi_2 - \left(1 - \frac{V_1}{V_3}\right)\phi_3 - \frac{p_1^0}{RT}(B_{11} - V_1) \qquad 3.52$$

from which χ_{23} may be determined.

Recent theories of polymer solution thermodynamics[17] have also been applied to these problems. These include the effect of a difference in free volume between the components which leads to a volume change on mixing. The interaction between molecules is associated with surfaces of the molecules considered as 'hard cores'. Also, the combinational entropy is expressed in terms of segment fractions, which deal

with the hard core volumes, not the macroscopic volumes used in the familiar volume fractions of the Flory-Huggins theory.

When the stationary phase contains only one adsorbed component the usual expression is[101] from equation 3.49 :

$$\chi^* = \ell n \left| \frac{273.2\ R\ v_2^*}{V_g^{\,o} V_1^*\ p_1^{\,o}} \right| - \left| 1 - \frac{V_1^*}{M_2 v_2^*} \right| - \frac{p^{\,o}}{RT} (B_{11} - V_1) \qquad 3.52$$

This can be compared with the theoretical expression of Flory[17] which expresses χ^* as the sum of contributions from equation of state and contact interaction concepts :

$$\chi^* RT = P_1^* V_1^* \left\{ (3\tilde{T}_1\ \ell n \frac{\tilde{v}_1^{1/3} - 1}{\tilde{v}_2^{1/3} - 1} + \tilde{v}_1^{-1} - \tilde{v}_2^{-1}) + \frac{X_{12}}{P_1^* \tilde{v}_2} \right\} \qquad 3.53$$

where starred terms relate to hard-core volumes,

$$(\tilde{v})^{1/3} = \frac{1 + \alpha T}{3(1 + \alpha T)}\ , \quad \tilde{T} = \frac{T}{T^*} = (\tilde{v}^{1/3} - 1)/\tilde{v}^{4/3}$$

where α is the thermal expansion coefficient.

The first term in the Flory expression arises from differences in the thermal expansion coefficients, and the second arises from potential differences in the components identified by the contact interaction parameter χ_{12} .

Patterson et al[102] have identified χ_{12} normalised to s_i (molecular surface : volume ratios) with the experimental interfacial free energy. In an extension to the above treatment they derived an expression for $\chi_{1(23)}^*$ in a column containing two compatible polymers.

$$\left(\frac{\mu_1 - \mu_1^{\,0}}{RT} \right)_{\text{noncomb}} = \chi_{1(23)}^* = \left[\left(\frac{X_{12}}{s_1} \right) \theta_2 + \left(\frac{X_{13}}{s_1} \right) \theta_3 - \left(\frac{X_{23}}{s_2} \right) \theta_2 \theta_3 \right]$$

$$\times \left[\frac{s_1 M_1 v_1^*}{RT}\ (\tilde{U}(\tilde{T}_0)) \right] + \left[\tilde{U}(\tilde{T}_0) - \tilde{U}(\tilde{T}_1) + \tilde{T}_1 \{ \tilde{S}(\tilde{T}_1) - \tilde{S}_0(\tilde{T}_0) \} \right] \times \frac{P_1^* M_1 v_1^*}{RT} \qquad 3.54$$

If the hard-core volumes are substituted in the normal expression for χ^*_{23}, the value of χ^*_{23} may be determined from[42]:

$$\left|\frac{\chi^*_{23}}{V_2^*}\right| \theta_2\theta_3 V_1^* = \ell n \frac{273.2\ R\ (\omega_2 v_2^* + \omega_3 v_3^*)}{P_1^o V_g^o V_1} - \left(1 - \frac{V_1^*}{V_2^*}\right)\theta_2 - \left(1 - \frac{V_1^*}{V_3^*}\right)\theta_3$$

$$- \frac{P_1^o}{RT}(B_{11} - V_1) - \chi^*_{12}\theta_2 - \chi^*_{13}\theta_3 \qquad 3.55$$

where θ_i is the surface fraction $= \dfrac{\omega_i v_i^* S_i}{\Sigma\, \omega_i v_i^* S_i}$

From this value the exchange energy can be calculated.

It has been shown that the technique of Inverse Gas Chromatography can give information on the interaction between a polymer and various solvents, between polymers and surfaces, and between compatible polymers. The absolute values are open to some criticism, but the use of the technique in detecting transitions in isothermal studies will be shown to be of importance in investigating polymers in composite.

3.10.2 Polymer-Solvent Interactions

The apparatus used was a Pye Unicam 104 series Gas Chromatograph (GC) which was fitted with a thermal conductivity detector and other ancilliaries, as in Fig. (3.52). Helium was used as the carrier gas and the flow rate was measured with a soap-bubble flow meter. P.T.F.E. beads (40 - 60 mesh) were supplied by Phase Separations Ltd. A 5% solution of the polymer in 2-butanone (M.E.K.) was prepared by warming a known weight of pure polymer with the solvent to 50°C. The appropriate weight of P.T.F.E. beads ($\sim$ 10g) was then added, and the mixture stirred with a magnetic stirrer bar in a stream of air. When the mixture became viscous, stirring was continued using a spatula to prevent aggregation. The beads were then dried at 50°C

for 24 hours at 10^{-2} torr. These beads were then screened in a 15 mesh B.S.S. sieve. Finally the screened beads were loaded into a 160 cm glass column of 4 mm outer diameter.

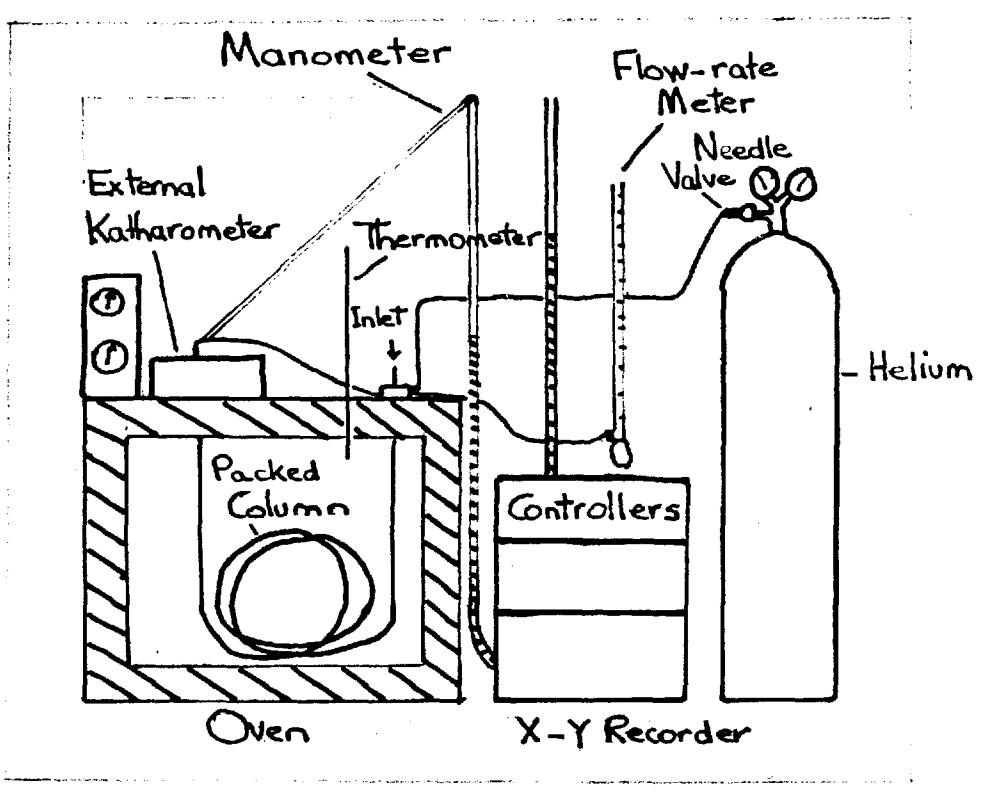

Fig. (3.52) The apparatus for I.G.C. studies

The packed column was inserted in the oven of the G.C. for equilibration for 12 hours at the experimental temperature. Injections were normally 0.1 µl measured by a S.G.C. B17 1 µl syringe supplied by Scientific Glass and Engineering Ltd. Solvents used were A.R. grade, as supplied by B.D.H. Silicone septa, used as seals for the injector, were replaced often to prevent leaks and maintain a constant flow rate.

For most experiments the loading was approximately 15% wt/wt of polymer on the P.T.F.E. Some experiments on the effect of loading used different quantities of polymers. In general, peaks obtained were symmetrical, and the retention times measured relative to air were not found to vary greatly with the quantity of solute

injected. Measurements were carried out in triplicate and the values were then extrapolated to zero flow rate. A typical extrapolation is shown in Fig. (3.53).

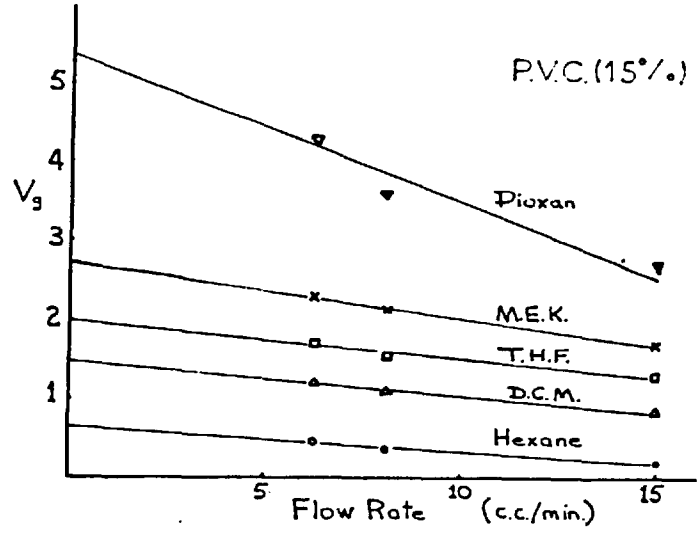

Fig. (3.53) The evaluation of V_g° for a P.V.C. column

In accordance with the recommendations of Prausnitz and Newman[103], the flow rates were kept as low as possible. Values of χ_{12} and χ_{12}^* were determined for each experiment from equations 3.49 and 3.52. The solvent parameters for these calculations were obtained from the literature[104-107]. The Fortran programs used to calculate these are shown in Appendix 1.

Weights of polymer loading were checked by extraction in T.H.F. and gravimetric analysis[108]. The results were found to agree closely with the calculated loading value.

It is apparent from equation 3.45 that there may be a surface component contributing to the sorption which determines the retention volume. P.T.F.E. is considered inert by most authors[103], but the surface area of P.T.F.E. has been measured as 20 m^2/g[109]. If the P.T.F.E. beads are run alone, it is impossible to obtain V_g in equation 3.45 as the mass of coating is zero. Because of this, the mass term was

altered to the total weight of support and polymer coating. In the original theories of Young et al[100] the volume is used, but the weight is more accurately known due to the uncertainty of the density of polymers near surfaces.

A plot of V_g (total) against the weight loading shows the influence of coating thickness from equation 3.45, shown in Fig. 3.54.

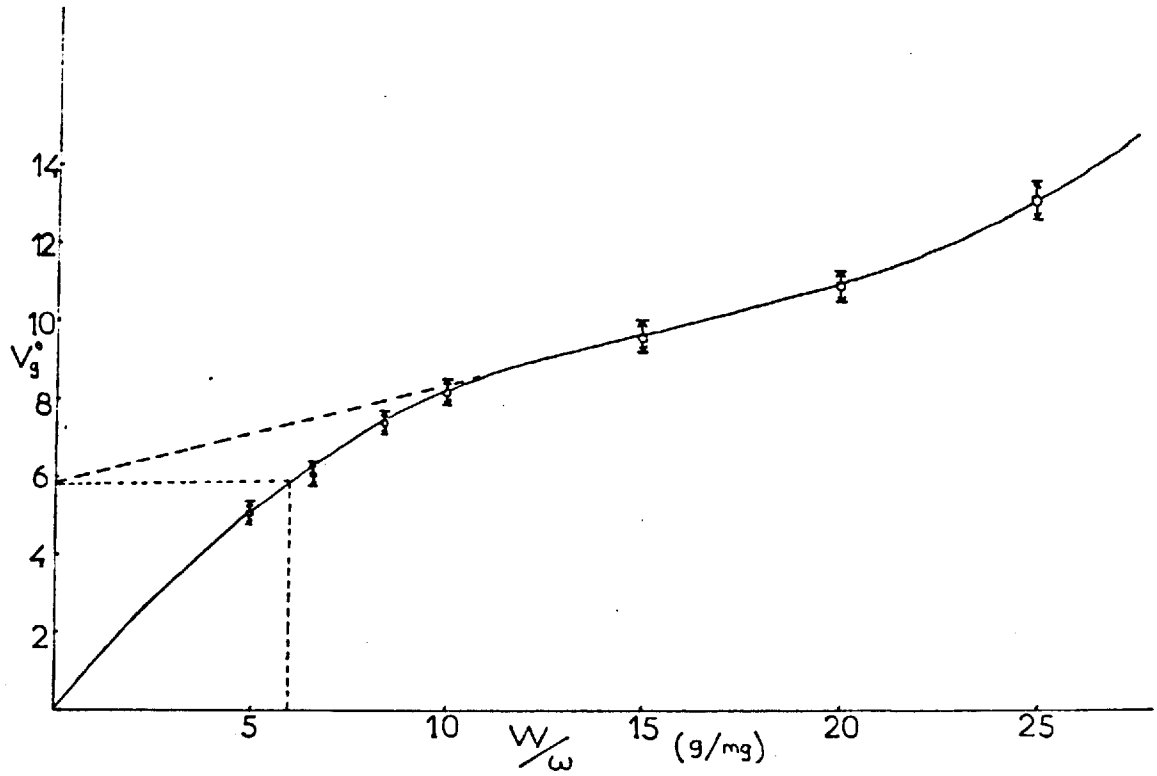

Fig. (3.54) The variation in retention volume with coating thickness

Above 20 the surface influence dominates, and below 10 there are rate effects due to diffusion control.

Extrapolation of the linear section of this curve shows that the use of approximately 15% wt. coverage is equivalent to bulk polymer (infinite coverage). The logarithmic term in equation 3.49 reduces the error caused by using other coverages. However, it is evident that coverages less than 5% will result in spuriously high values of V_g and hence χ due to the interaction of the solvent with the surface[110]. Such problems suggest the technique should be more standardised and a non-porous inert support should be used. Glass spheres coated with Dimethylchlorosilane (D.M.C.S.) would have

Solvent	Pure S.C.P.E. 20% (Coverage)	Pure S.C.P.E. 10% (Coverage)	Blend SCPE: PVC 3 : 1	Blend (100°C) SCPE : PVC 1 : 1	Blend SCPE : PVC 1:3	Blend SCPE: PVC 1: 5
Hexane	1.08	1.11	1.69	1.66	2.79	2.90
D.C.M.	.56	.91	.84	.85	1.37	1.46
$CHCl_3$	.45	.61	.81	.75	1.42	1.66
Acetone	.87	.99	1.04	.44	1.48	1.54
T.H.F.	.21	.43	.59	.41	.99	1.33
Dioxan	.39	.65	.74	.57	1.13	1.37
CH_3CN	1.61	1.89	1.62	1.65	1.98	1.92
M.E.K.	.41	.76	.75	.65	1.07	1.31
Ethyl Acetate	.52	.86	.86	.80	1.37	1.52
n-Propanol	1.54	1.86	1.84	2.01	2.48	2.47

Table 7 Polymer-Solvent Interaction Parameters for various solvents *

* 120°C (or as indicated)

Coverage (wt.) Pure P.V.C.	5%	6.8%	10%	12%	15%	20%	15% at 130°C	15% at 140°C	15% at 150°C
Hexane	1.33	1.48	1.86	3.61	2.78	3.07	2.07	2.42	2.89
DCM	.65	1.11	1.14	1.44	1.43	1.96	1.71	2.04	2.08
$CH Cl_3$	1.08	1.05	1.17	1.65	1.73	2.28	1.62	2.05	2.32
Acetone	1.02	.96	1.08	1.32	1.63	1.58	1.65	1.99	2.42
T.H.F.	.39	.66	.80	.93	1.33	1.72	1.46	1.66	1.74
Dioxan	.67	.89	1.08	1.54	1.44	1.95	1.62	1.79	1.89
CH_3CN	1.51	1.94	1.94	1.78	2.11	2.34	2.59	2.83	3.01
M.E.K.	.59	.81	1.07	1.22	1.50	1.82	1.69	1.78	1.88
Ethyl Acetate	.61	.93	1.23	1.46	1.58	2.07	1.61	2.04	1.85
n-Propanol	1.55	1.87	1.97	2.29	2.47	2.89	2.35	3.00	2.70

Table 7 (continued) Polymer-Solvent Interaction Parameters for various solvents

* 120°C (or as indicated)

Solvent	Pure SCPE 20% (Coverage)	Pure SCPE 10%	P.V.C. : C.P.E. Blend 25% wt.	Blend 50% wt. (100°C)	75% wt.	85% wt.
Hexane	1.16	1.19	1.78	1.76	2.90	3.02
D.C.M.	.64	.99	.93	.96	1.49	1.58
$CHCl_3$	.52	.68	.89	.84	1.53	1.77
Acetone	.96	1.08	1.14	1.06	1.61	1.67
T.H.F.	.25	.47	.64	.47	1.06	1.41
Dioxan	.43	.69	.79	.63	1.21	1.45
CH_3CN	1.70	1.98	1.22	1.76	2.1	2.04
M.E.K.	.48	.83	.83	.75	1.19	1.42
Ethyl Acetate	.60	.94	.94	.91	1.48	1.64
n-Propanol	1.55	1.87	1.86	2.05	2.53	2.52

Table 8 Equation of State interaction parameters for various solvents *

Pure P.V.C. Coverage (wt.)	5%	6.8%	10%	12%	15%	20%	15% at 130°	15% at 140°	15% at 150°C
Hexane	1.45	1.60	1.99	3.73	2.91	3.19	2.19	2.53	3.00
DCM	.77	1.23	1.27	1.56	1.86	2.08	1.83	2.16	2.20
$CH Cl_3$	1.19	1.16	1.28	1.76	1.84	2.39	1.73	2.16	2.42
Acetone	1.15	1.09	1.22	1.46	1.77	2.01	1.78	2.12	2.54
T.H.F.	.47	.75	0.89	1.02	1.41	1.80	1.54	1.74	1.82
Dioxan	.76	.97	1.16	1.62	1.52	2.03	1.69	1.88	1.97
CH_3CN	1.64	2.06	2.07	1.90	2.24	2.47	2.72	2.96	3.13
M.E.K.	.71	.92	1.18	1.34	1.61	1.94	1.80	1.89	1.98
Ethyl Acetate	.73	1.05	1.35	1.59	1.71	2.20	1.73	2.16	1.97
n-Propanol	1.61	1.93	2.03	2.36	2.53	2.95	2.41	3.06	2.74

Table 8 (continued) Equation of State interaction parameters for various solvents

minimum surface forces, but only glass beads have been used with some success[99].

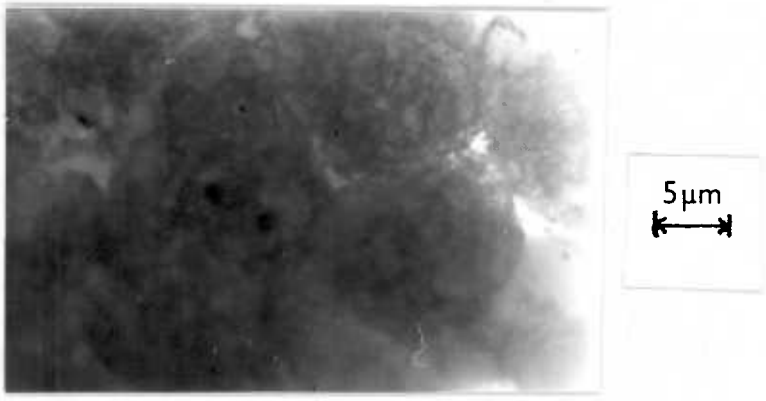

Fig. (3.55) A micrograph from the Zeiss microscope of a section from a P.T.F.E. bead coated with P.V.C. is shown in Fig. (3.55). The P.V.C. appears darker as it has a higher refractive index. The pores in the P.T.F.E. particles are immediately apparent.

Results of the calculations for χ and χ^* are listed in Tables 7 and 8 respectively.

3.10.3 Polymer-Polymer Interactions

The Flory-Huggins polymer-polymer interaction parameter χ_{23} and those of the Equation of State χ_{23} and χ^*_{23} can be calculated from the results in Tables 7 and 8, using equations 3.52 and 3.54.

Table 9 lists the values obtained for the mixed columns.

This technique is only valid for compatible polymers. If phase separation occurs on heating, there will be a discontinuity corresponding to the temperature of phase separation. Fig. (3.56)[a] shows the results of a number of experiments carried out to determine how V_g would vary with temperature. The column containing a mixed polymer of 15% wt coating on P.T.F.E. was injected with solvents to measure V_g

Solvent	$\left[\frac{\chi_{23}}{V_2}\right]$ at 120 °C Blend 25% PVC	75% PVC	85% PVC
Hexane	+0.0021	- 0.015	- 0.018
DCM	+0.0008	- 0.014	- 0.019
$CHCl_3$	+0.0025	- 0.0023	- 0.011
Acetone	+0.0055	- 0.004	- 0.003
THF	- 0.0007	+0.0023	- 0.014
Dioxan	- 0.0005	+0.001	- 0.008
MEK	+0.0006	- 0.009	+0.002
Ethyl Acetate	- 0.0005	- 0.003	- 0.006
Propanol	- 0.0002	+0.015	- 0.013
	$\left[\frac{\chi^*_{23}}{V_2}\right]$ at 120 °C		
Hexane	- 0.004	+0.021	- 0.028
DCM	+0.002	- 0.007	- 0.018
$CH\,Cl_3$	+0.008	- 0.0001	- 0.015
Acetone	+0.012	- 0.0008	+0.002
THF	+0.007	+0.013	- 0.016
Dioxan	+0.010	+0.011	+0.0004
MEK	+0.014	+0.02	+0.014
Ethyl Acetate	+0.012	+0.004	- 0.001
Propanol	+0.016	- 0.013	+0.012

Table 9 Polymer-Polymer interaction parameters calculated from Tables 7 and 8

at temperatures 5°C apart. These measurements were made after 30 minutes for equilibration to ensure isothermal conditions were used.

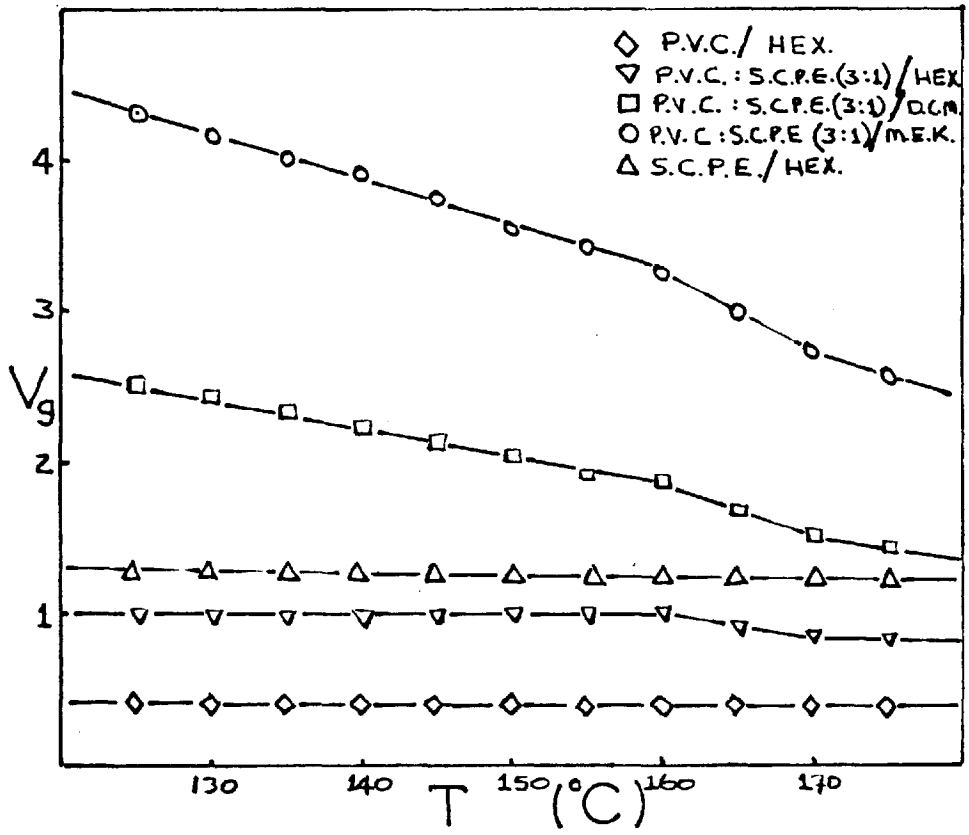

Fig. (3.56)[a] A plot of V_g against temperature for mixed columns

Three of the solvents show the transition more markedly, and these are the solvents 2-butanone, dichloromethane and benzene.

If the temperature of deviation from linearity is taken as the point of phase separation, a phase diagram can be constructed. This was important for low ratio mixtures where other techniques had not been successful.

Fig. (3.56) shows the results of this procedure. (See next page)

Results from the technique of I.G.C. have shown that it is not capable of systematic results for polymer-solvent interactions. Variation in the literature is extensive and the technique requires further development before these can be considered reliable. However, it is an excellent technique for determining transitions, as shown by its ability to produce this phase diagram.

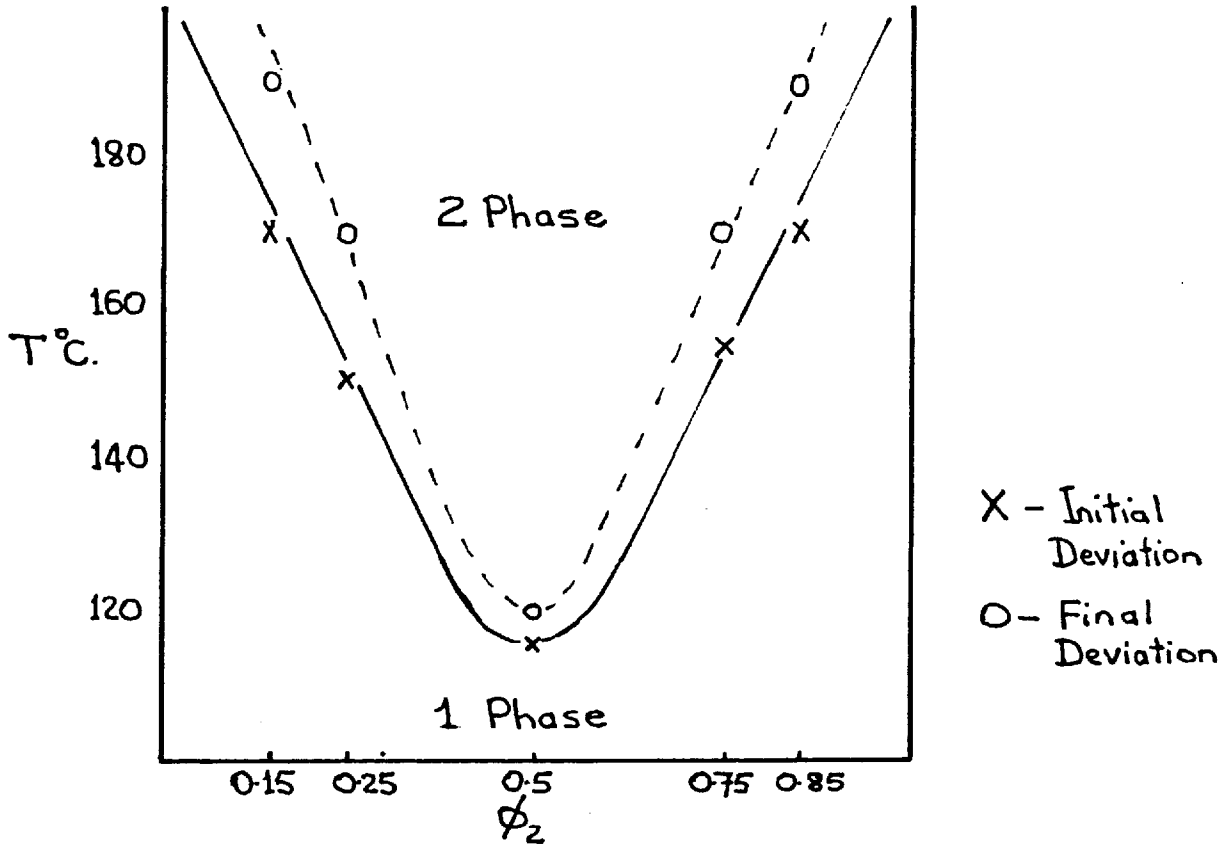

Fig. (3.56) The phase diagram obtained by I.G.C.

CHAPTER 4

MEASUREMENT OF POLYMER - FILLER INTERACTIONS

4.1 Introduction

The measurement of interactions between mineral surfaces and bulk polymers has been limited by the difficulty of establishing rapid equilibrium for viscoelastic materials. This problem precludes the possibility of directly measuring the heat of adsorption for the bulk polymer. Normal techniques for adsorption studies from solution are limited by the complexity of the solvent interaction with the surface. Because of these problems, most work has been directed at estimating the polymer-surface interaction after it has been formed. The most important techniques have been both visible and electron microscopy, but particularly scanning electron microscopy, in observing the mechanism of failure. Another technique which has been used with some success to determine the thickness of adsorbed films has been ellipsometry, but this is limited to transparent polymers. For some substrates, Infra-Red Spectroscopy has been used very successfully in determining the existence of chemisorption and estimating the strength of physisorption. Particularly useful is the Si OH absorption, which can be accurately measured using a high resolution Infra-Red spectrometer.

The most important parameter in polymer-surface interactions is the free energy of adsorption, also called the work of adhesion[44]. Such quantities as the particle size and size distribution or the degree of dispersion relate to the surface area of contact. The object of this investigation was to examine the interactions in the system chosen, and to quantify them. This was attempted using Differential Scanning Calorimetry (D.S.C.) and Inverse Gas Chromatography (I.G.C.). These results were then tested by mechanical measurements on Kaolin-polymer composites.

4.2 D.S.C.

The apparatus was the Perkin-Elmer D.S.C.-2 described in 3.6.2. Kaolin was prepared by heating to 120°C for two hours and then stored under nitrogen. The D.S.C. trace for 20 mg Kaolin did not have any endotherm for water desorbing from the surface of the clay from 100 - 200°C.

Traces obtained for P.V.C. and S.C.P.E. also gave no significant peaks in the range 50°- 200°C.

Films of P.V.C. or S.C.P.E. cast from M.E.K. and Kaolin which had been coated with M.E.K. were run on the D.S.C. In all cases, there was an endotherm for the solvent near its boiling point and no other change.

The surface area of Kaolin has been given as 20 m^2/g,[48] and the loading to produce a monolayer in other studies as 10 mg/g [34]. Thus, the quantity for a monolayer on 20 mg Kaolin was 0.5×10^{-3} mg polymer. This was added as 0.05 ml of a solution of 1.0 mg of polymer in M.E.K. The solvent was allowed to evaporate and the mixture run in the D.S.C. The solvent endotherm was present at 85°C, but there were extra peaks at 170°C (Fig. 3.57).

Problems with the apparatus precluded further studies of this type. The results were inconclusive.

The manufacturers of the S.C.P.E. have suggested that the reaction[111]

$$RSO_2Cl + MOH \rightarrow (RSO_2) - OM + HCl$$

(where MOH is any species with an active hydrogen) may occur on heating the S.C.P.E., due to the sulfonyl chloride groups present.

It is possible that D.S.C. could be used to measure the heat of reaction, such as that postulated in the solid or molten state, but that has not been proved.

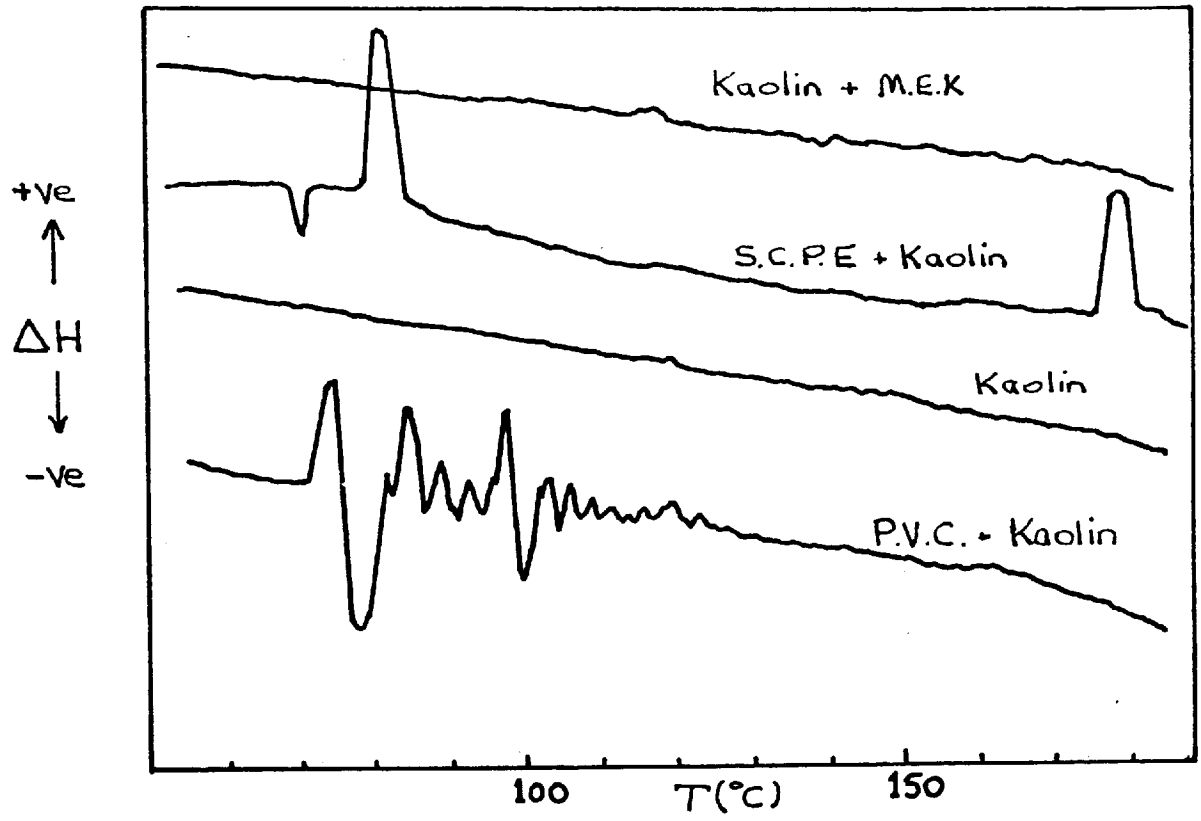

Fig. (3.57) D.S.C. traces for polymers adsorbed on Kaolin

4.3 Inverse Gas Chromatography (I.G.C.)

4.3.1 Theory

From the review by Guillet and Braun[42] it is apparent that the technique of I.G.C. is very sensitive to the influence of the underlying stationary phase - so much so that it is normal to resort to so-called 'inert' supports such as Polytetrafluoro-ethylene (P.T.F.E.) and Silane treated Glass Spheres. The technique has been used to measure adsorption isotherms for solvents on various solids, including polymers below their

T_gs[112], where physisorption is the main mechanism. One of the principal assumptions of the technique is that for an equilibrium partitioning process the chemical potential of the solvent sorbed on the polymer when the polymer coating is 50° above its glass transition.

$$\mu_{solvent/vap} = \mu_{solvent/polymer}$$

It has already been mentioned that the conformation of a polymer on a surface is determined by the extent of interaction with the surface[34]. The solvent can be used to probe the variation of the chemical potential of the polymer on the surface, as the surface coating is increased. It would be expected that at some point the polymer should reach theta dimensions when the influence of the surface diminishes. The distance to reach this value should give a measure of the interaction with the surface. Each measurement is separate and the column packings are prepared independently for isothermal testing.

4.3.2 Experimental and Results

The apparatus used was the same as that described in 3.10.2. Approximately 5g Kaolin was dried at 120°C for 2 hours for the column packings. The required weight of polymer was dissolved in 50 c.c. of 2-butanone, and this solution was added rapidly to the dry Kaolin. This suspension was stirred with a magnetic stirrer as the solvent was evaporated in a stream of air. Stirring was continued using a spatula to prevent aggregation when the suspension became viscous. As polymer loadings were increased, the packings had a marked tendency to aggregate, and it was necessary to grind the composition in a mortar and pestle. The packings were then dried for 24 hours at 50°C and 10^{-2} torr. Glass columns were packed by connecting a vacuum to one end of the column, and applying the other end to the stationary phase. The packed columns were loaded in the oven for equilibration at the experimental

temperature. As the retention times varied with the injection quantity for asymmetric points this was standardised at 0.1 µl.

Results for the various columns are listed in Table 10.

It was noticeable that the asymmetry of the peaks decreased as the column loading was increased. This change occurred at similar loadings as the tendency to aggregate was observed. When the V_g values are calculated for high loadings as a function of polymer weight only, the results are equivalent for Kaolin and P.T.F.E., indicating the absence of a support effect.

Fig. (3.58) shows the result for V_g values calculated on the total weight of packing (i.e. Kaolin and polymer) as a function of the loading of the polymer on the Kaolin.

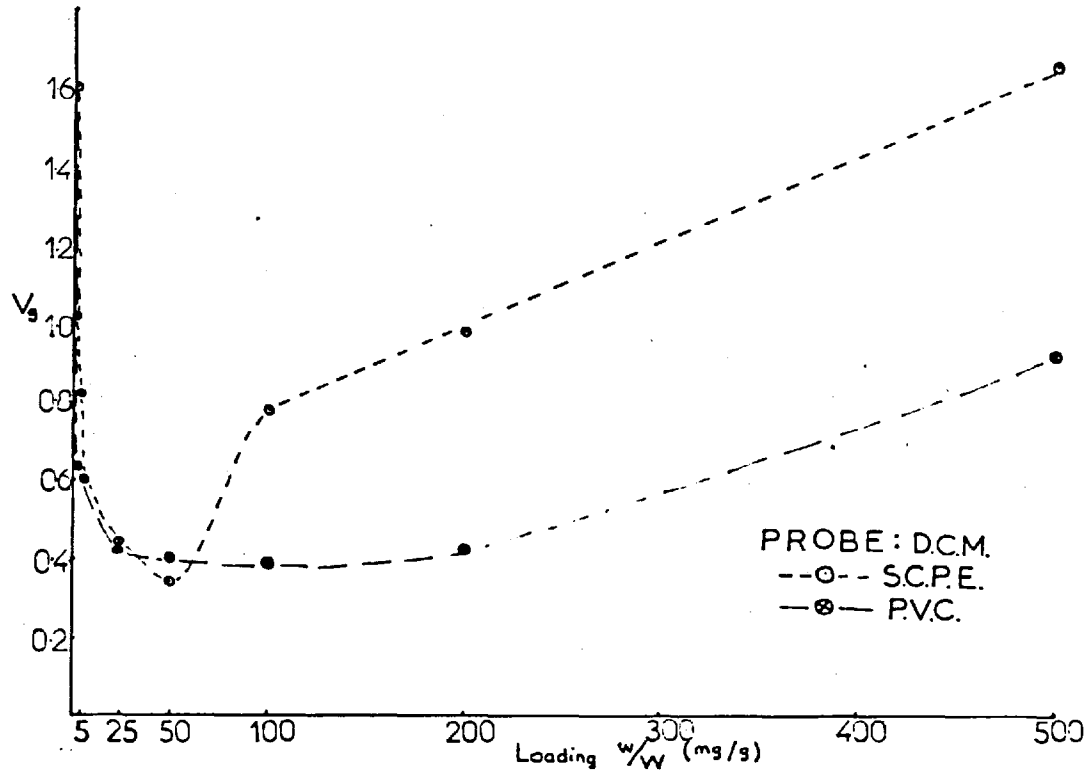

Fig. (3.58) The effect of polymer coverage on V_g for Kaolin

This shows a marked minimum which should correspond to the formation of a monolayer where the polymer 'screens' the active surface of the clay. At some further point the polymer exhibits bulk (theta) dimensions, and the value of V_g

becomes effectively constant. The results vary for different probes but are consistent for molecules which are solvents for both polymers.

This can be seen by combining equation 3.43 and 3.44 to give :

$$V_g = \frac{V_N k}{W_L + W_s} \qquad 3.56$$

where W_s is the weight of support.

As the weight of polymer becomes large, V_N will be proportional to the weight of polymer only. As the denominator increases, the value of V_g will tend to become constant. Any non-equilibrium effects would result in V_g decreasing with increasing polymer loading.

The minimum for S.C.P.E. was at lower loadings than that for P.V.C., and the increase in V_g was greater. This suggests the S.C.P.E. may adsorb more strongly on the clay.

The results for P.T.F.E. beads coated with P.V.C. may be plotted in a similar fashion, and the results are shown in Fig. (3.59).

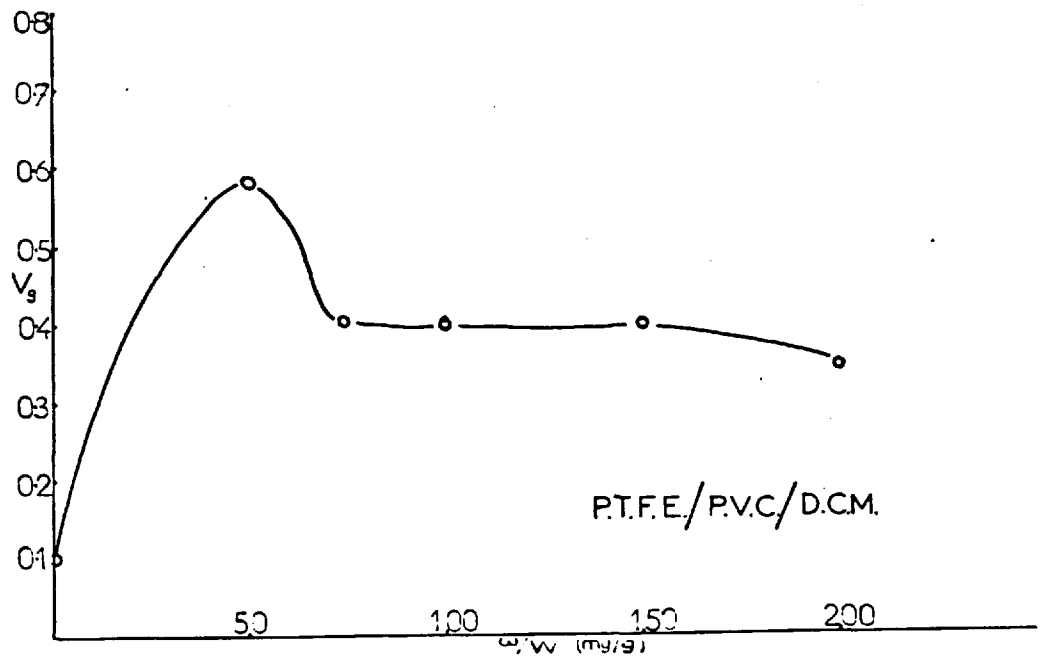

Fig. (3.59) The effect of polymer coverage on V_g for P.T.F.E.

V_g per g stationary phase for the system S.C.P.E./Kaolin								
Column	I	II	III	IV	V	VI	VII	VIII
Loading mg/g	0	1	5	25	50	100	200	500
Solvent								
Hexane	1.46	0.82	0.66	0.33	0.21	0.49	0.58	0.78
Dichlomethane	1.60	1.02	0.82	0.44	0.34	0.78	0.98	1.67
Chloroform	1.74	1.23	1.15	0.59	0.52	1.11	1.53	2.6
Acetone	45.06	26.38	20.40	9.43	6.19	2.63	2.62	3.5
T.H.F.	34.69	20.20	12.17	7.77	4.82	3.18	3.27	5.3
Dioxan	38.82	21.44	12.10	5.35	3.96	4.78	4.80	8.1
Acetonitrile	28.43	20.61	15.30	5.77	4.73	5.3	5.61	6.29
2 Butanone	59.7	34.63	22.04	6.1	3.3	2.97	3.86	6.0
Ethyl Acetate	45.76	39.57	25.33	5.66	3.1	2.92	2.97	3.0
n-Propanol	36.86	26.38	18.75	8.88	6.45	4.24	5.19	6.67
Polymer SCPE								
V_g per g stationary phase for the system P.V.C./Kaolin								
Solvent								
Hexane	1.46	0.52	0.41	0.30	0.20	0.18	0.15	0.28
Dichloromethane	1.60	0.63	0.60	0.42	0.40	0.39	0.42	0.92
Chloroform	1.74	0.74	0.74	0.51	0.50	0.48	0.50	1.1
Acetone	45.06	23.22	16.18	3.45	3.04	2.05	1.87	2.9
T.H.F.	34.69	13.76	9.96	3.85	2.68	2.22	1.87	3.28
Dioxan	38.82	15.4	14.3	4.68	3.51	2.93	2.85	5.63
Acetonitrile	28.43	17.18	14.3	3.66	3.22	2.65	3.15	7.13
2-Butanone	59.7	20.00	20.5	4.27	4.05	3.60	2.91	4.99
Ethyl Acetate	45.76	26.66	19.9	7.32	5.41	2.29	1.37	3.31
n-Propanol	36.86	19.78	19.9	13.42	6.72	3.37	3.49	4.80
Polymer P.V.C.								

Independent of sample size

Table 10 Table of V_g at different surface coatings

These results indicate a different mechanism to simple monolayer formation. There is a finite adsorption term and this is consistent with the quoted surface area of 20 m^2/g.[109] This value may be explained by the fact that the beads of $\sim$ 100μ diameter consist of sintered smaller beads of $\sim$ 2μ diameter. Both morphologies may contain capilliaries and this would explain the result in Fig. (3.59) as a 'pore filling' mechanism. Such an explanation is consistent with the morphology of the P.T.F.E. beads, as shown in Fig. (3.55). This question has been discussed by Conder[113], who was not able to resolve the matter.

All these results are different from those of Kieselev et al[41]. They found that V_g remained constant over three degrees of coverage after monolayer formation in the system Polyethylene glycole/rutile.

Another important result was that the drying of the Kaolin was critical to the results. Any Kaolin which was not dehydrated as specified gave higher values of V_g in the region of monolayer formation. This implies the adsorbed water was interfering in the adsorption process of the polymer.

These results demonstrate the use of I.G.C. in observing qualitative changes in states of matter, but not in obtaining quantitative results.

4.4 Preparation and Mechanical Testing of Composites

Composites were prepared on two different scales, the 30 c.c. Brabender Mixing Chamber, and the 2 kg Laboratory Banbury. Both are twin-rotor intensive internal mixers. Compositions were prepared as in 3.2 , and the scale of mixing is listed in Table 11. In these preparations the Kaolin was not normally pre-dried as this step should occur in the mixer. Each composition was tested in the Rheovibron, as described in 3.3.2.

In each case the samples were formed into an ASTM tensile dumbell (by

No.	P.V.C.	S.C.P.E.	KAOLIN	T°C	Quantity	T_g
1	100	100	100	160°	30 g	76°C
2	100	100	50	"	"	80°
3	100	0	100 (wet)	160°	30 g	88°
4	100	0	100 (dry)	160°	"	88°
5	100	0	100	180°	2 kg	86°
6	100	1	100	180°	2 kg	86°
7	100	10	100	180°	2 kg	86°
8	100	100	100	180°	2 kg	82°
9	100	0	0	180°	2 kg	84°
10	90	10	0	160°	30 g	82°

Table 11 Glass transition temperatures of composites

Sample	Composition	Initial Modulus (MN/m^2)	U.T.S. (MN/m^2)	Elongation at Break (%)	Charpy Impact $J/m^2 \times 10^3$
1	100 PVC 0 SCPE	2900	56.5	1.5	1.4
2	90 PVC 10 SCPE	3200	49.1	33	4.5
3	80 PVC 20 SCPE	1800	26.8	92	88.7
4	70 PVC 30 SCPE	1100	15.7	115	165
5	60 PVC 40 SCPE	610	15.0	152	169
6	100 PVC 0 SCPE 100 Kaolin	5460	35.9	1	2.0
7	100 PVC 1 SCPE 100 Kaolin	4900	55.3	3	1.7
8	100 PVC 10 SCPE 100 Kaolin	7850	51.5	6	2.6
9	100 PVC 25 SCPE 100 Kaolin	5090	42.0	13	3.0
10	100 PVC 50 SCPE 100 Kaolin	1470	16.9	89	8.5
11	100 PVC 100 SCPE 100 Kaolin	600	10.6	149	22.2
12	90 PVC 10 HCPE	2740	43.8	59	15.4
13	100 PVC 25 HCPE 100 Kaolin	4050	30.4	2	5.4

Table 12 Mechanical Properties of Composites

PVC : SCPE : Kaolin			Charpy Impact $Jm^{-2} \times 10^3$	G_c $Jm^{-2} \times 10^3$	γ_c $Jm^{-2} \times 10^3$	$W_{ads.}$ $Jm^{-2} \times 10^3$
100	0	0	1.4	1.6	0.8	77
90	10	0	4.5	5.0	2.5	77
80	20	0	88.7	100	50	77
70	30	0	165	185	93	77
60	40	0	169	190	95	77
100	0	100	2.0	2.3	1.2	243
100	1	100	1.7	1.9	0.9	243
100	10	100	2.6	2.9	1.5	281
100	25	100	3.0	3.4	1.7	281
100	50	100	8.5	9.6	4.8	281
100	100	100	22.2	25	12.5	281

Table 13 A comparison of surface free energy at fracture and in bulk

compression moulding) and using the I.C.I. router. The Ultimate Tensile Stress, Yield Stress, Youngs Modulus and elongation at break were then measured using an Instron Tensile tester according to A.S.T.M. D 1708-66 (1970) .

The composites were also tested according to the Charpy Impact test, using a blunt notch of 1 mm depth and radius of curvature 0.25 mm.

The results from these tests are given in Table 12.

The increase in impact strength in samples 1 - 5 is offset by the decrease in tensile properties. Similarly, in sample 6 - 11 the impact strength increases; however, samples 7 and 8 have superior tensile and impact properties. This implies the S.C.P.E. is effective at low loadings in modifying the impact properties, whilst not detracting from the tensile properties. It is possible that the elastomer is acting as a process aid, which improves dispersion of the Kaolin.

The mechanical properties of the different compositions prepared can now be discussed in terms of the interactions of the components. Most important is the effect of the S.C.P.E. on the Kaolin, as this influences the impact strength of the composites. From the expression of Williams[48] the value of the fracture toughness (G_c) may be calculated. From the fracture toughness and the Griffiths condition the surface fracture energy can be calculated. This can then be compared with the calculated work of adhesion W_{ADS} from equation (2.54), with values obtained from references 44 and 49, assuming $\gamma_{kaolin} \simeq \gamma_{mica}$. (Table 13)

It is also possible to calculate from reference 48 the critical crack length and crack opening displacement. These values are respectively 0.2 mm and 28 μ for P.V.C. and 1.3 mm and 46 μ for P.V.C./Kaolin.

This shows the substantial difference between the observed and theoretical values. The examples where these are similar are due to viscoelastic losses during fracture, so L.E.F.M. is not valid.

The values obtained for Young's Modulus for these compositions can be compared with those obtained from equation (2.55). These may also be compared with values predicted by the 'Law of Mixtures', which assumes perfect adhesion[53]:

$$E_c = E_p\phi_p + E_{f_2}\phi_{f_2} \qquad (3.57)$$

where : E_c is the modulus of the composite, E_p is the modulus of the polymer, E_f the modulus of the filler, ϕ_p the volume fraction of the polymer, and ϕ_f the volume fraction of the filler. E_f is taken as 20 GN/m^2 for Kaolin (Granite is 30 GN/m^2).

Composition	E_{exp}	$E_{calc.}$	$E_{L.O.M.}$
PVC : SCPE : Kaolin	$GN\,m^{-2}$	$GN\,m^{-2}$	$GN\,m^{-2}$
100 : 0 : 0	2.9	2.9	2.9
90 : 10 : 0	3.2	3.6	2.6
80 : 20 : 0	1.8	4.4	2.3
70 : 30 : 0	1.1	5.1	2.0
60 : 40 : 0	0.6	6.5	1.7
100 : 0 : 100	5.5	5.5	9.1
100 : 1 : 100	4.9	5.5	9.0
100 : 10 : 100	7.8	5.7	8.4
100 : 25 : 100	5.1	6.2	7.6
100 : 50 : 100	1.5	6.7	6.7
100 : 100 : 100	0.6	7.7	5.6

Table 14 A comparison of calculated and experimental values of Young's Modulus

These values show the difference in the potential and realised values for the modulus of composites. The Law of Mixtures is inferior to the equation (2.55), except when there is a large quantity of elastomer present.

It is possible that the elastomer acts as a processing aid to dispersion which reduces high energy Kaolin - Kaolin interfaces and voids. The proportion of elastomer is critical for improving the mechanical properties. It may be possible to improve these results by varying the level of S.C.P.E. from 5 - 25 g/100 g Kaolin.

4.5 Electron Microscopy

The apparatus used in this work was the same as that in Section 3.5. Initial investigations made on the JEM 100B were of sections from samples containing 100 : 100 g of P.V.C. : S.C.P.E. : Kaolin (Sample 11). This showed the structure reproduced in Fig. (3.60).

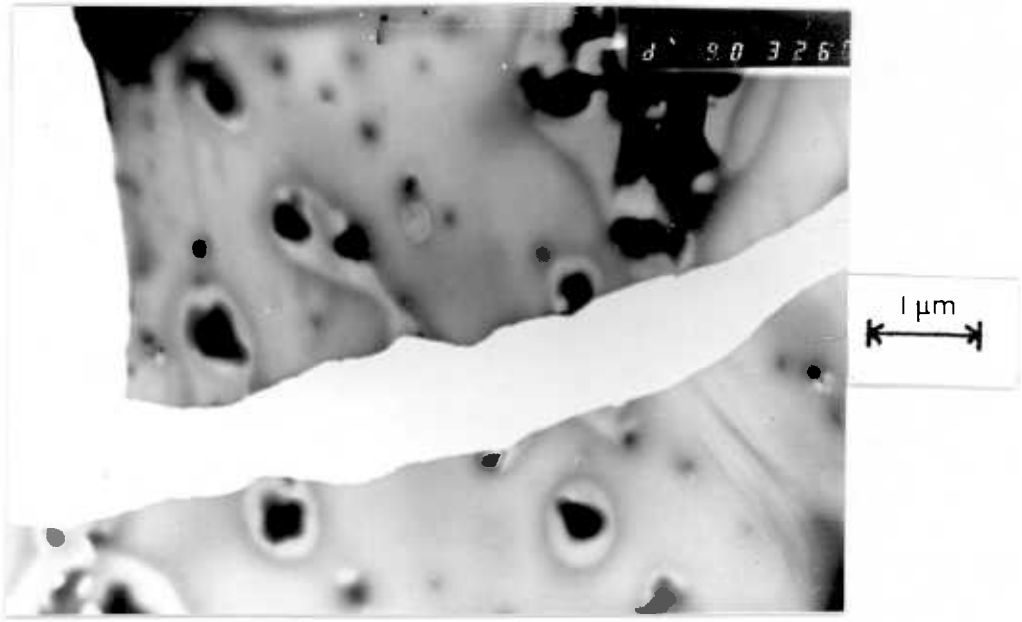

Fig. (3.60) The microstructure of P.V.C./S.C.P.E./Kaolin composites

It is not possible to resolve the origin of the contrast on a normal T.E.M., but it is possible to observe crystalline regions by electron diffraction. Fig. (3.61) is the diffraction pattern from Kaolin, which enabled the darkest regions in Fig. (3.60) to be identified as Kaolin.

Further studies on Samples 6 - 10 of Table 12 showed the poor dispersion of the Kaolin platelets in various stages of deformation. This was attributed to

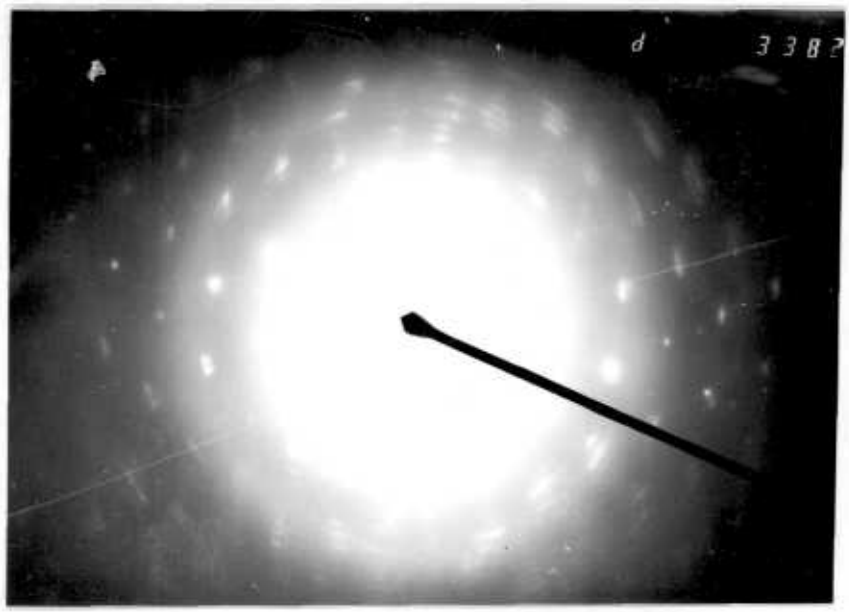

Fig. (3.61) The electron diffraction pattern of Kaolin

problems with the loading factor in the Banbury mixer, i.e. inadequate charging.

The JEM 100 C was used to analyse the sections from Sample 8 for Silicon and Chlorine. Fig. (3.62) contains the Si analysis at left and the Cl analysis at right. Each photograph contains the S.T.E.M. image, X-ray line trace, the trace line on the image and the base line of the X-ray signal. These results, together with those from 3.5.4, suggest the contrast originates as black for Kaolin, dark grey for P.V.C. and light grey for S.C.P.E.

Fig. (3.60) can then be explained as the encapsulation of Kaolin particles by the S.C.P.E. which then forms a second 'interface' with P.V.C., which acts as the matrix. Coatings of less than 0.1 μ are beyond the capability of the line analysis on the 100 CX.

The area analysis in Fig. (3.63) shows the presence of K, Al, Si from the Kaolin, together with Cl from the polymer. There is also a small peak for Fe, which could originate from the P.V.C. or the Kaolin, and which may be responsible for the catalysis of degradation reactions[114].

The resolution and identification of the components of complex morphologies

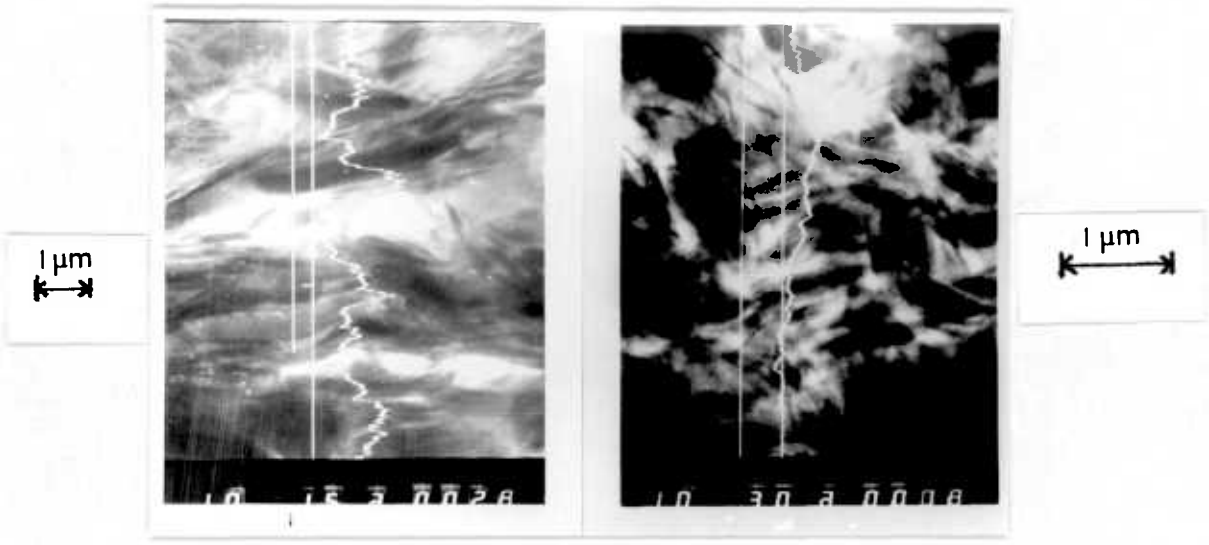

Fig. (3.62) The S.T.E.M. images and line analyses of composites for Silicon on the left and Chlorine on the right

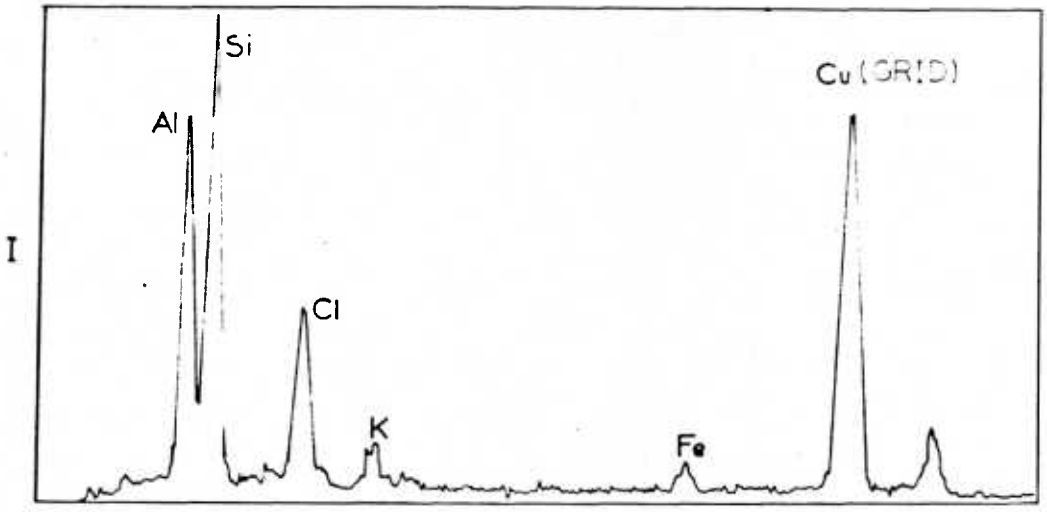

Fig. (3.63) The area analysis of a section from a P.V.C./Kaolin composite

is very difficult, even with the new generation of scanning /analytical microscopes.

These results are discussed within the context of the other experimental findings in the next section.

CHAPTER 5

DISCUSSION

5.1 Polymer - Solvent Interactions

The solvents used in the I.G.C. work were selected on the same basis as in other studies[115]. Hexane was used to test non-polar interactions, and acetonitrile or propanol were used for polar interactions. Chloroform was used to test the proton accepting strength of the polymer. Ethyl Acetate, T.H.F., 2-butanone (M.E.K.), acetone and dioxan were used to test the proton donating strength of the polymer. Finally D.C.M. was used to test the compatibility of a solvent which was chemically similar to the polymers.

Results from the I.G.C. indicate that hexane, propanol, and acetonitrile interact very weakly with both polymers, so the interactions of these polymers cannot be considered as non-polar or strongly polar. However, all other solvents show strong interactions with both polymers. Such a comparison is the main value of results from the I.G.C. studies. Instances where correlation between I.G.C. and other techniques have been found[110] are open to doubt because of the problems associated with I.G.C. This is apparent from the comparison of χ values measured at the same temperature for P.V.C. with chloroform and M.E.K. (1.73 and 1.50) and those in references 115 and 116 respectively (1.23 and 0.85, — and 0.5). There is a significant discrepancy from the reported results because other workers have values at one low coverage ratio only.

Calculations of χ^* are generally higher than those for χ, as expected. However, either of these give an experimentalist greater ability to select good solvents from the results. For example, the values of the interaction parameters for D.C.M. with P.V.C., and M.E.K. with P.V.C. are similar both for χ and χ^*. D.C.M. does dissolve P.V.C. (as it does S.C.P.E. where χ and χ^* have lower values). By comparison, chloroform is predicted to be a solvent for S.C.P.E., but not for P.V.C., and this was observed experimentally.

Although the high values of χ for M.E.K. with P.V.C. at 120°C suggest it is a non-solvent at that temperature, the cloud point data (T_c = 160°C) indicate it is still a solvent at low polymer concentration,at higher pressures. L.C.S.T.'s for polymer-solvents are asymmetric, as in Fig. 2.1, so the solvent at high polymer concentration could be expected to solvate the polymer, well above T_c.

All the proton-accepting (i.e. hydrogen bonding) solvents give lower values of χ and χ^* for both polymers. This suggests there is an interaction between the proton associated with the chlorine on the polymer chain, and the proton accepting group. Such an interpretation is supported by the I.R. absorption frequencies of the residual solvent in polymer films. In spite of this, ethyl acetate and acetone are not solvents. This may be explained by δ values from solubility parameter theory[65]. The values in $(\text{cal cm}^{-3})^{\frac{1}{2}}$ are 9.9 for acetone, and 9.1 for ethyl acetate, whereas M.E.K. has a value of 9.3, closer to the value of 9.5 for P.V.C.

The difference in the relative values obtained for chloroform with S.C.P.E. and P.V.C. may also be explained in terms of solubility parameter theory. Solubility parameters are 9.3 for chloroform, 9.7 for D.C.M., 9.5 for P.V.C. and $\sim$ 8.8 for S.C.P.E. This would imply that chloroform should be a solvent for P.V.C., as it is for S.C.P.E. It is possible that there is some ordering in P.V.C., which means it swells in many solvents, but only dissolves in solvents with very similar solubility parameters, or which form specific interactions. The difference in the heats of solution for D.C.M. and chloroform with P.V.C. would be small, as no hydrogen bonds are formed.

Many vinyl polymers dissolve in a wide range of solvents without specific interactions. However, P.V.C. dissolves only in solvents which are capable of forming hydrogen bonds, so that ΔH_m will be negative, or chemically similar to P.V.C., so

that ΔH_m will be very close to zero, i.e. P.V.C. dissolves naturally in a much more narrow range of solvents.

Values of χ obtained at different temperatures (120 - 150°C) increase with temperature, as predicted by the simple lattice theory[19]. The equation of state theory predicts χ should give a minimum with increasing temperature, as observed by some workers[116]. However, there are problems due to the onset of the T_g of P.V.C. at lower temperatures, which cause complications in interpretation in this region.

The variation in the compatibility of polymer blends cast from different solvents has been explained by Patterson[61] as due to the difference in the interactions between the two polymers and some solvents. In the case of M.E.K. the polymer-solvent interaction parameters χ_{12} and χ_{13} must be similar. However, when D.C.M. is used as a solvent there may be a stronger interaction with the S.C.P.E. than with the P.V.C. This asymmetry would lead to phase separation before all the solvent is removed.

It has been shown that residual solvent can be a serious problem in the study of compatible polymer pairs. The technique of solvent casting films has been criticised[61,117] but there are no instances of the use of 'in-situ' polymerisation to solve these problems. Residual solvent may cause spurious effects in T_g studies and in heat of mixing analyses, particularly in cases where a specific interaction is possible.

When vinyl chloride is used to make polymer blends by 'in-situ' polymerisation it is possible that it acts as a 'solvent'. The technique of I.G.C. could be a good way to investigate this. Since the structure of vinyl chloride is analogous to both polymers and there are no specific interactions, there should be little difference in their interactions. Because of this it should not interfere in the interactions between the two polymers.

It is also possible to control grafting and crosslinking in the preparation of the

'in-situ' blends in order to change the position of the phase diagram, or to suppress phase separation. Such work was beyond the scope of this investigation. The phase diagram also varies with molecular weight, but the interest here was in polymers with a degree of polymerisation greater than 1000. At this value the mechanical properties reach a steady value[62].

5.2 Polymer-Polymer Interactions

The questions regarding polymer compatibility have been discussed by McMaster[27] but recently Patterson and Robard[118] have published a different analysis. The former suggests that L.C.S.T.'s are due to a free volume effect which becomes less favourable with increasing temperature. This is attributed to the difference in expansion coefficients of the two polymers. The latter states that there must be a specific interaction, such as a hydrogen bond between the two polymers for compatibility to occur.

In this system there is no possibility of specific interactions. The only interactions would be dipolar forces between the molecules and these have been shown to be small relative to London forces[44]. This is supported by the low value for the heat of mixing obtained (-0.15 cal/cm^3) compared with that of the polystyrene-poly(vinyl-methyl ether) system, where a specific interaction (charge-transfer) has been postulated[1] (-16 cal/cm^3).

The explanation for the L.C.S.T. here must be that there is a free volume effect which is made manifest by the small negative heat of mixing. This may result from favourable packing arrangements which reduce the free volume and may cause a negative non-combinational entropy of mixing. This is in agreement with the work of McMaster[27] who postulated that the expansion coefficients for the two polymers should be similar. Those measured for liquid P.V.C. and poly(chloroprene) (P.C.P.) are similar[49]. P.C.P. is chemically and physically analogous to S.C.P.E.

It is difficult to estimate the importance of the dipole forces, as this is the only

known system which has only dipole forces contributing to an L.C.S.T. These should be unfavourable for mixing, as contacts between unlike chain segments would be higher energy than for like contacts. There must be a free volume effect as the driving force for compatibility.

Results from the analysis of the structure of single phase blends do not agree with the hypothesis of Geil et al[119] that the structure is due to 'nodules' or para-crystallites. The absence of any diffraction peaks from diffraction studies precludes the notion of long range 'order'. Similarly, the explanation of Uhlmann et al[83] that high resolution electron microscope images are artefacts has been disproved.

The structure can be seen as originating in local density fluctuations associated with polymer coils. This implies the polymers are miscible on a molecular level. Data obtained from neutron studies can be used to estimate the extent of 'phase separation'. It can be shown from simple considerations that if unperturbed polymer coils are placed randomly to fill a volume element, then the distance between the coil centres would be 66 Å. This illustrates that it is not necessary to imply any order in an amorphous polymer in order to obtain density fluctuations. If they are regarded as random coils, a photon should experience a greater density of chlorine atoms as it passes through the major axis than if it passes through a minor axis. This is implied in the definition of the Gaussian coil.

S.A.X.S. results have been criticised[120] because of the correction for de-smearing. In these results, absolute intensity units have been obtained from neutron scattering at different Q values, and these all indicate the existence of density fluctuations obtained from monotonically decreasing scattering curves.

This type of behaviour has been observed in amorphous poly(ethyleneterephthalate) poly(styrene) and poly(methyl methacrylate)[120]. The great problem with P.V.C. has

been the presence of other scattering centres[93] which have caused ambiguity in the analysis of the structure[120]. The formation of these so-called 'primary particles' has here been suppressed by the use of 'in-situ' polymerisation to prepare the blends. This polymer blend can be considered similarly to other amorphous polymers.

The 'd' spacing of the paracrystalline primary particles of 142 Å obtained from the 'Bragg' peak suggests the particles would be in multiples of this - 282 or 426Å in size. These must be responsible for the large value (300 Å) of the characteristic correlation length for P.V.C. found by others[120].

Radii of gyration (R_g) measurements give a value of $(R_g^2/M.W.)^{\frac{1}{2}}$ of 0.33, compared with 0.37 theoretically estimated for theta dimensions, and 0.30 found by others[124]. The decrease in R_g with increasing elastomer content is similar to other results for polystyrene/poly α-methylstyrene[120], which indicate the second polymer is a 'poor' solvent for the first.

The characteristic ratio C_∞ for P.V.C. may also be estimated from the expressions of Flory[121] to be 8.3 ± 2.0. This value is higher than those obtained by light scattering for P.V.C. in T.H.F. and other good solvents[65] (which may be because for light scattering P.V.C. aggregates in solution).

These results suggest that P.V.C. is expanded in the solid state, presumably by steric effects along the chains.

It may be that the propagating P.V.C. polymer entangles with the S.C.P.E. present for 'in-situ' polymerisation which stops ordering in P.V.C. This is supported by the hypothesis put forward by Wenig[93] that the primary particles in P.V.C. are formed due to self association of propagating chains in the early stages of polymerisation. These ordered molecules precipitate from solution entangled with other growing chains which then form larger particles. It is because of their network-like structure that P.V.C. can be swollen by many solvents but can only dissolve in a narrow range of solvents.

Another important result is the variation in the characteristic correlation length for the 50% d P.V.C./S.C.P.E. blend prepared by 'in-situ' polymerisation. The neutron scattering results show this distance between scattering centres decreases with increasing temperature, although this change is within experimental error. When phase separation is initiated, one could expect polymers of the same type to move closer together, as has been observed. The results also indicate phase separation did not occur after the short heating time for these large specimens.

It is possible that the absence of 'primary particles' could influence the mechanical properties of P.V.C. compositions, as these could act as stress concentrators in the solid state. The diffusion of small molecules would also be affected by the reduction in the 'tortuosity factor' for the diffusion path length[62].

Results obtained from mechanically mixed samples confirm others[59] that impact properties increase on crossing a phase boundary from single phase to two phase mixtures. It is possible to locate the phase boundary by studies of impact properties of mechanically mixed blends. However, an independently obtained phase diagram is more useful in determining other thermodynamic data. This may be advantageous because the components can also be studied. For example, some workers have concluded that C.P.E. and P.V.C. are incompatible from studies of mechanical blends of surface chlorinated or heterogeneously chlorinated polyethylene (H.C.P.E.)[122,123].

It may be possible to calculate further data such as contact parameters from accurate values of the polymer-polymer interaction parameter for P.V.C./S.C.P.E. However, the values obtained by I.G.C. for mixtures of these polymers adsorbed on the support vary greatly with the solvent probes used. Both for χ_{23} and χ^*_{23} the values do not have appropriately positive or negative values which agree with results from solvent casting. Some workers have commented on the variation between bulk and I.G.C. values of χ for compatible polymers[115], whereas others assert that

the consistency of the results makes them reliable[102].

In a discussion on the activity of P.T.F.E., Conder[113] states that previous workers unsuccessfully attempted to observe capilliaries by electron microscopy. It is well known[78] that P.T.F.E. degrades rapidly under electron irradiation, so the result is not surprising. Rather larger capilliaries have been observed in this work by optical microscopy. Braun and Guillet[99] have argued that the influence of the substrate can be isolated, whereas Silberberg[124] and Lipatov[125] argue that the adsorbed polymer is changed by the substrate. Olabisi[115] is the only experimentalist to give details of the method of preparation of the I.G.C. columns.

If the technique of I.G.C. is to be improved it would be necessary for standard techniques to be used. These could be based on the use of glass spheres or beads of low surface areas which have been treated with D.M.C.S. as supports. Polymers should be coated and dried by a standard method, such as the use of a fluidised bed. The optimum loading ratio should be obtained by a measurement of the variation of retention volume with loading. All stationary phases should be sieved to the appropriate size calculated from the size of the support, and the method of column packing should be specified.

When all these factors are controlled it will be possible to assess the accuracy of the technique.

5.3 Polymer-Kaolin Interactions

The values of coverage obtained for the formation of 'monolayers' of P.V.C. and S.C.P.E. on Kaolin, using D.C.M. as the probe in I.G.C., were 50 and 100 mg per g of substrate respectively. This value is significantly larger than the value of 10 mg/g which has been measured by other workers[34,41] for systems with greater interactions.

One explanation for the difference in the values of the coverage for those polymers is that the interaction with the surface is responsible. This causes S.C.P.E. to bind more strongly than P.V.C. to this surface, but less strongly than other polymers.

Because of this, less S.C.P.E. than P.V.C. is required for monolayer formation. The increase in the value of V_g after the minimum in Fig. (3.58) is much greater for S.C.P.E. than P.V.C. and this supports the analysis. Chloroform and D.C.M. are considered the best probes because they do not hydrogen bond with the polymers.

The thickness of this coverage is $\sim 40\text{Å}$, assuming a value of 10 m^2/g for the surface area[55]. Some workers have criticised the use of B.E.T. surface areas, arguing that nitrogen molecules can adsorb on areas where polymers cannot[99]. Kaolin has a regular surface and the polymers have a small cross-sectional area, so these objections should not be valid.

From this result the order of magnitude of the effective thickness of polymers on surfaces can be estimated. This is particularly important in composites where mechanical properties of a polymer are modified. The thickness of a coating can determine its effectiveness in dissipating energy or preventing crack propagation[51,53].

In this case there is no correlation between the dimensions associated with the critical crack opening displacement and the dimensions of the polymer coating. The low coating thickness has been effective in improving impact properties, while tensile properties have not been greatly reduced. Also, there is only a small difference in the surface free energy of the two polymers used in composites with the clay. It may be that the S.C.P.E. acts as a 'weak boundary layer' or it may be that there are covalent bonds at the surface which are significant.

Results obtained here may be improved by controlled coating of fillers by elastomers from solution before mixing in composites. This might be useful to resolve the questions regarding chemical and physical effects at interfaces.

CHAPTER 6

CONCLUSIONS

The object of this work was to study the interactions between the components of a composite system consisting of P.V.C., S.C.P.E. and Kaolin. This has resulted in the discovery that the two polymers are compatible at room temperature, and that they phase separate at higher temperatures. This behaviour has been proved to result in a phase diagram which is an L.C.S.T. with a critical temperature near 120°C. A technique has also been found for evaluating the interactions of the polymers with Kaolin and other substrates.

Interactions of chlorinated polymers with solvents have been adequately explained by solubility parameter theory. They have been found to dissolve the polymers if their solubility parameters are within a narrow range near that of the polymer, unless there is a specific interaction. P.V.C. has been shown to have unusual solubility characteristics which may be associated with its structure. Values of polymer-solvent interaction parameters calculated from Inverse Gas Chromatograph experiments at 120°C are higher than expected, but can be explained by the simple Flory-Huggins theory.

The polymer-polymer interactions are best explained by an equation-of-state approach. Polymer-polymer interaction parameters obtained experimentally did not always have the negative values which were expected. This has been explained as due to difficulties with the I.G.C. procedure used.

Different techniques have been shown to be useful in these studies. 'In-situ' polymerisation, when used with solvent casting, provides an independent test of polymer compatibility. The main technique of evaluating T_g by Dynamic Mechanical Spectroscopy has been useful for establishing compatibility, but a more sophisticated instrument would be preferable. Facilities for a wide range of accurate modulus measurements, programmed

isothermal heating and a wide range of vibration frequencies would be useful.

Combined optical and electron microscopic studies have been shown to be useful for the development of models of the system, provided these instruments are used in a systematic way. It was particularly important that the specimen preparation, treatment and radiation resistance were considered before any interpretations were made. Using these instruments, it was found that phase separation could be observed in the optical and electron microscopes. A scanning/analytical microscope was found to be useful in determining the origin of contrast variations observed in the images which were due to chlorine. A 'fine structure' with separation of molecular dimensions was also observed in single phase blends.

There were limitations to the direct attempts which were made to measure the heat and volume of mixing. However, these were simpler than other indirect techniques and give reliable data. In this way it was shown that : $\Delta H_m = -0.15 \pm 0.05$ cal/g, and $\Delta V_m = -0.007 \pm 0.003$ cm^3/g.

Scattering experiments such as S.A.X.S. and S.A.N.S. were used to obtain molecular models to check results from electron microscopy. These showed that the blends had no preferential orientation or structure, other than random coils whose centres were $\sim$ 48 Å apart. Radii of gyration were obtained which decreased from 134 Å in P.V.C. to 109 Å in 50% blends, and this was consistent with other studies. The blends prepared by 'in-situ' polymerisation show no evidence of the 'primary particles' which occur in P.V.C., so the technique could be used as a way of suppressing the formation of these particles. A characteristic ratio of 8.3 was obtained for P.V.C. which indicates the homopolymer is more expanded than previous studies suggest.

The technique of Inverse Gas Chromatography has been shown to be capable of useful measurements. Trends in the calculated values of interaction parameters were useful for predicting the behaviour of different solvents. It was concluded that absolute

values will be possible, but only when a rigorous standard procedure is developed. I.G.C. was shown also to be useful in observing the phase separation of single phase polymer blends under isothermal conditions. This gave an independent determination of the phase diagram.

The technique was further used to measure the influence of surfaces on adsorbed polymers. Both on Kaolin and P.T.F.E. the point of complete coverage could be measured, and this was near 50 mg/g loading of polymer on substrate. This has been shown to correspond to a layer 40 Å thick, which is higher than values previously reported for other systems. The results were interpreted as showing S.C.P.E. interacted more strongly than P.V.C. with active Kaolin surfaces. This confirmed observations in the electron microscope that S.C.P.E. was preferentially encapsulating the Kaolin particles.

Problems of combining theoretical predictions from surface free energy measurements with fracture mechanics have not been overcome, because of the viscoelastic properties of these composites. There is no evidence that the deformation zone in fracture mechanics is similar to the thickness of coating required to improve the properties of composites.

The impact properties of blends prepared by hot mixing have shown an increase on changing from single phase to two phase blends. Knowledge of the location of this phase boundary means the change can be studied in more detail. Similarly, the impact properties of composites containing Kaolin and P.V.C. increase with an increase in the level of S.C.P.E. For the same compositions the modulus increases until the level which corresponds to monolayer coverage has been reached. This indicates the elastomer is important in improving the mechanical properties of composites. It has been suggested that the elastomer reduces the area of high energy interfaces.

This investigation has shown that using appropriate techniques it is possible to

develop a systematic analysis of the properties and performance of composites on a molecular basis.

```
UNIVERSITY OF MINNESOTA FORTRAN COMPILER (VERSION 5.3 - 79/01/12) ON THE C174 UNDER  N O S 1.1.0 ON 79/08/13 AT 15.49
                    MNF5(1)  PROGRAM FOR χ FROM I.G.C.
                    C      MA,MASS MW,MOL.WT. FR,FLOW RATE TE,EXP.TEMP. BST,B STAR ALF,ALPHA
                    C      TR,REF.TEMP. DENL1,LIQUID DENSITY AT TR1 , T DEG CEN (ALL)
                    C      AZ,LIL A BZ,LILB Z11,D VAP AT TR1
                    C      M=NUMBER OF SOLVENTS,CHIA=CHI(ARRAY)
      1.  000000B           REAL MA,MW,NU2,M2N
      2.  000000B           DIMENSION CHIA(15),VGOA(15),V1A(15),P0A(15),TEA(15),TIM1(15),TIM2(
                           115)
      3.  002131B           M=10
      4.  002306B           READ,((TIM1(I),TIM2(I)),I=1,M)
      5.  002336B           READ,P0,PI,FR1,FR2,RO,ALF,M2N
      6.  002350B           READ,MA,TE
      7.  002355B           DO 4 N=1,M
      8.  002364B           READ,A,B,MW,E,BST,TR1,TR2,DENL1,DENL2,B11
      9.  002402B           AST=ALOG(MW)/2.303-E
     10.  002407B           Z1=AST-(BST/(TR1+230.0))
     11.  002412B           Z2=AST-(BST/(TR2+230.0))
     12.  002415B           Z11=EXP(Z1*2.303)
     13.  002424B           Z12=EXP(Z2*2.303)
     14.  002432B           BZ=(DENL1-DENL2-Z12+Z11)/(TR1-TR2)
     15.  002440B           AZ=DENL1+Z11-BZ*TR1
     16.  002443B           DVE=EXP(AST-(BST/(TE+230.0)))*2.303
     17.  002454B           DLQ=(AZ+BZ*TE)-DVE
     18.  002457B           V1=MW/DLQ
     19.  002461B           NU2=1.0/(RO-ALF*(TE-TR1)/RO)
     20.  002466B           V5=(PI*PI)/(P0*P0)
     21.  002471B           V6=(PI*PI*PI)/(P0*P0*P0)
     22.  002475B           VG1=(1.5*(V5-1)/(V6-1)*FR1*273.0)/(MA*(273.0+TE))*TIM1(N)/60.0
     23.  002515B           VG2=(1.5*(V5-1)/(V6-1)*FR2*273.0)/(MA*(273.0+TE))*TIM2(N)/60.0
     24.  002534B           SL=(VG1-VG2)/(FR1-FR2)
     25.  002541B           VG0=VG1-(SL*FR1)
     26.  002543B           RC=82.05
     27.  002544B           BA=(A-(B/(TE+230.0)))*2.303
     28.  002551B           P0=EXP(BA)//60.0
     29.  002566B           CHI = ALOG((273.0*RC*NU2)/(VG0*P0*V1)) - (1.0-V1/(M2N*NU2))
                           1-P0/(RC*(TE+273.2))*(B11-V1)
     30.  002604B           CHIA(N)=CHI
     31.  002611B           VGOA(N)=VG0
     32.  002615B           V1A(N)=V1
     33.  002622B           P0A(N)=P0
     34.  002627B           TEA(N)=TE
     35.  002633B      4    CONTINUE
     36.  002641B           PRINT1
     37.  002647B           DO 5 N=1,M
     38.  002656B           READ(5,6)NAME
     39.  002666B      5    WRITE(6,2)NAME,CHIA(N),VGOA(N),V1A(N),P0A(N),TEA(N)
     40.  002731B           PRINT8
     41.  002740B      1    FORMAT(///10X,7HSOLVENT,14X,7HCHI 1-2,10X,3HVG0,10X,2HV1,10X,2HP0,
                           110X,2HTE//)
     42.  002740B      2    FORMAT(10X,A10,10XF7.3,8XF6.2,7XF7.2,5XF7.4,5XF7.2//)
     43.  002746B      6    FORMAT(A10)
     44.  002748B      8    FORMAT(//)
     45.  002750B           STOP
     46.  002751B           END
```

APPENDIX 1

PROGRAM FOR χ^* FROM I.G.C.

```
UNIVERSITY OF MINNESOTA FORTRAN COMPILER (VERSION 5.2 - 78/07/25) ON THE C174 UNDER  N O S 1.1.0 ON 79/06/11 AT 10.36

                      MNFS(T)
                      C     MA,MASS MW,MOL.WT. FR,FLOW RATE TE,EXP.TEMP. BST,B STAR ALF,ALPHA
                      C     TR,REF.TEMP. DENL1,LIQUID DENSITY AT TR1 , T DEG CEN (ALL)
                      C     AZ,LIL A BZ,LILB ZI1,D VAP AT TR1
                      C     M=NUMBER OF SOLVENTS,CHISA=CHIS(ARRAY)
     1.    000000B          REAL MA,MW,NU2S,M2N,NUTILDE
     2.    000000B          DIMENSION CHISA(15),VG0A(15),V1SA(15),P0A(15),TEA(15),TIM1(15),
                           +TIM2(15)
     3.    002151B          M=10
     4.    002307B          READ,((TIM1(I),TIM2(I)),I=1,M)
     5.    002337B          READ,PO,PI,FR1,FR2,RUS,ALF,M2N
     6.    002351B          READ,MA,TE
     7.    002356B          DO 4 N=1,M
     8.    002365B          READ,A,B,MW,E,BST,TR1,TR2,DENL1,DENL2,B11,NUTILDE
     9.    002404B          AST=ALOG(MW)/2.303-E
    10.    002411B          Z1=AST-(BST/(TR1+230.0))
    11.    002414B          Z2=AST-(BST/(TR2+230.0))
    12.    002417B          ZI1=EXP(Z1*2.303)
    13.    002426B          ZI2=EXP(Z2*2.303)
    14.    002434B          BZ=(DENL1-DENL2-ZI2+ZI1)/(TR1-TR2)
    15.    002442B          AZ=DENL1+ZI1-BZ*TR1
    16.    002445B          DVE=EXP(AST-(BST/(TE+230.0))*2.303)
    17.    002456B          DLQ=(AZ+BZ*TE)-DVE
    18.    002461B          V1S=MW/(DLQ*NUTILDE)
    19.    002464B          NU2S=1.0/(RUS-ALF*(TE-TR1)/RUS)
    20.    002470B          V5=(PI*P1)/(P0*P0)
    21.    002473B          V6=(PI*P1*P1)/(P0*P0*P0)
    22.    002477B          VG1=(1.5*(V5-1)/(V6-1)*FR1*273.0)/(MA*(273.0+TE))*TIM1(N)/60.0
    23.    002517B          VG2=(1.5*(V5-1)/(V6-1)*FR2*273.0)/(MA*(273.0+TE))*TIM2(N)/60.0
    24.    002536B          SL=(VG1-VG2)/(FR1-FR2)
    25.    002543B          VG0=VG1-(SL*FR1)
    26.    002545B          RC=82.05
    27.    002554B          BA=(A-(B/(TE+230.0)))*2.303
    28.    002563B          P0=EXP(BA)/760.0
    29.    002606B          CHIS = ALOG((273.0*RC*NU2S)/(VG0*P0*V1S)) - (1.0-V1S/(M2N*NU2S))
                           +-P0/(RC*(TE+273.2))*(B11-V1S)
    30.    002606B          CHISA(N)=CHIS
    31.    002613B          VG0A(N)=VG0
    32.    002617B          V1SA(N)=V1S
    33.    002624B          P0A(N)=P0
    34.    002631B          TEA(N)=TE
    35.    002655B     4    CONTINUE
    36.    002643B          PRINT1
    37.    002651B          DO 5 N=1,M
    38.    002660B          READ(5,6)NAME
    39.    002670B     5    WRITE(6,2)NAME,CHISA(N),VG0A(N),V1SA(N),P0A(N),TEA(N)
    40.    002732B          PRINT3
    41.    002742B     1    FORMAT(///10X,7HSOLVENT,15X,3HCHIS 1-2,10X,3HVG0,09X,3HV1S,
                           +10X,2HP0,10X,2HTE//)
    42.    002742B     2    FORMAT(10X,A10,10XF7.5,6XF6.2,7XF7.2,5XF7.4,5XF7.2//)
    43.    002742B     6    FORMAT(A10)
    44.    002742B     3    FORMAT(//)
    45.    002742B          STOP
    46.    002743B          END
```

REFERENCES

1. NISHI, T., KWEI, T.K., WANG, T.T. Macromolecules 8, p.227 (1975)
2. ARRIDGE, R.G.C. 'Mechanics of Polymers' (1975) Oxford U. Press
3. SMALL, P.A. J. Appl. Chem. 3, p.71 (1953)
4. ERA, V.A. Die Makromol. Chem. 175 (7), p.2199 (1974)
5. MORTON, M. Rubber Technology, p.322 (1973) 2nd Ed. Van Nostrand
6. DANNENBERG, E.M. Rubber Chemistry and Technology 48, p.410 (1975)
7. YEUNG, P., BROUTMAN, L.J. S.P.E. Polymer Eng. & Sci. 18, (2), p.62 (1978)
8. SOLOMON, D.H. J. Macromol. Sci. (Chem.) A5 (3), p.587 (1971)
9. GEE, G., TRELOAR, L.R.G. Trans. Faraday Soc. 38, p.147 (1942)
10. FLORY, P.J. J. Chem. Physics 10, p.51 (1942)
11. HUGGINS, M. J. Phys. Chem. 46, p.151 (1942)
12. TOMPA, H. Trans. Faraday Soc. 45, p.1142 (1949)
13. SCOTT, R.L. J. Chem. Physics 17, p.279 (1949)
14. FREEMAN, P.I., ROWLINSON, J.S. Polymer 1, p.20 (1959)
15. PATTERSON, D., DELMAS. G., SOMCYNSKY, T. J. Pol. Sci. 57, p.79 (1962)
16. PRIGOGINE, I. "The Molecular Theory of Solutions" Chap. 16 (1957) North-Holland Publishing Co.
17. FLORY, P.J., EICHINGER, B.E. Trans. Faraday Soc. 64, p.2053 (1968)
18. HILDEBRAND, J.H., SCOTT, R.L. 'The Solubility of non-electrolytes' 3rd Ed. Reinhold N.Y. (1950)
19. FLORY, P.J. 'Principles of Polymer Chemistry' Cornell U. Press (1953) 2nd Ed.
20. KONNINGSVELDT, R., STAVERMAN, A.J. J. Pol. Sci. A-2, 6, p.325 (1968)

21. EWING, M.J. Trans. Faraday Soc. 46, p.613 (1950)

22. BOOTH, C., GEE, G., JONES, M.N., TAYLOR, W.D. Polymer 5, p.353 (1964)

23. SCHULTZ, A.R., FLORY, P.J. J.A.C.S. 74, p.4760 (1952)

24. GORDON, M. J. Pol. Sci. Polymer Symposia 61, p.41 (1977)

25. MORAWETZ, H. "Macromolecules in Solution", p.40 (1965) High Polymers Vol. XXI. Interscience

26. ALLEN, G., GEE, G., NICHOLSON, J.P. Polymer 2, p.8 (1961)

27. PATTERSON, A. Macromolecules 10, p.74 (1974)

28. McMASTER, L. Macromolecules 6, p.760 (1973)

29. TONKS, L. Physic Rev. 50, p.955 (1936)

30. ROSENBLUTH, M.N., ROSENBLUTH, A.W. J. Chem. Phys. 22, p.881 (1954)

31. CAHN, J.W. J. Chem. Phys. 42, p.93 (1965)

32. GIBBS, J.W. Collected Works, Yale University Press (1948)

33. GRIFFITH, A.A. Phil. Trans. Roy. Soc. A 221, p.163 (1921)

34. ADAMSON, A.W. 'Physical Chemistry of Surfaces' 2nd Ed. Interscience p.411 (1967)

35. ZISMAN, W.A. J. Phys. Chem. 58, p.260 (1954)

36. SILBERBERG, A. J. Phys. Chem. 66, p.1872 (1962)

37. DERJAGUIN, A.V. Kolloid Z. 69, p.155 (1934)

38. HAMAKER, H. Physica 4, p.1058 (1937)

39. BAILEY, A.T., COURTNEY-PRATT, J.S. Proc. Roy. Soc. A, p.227 (1955)

40. ISRAELACHVILI, J.N. Faraday Discussions of the Chem. Soc. "Colloid Stability" 65, p.23 (1978)

41. KISELEV, A.V., KOVALEVA, N.V., KHOPINA, V.V., YU, A. Vysokomol. Soyed A16, p.1142 (1974)

42. BRAUN, J.M., GUILLET, J.E. Adv. Pol. Sci. 21, p.107 (1976)

43. GOOD, R.J., GIRIFALCO, L.A. J. Phys. Chem. 64, p.561 (1960)

44. LEE, L.H. (Ed.) Advances in Adhesion, p.364 (1973) Gordon and Breach

45. NIELSEN, L.E., WALL, R.A., RICHMOND, P.G. S.P.E. J. 11, p.22 (1955)

46. EINSTEIN, A. Ann. Phys. 34, p.591 (1911)

47. NIELSEN, L.E. J. Appl. Pol. Sci. 10, p.97 (1966)

48. WILLIAMS, J.G. Adv. Pol. Sci. 27, p.67 (1978)

49. VAN KREVELEN, D.W. 'Properties of Polymers' Elsevier (1972)

50. TABOR, D. 'Gases, Liquids and Solids', p.130 (1970) Penguin

51. BUCKNALL, C. Adv. Pol. Sci. 27, p.121 (1978)

52. BROUTMAN, L.J., KROCK, R.H. 'Composite Materials' 6 (1974)
Ed. Plueddmann E. Academic Press

53. MASON, J.A., SPERLING, L.H. 'Polymer Blends and Composites', p.442
(1976) Plenum

54. VAN OLPHEN, H. 'An Introduction to Clay Colloid Chemistry' (1963)
Interscience

55. MATJEVIC, E., SWARTZEN-ALLEN, S.L. Chem. Revs. 74, p.387 (1974)

56. SOLOMON, D.H., HODGKINS, J. J. Macromol. Sci. (Chem.) A8,
p.635 (1974)

57. HAWTHORNE, D.G., SOLOMON, D.H. J. Macromol. Sci. (Chem.) A8,
p.659 (1974)

58. English China Clay Ltd. 'Speshwhite' technical literature

59. BLANCHARD, R.R., BURNELL, C.N. S.C.P.E. J 24, p.74 (1968)

60. REBENFELD, L. et al. J. Macromol. Sci. Revs. Macromol. Chem. C15 (2)
p.325 (1976)

61. PATTERSON, D. Macromolecules 10 (5) p.1021 (1977)

62. HAWARD, R.N. 'The Physics of Glassy Polymers', p.26 (1973) Applied Science

63. IVIN, K. Ed. 'Structural Studies of Macromolecules by Spectroscopic Methods', p.1 (1976) Wiley

64. EVANS, J.M., MAISEY, L.J. 'Industrial Polymers : Characterisation by Molecular Weight'. Symposium at National Physical Laboratory, May 1973, Transcripta Books, London

65. BRANDRUP, J, IMMERGUT, E.H. Polymer Handbook, 2nd Ed. (1975) Wiley

66. HASLAM, J., WILLIS, H.A. 'Identification and Analysis of Plastics', p.199, 2nd Ed. (1972) Iliffe

67. WING Yip. Personal communication (I.C.S.T.)

68. ALLEN, G., BOWDEN, M.J., BLUNDELL, D.J., JEFFS, G.M., VYVODA, J. and WHITE, T. Polymer 14, p.604 (1973)

69. CHAPIRO, A. 'High Polymers' Vol. XV, p.468 (1962) Interscience

70. FERRY, J.D. 'Viscoelastic Properties of Polymers', p.9 (1970) 2nd Ed. Wiley

71. McCRUM, N.G., READ, B.E., WILLIAMS, G. Anelastic and Dielectric Effects in Polymeric Solids' p.208 (1967) Wiley

72. WILLIAMS, G., WATTS, D.C. NOTTIN, J.P. J.C.S. Faraday Trans. II, 68, p.16 (1972)

73. HARTSHORN, N.H., STUART, A. 'Crystals and the Polarising Microscope', p.422, 4th Ed. (1970) Arnold

74. ZERNIKE, from VEB Carl Zeiss JENA. Technical literature

75. BENNETT, A.H. et al. 'Phase Microscopy' (1951) Wiley

76. KAY, D. 'Techniques for Electron Microscopy' (1961) Blackwell

77. COSLETT, V.E. Br. J. of Appl. Phys. 7, p.10 (1956)

78. SPINKS, J.W.T., WOODS, R.J. 'An Introduction to Radiation Chemistry', p.383, 2nd Ed. (1976) Wiley.

79. SUZUKI, T. Pure and Applied Chemistry 49, (5) p.539 (1977)

80. BOWEN, D.K., HALL, C.R. 'Microscopy of Materials', p.145 (1975) Macmillan

81. BARCLAY, L.M. Die Angewandte Makromol. Chem. 52, p.1 (1976)

82. CHRISTNER, G.L., THOMAS, E.L. J. Appl. Phys. 48, (10) p.4063 (1977)

83. MEYER, M., VANDERSANDE, J., UHLMANN, D.R. J. Pol. Sci. Pol. Phys. Ed. 16 (11) p.2005 (1978)

84. WEEKS, N.E., KARASZ, F.E., MACKNIGHT, W.J. J. Appl. Phys. 48 (10) p.4068 (1977)

85. KONINGSVELDT, R., KLEINTJENS, L.A., SCHOFFELEERS, H.M. Pure and Applied Chem. 39, p.1 (1974)

86. CARROLL, B., MANCHE, E. 'Physical Methods in Macromol. Chem.' 2, Chap. 4, p.255 (1972) M. Dekker, N.Y.

87. REHAGE, G. Kolloid Z. Polymere 199, p.1 (1964)

88. Handbook of Chemistry and Physics CRC Press, 55th Ed., p. D 223

89. KELLER, A. J. Pol. Sci. Pol. Phys. Ed. 16 (8) p.1507 (1978)

90. KRATKY, O. Pure and Appl. Chem. 12, p. 483 (1966)

91. DEBYE, P., ANDERSON, H.R., BRUMBERGER, H. J. Appl. Phys. 28, p.679 (1957)

92. DUISER, J.A., KEIJZERS, A.E.M. Polymer 19 (8) p.889 (1978)

93. WENIG, W. J. Pol. Sci. Pol. Phys. Edn. 16 (9) p.1635 (1978)

94. MACONNACHIE, A., RICHARDS, R.W. Polymer 19, p.739 (1978)

95. ALLEN, G., HIGGINS, J.S. Rep. Prog. in Phys. 36, p.1073 (1973)

96. GHOSH, A. 'A computing guide for small angle scattering experiments'. Institut Laue - Langevin, 1978

97. DETTENMEIER, M., HERSCHENSCHROEDER, P. Personal Comm., University of Mainz

98. GUILLET, J.E., SMIDROD, O. Macromolecules 2, p.272 (1969)

99. BRAUN, J.M., GUILLET, J.E. Macromolecules 8, p.882 (1975)

100. YOUNG, C.L. Chrom. Revs. 10, p.129 (1968)

101. PATTERSON, D., TEWARI, Y.B., SCHREIBER, H.P. and GUILLET, J.E. Macromolecules 4, p.356 (1971)

102. DESHPANDE, D.D., PATTERSON, D., SCHREIBER, H.P. and SU, C.S. Macromolecules 7, p.530 (1974)

103. PRAUSNITZ, J.M., NEWMAN, R.D. J. Paint Technol. 45, p.33 (1973)

104. TIMMERMANS, I. 'Physico-Chemical Constants of Pure Organic Compounds', Elsevier, N.Y. (1960)

105. DREISBACH, R.R. 'Physical Properties of Chemical Compounds', A.C.S. Press, Washington (1955)

106. ALLEN, G., GEE, G. and WILSON, G.J. Polymer 1, p.456 (1960)

107. GALLANT, R.W. 'Physical Properties of Hydrocarbons' (1974) Gulf

108. HASLAM, J., WILLIS, H.A., SQUIRRELL, D.C.M. 'Identification and Analysis of Plastics', 2nd Ed., p.149 (1972)

109. GRAHAM, D.P. J. Phys. Chem. 69, p.4387 (1965)

110. TAIT, P.J.T., AMBUSHIHADA, A.M. Polymer 18, p.810 (1977)

111. MARK, H. (Ed.) Encyc. of Pol. Sci. and Tech. 6, p.442 (1967) Wiley

112. KESSAISSIA, Z., PAPIRER, E. J. Chim. Phys. 75, p.709 (1978)

113. CONDER, J.R. Anal. Chem. 43, p.367 (1971)

114. UEGAKI, Y., NAKAGAWA, T. J. Appl. Pol. Sci. 21, p.965 (1977)

115. OLABISI, O. Macromolecules 8, p.316 (1975)

116. TAIT, P.J.T., AMBUSHIHADA, A.M. Macromolecules 11, p.918 (1978)

117. KRAUSE, S.J. J. Macromol. Sci. C. 7, p.251 (1972)

118. PATTERSON, D., ROBARD, A. Macromolecules 11, p.690 (1978)

119. GEZOVICH, P.M., GEIL, P.H. Int. J. Polym. Mater. 1, p.3 (1971)

120. HIGGINS, J.S., STEIN, R.S. J. Appl. Cryst. 11, p.346 (1978)

121. FLORY, P.J. 'Statistical Mechanics of Chain Molecules' Interscience N.Y. (1969)

122. FLEISCHER, D., FISCHER, E., BRANDRUP, J. Die Ang. Makromol. Chem. 62, p.69 (1977)

123. HEDVIG, P. 'Dielectric Spectroscopy of Polymers', p.305 (1977) Adam Hilger Ltd.

124. SILBERBERG, A., PRIEL, Z. J. Pol. Sci. Pol. Phys. Ed. 16, p.1917 (1978)

125. LIPATOV, Y.S., NESTEROV, A.E. Macromolecules 8 (6) p.889 (1975).